S-Acylation is Crucial for ASBT-Mediated Bile Acid Uptake: Monitoring the Transport Activity in Real Time

BY

ALEXANDER L TICHO
B.A., St Olaf College, 2012

THESIS

Submitted as partial fulfillment of the requirements
for the degree of Doctor of Philosophy in Physiology and Biophysics
in the Graduate College of the
University of Illinois at Chicago, 2021

Chicago, Illinois

Defense Committee:

Mrinalini C Rao, Chair, Physiology and Biophysics
Waddah A Alrefai, Advisor, Medicine
Larry Tobacmen, Medicine
Pradeep K Dudeja, Medicine
Chong Wee Liew, Physiology and Biophysics
Daesung Lee, Chemistry

ACKNOWLEDGEMENTS

First and foremost, I must thank my family for their constant and unwavering support. My parents, who have always encouraged me to ask questions about the world, shaped my love for science. I could not be where I am today without your patience and guidance. To my wife and best friend, Katie, who has been my partner throughout this journey. Thank you for loving and supporting me, for taking care of me, and for making my life brighter.

I would also like to acknowledge my committee members, Drs. Meena Rao, Larry Tobacman, Pradeep Dudeja, Chong Wee Liew, and Daesung Lee. Thank you for challenging me and guiding me. You have always sought to make me a better thinker and communicator, and I hope to make you proud. Thank you also to everyone in the Department of Physiology and Biophysics. It has been a pleasure to train in a department that is so devoted to their students.

To my friends in the lab, thank you for teaching me, laughing with me, and putting up with me. A special thanks to Drs. Ravinder Gill and Seema Saksena, whose insight and conversations helped to shape my research.

To everyone in the Medical Scientist Training Program, thank you for being my second family. Because of your work, the future of science and medicine has never been stronger.

Finally, I would be remiss if I did not thank my mentor, Waddah. Your dedication and enthusiasm have inspired me to persevere during hard times, celebrate during good times, and appreciate the journey. You are a selfless mentor, and I cannot possibly thank you enough for your guidance, encouragement, and friendship.

CONTRIBUTION OF AUTHORS

The *in vitro* and *ex vivo* data presented in **chapter II** represent work that was published as part of a collaboration between our laboratory and the laboratory of Dr. Daesung Lee (Ticho AL, Lee H, Gill RK, Dudeja PK, Saksena S, Lee D, Alrefai WA. 2018. A novel bioluminescence-based method to investigate uptake of bile acids in living cells. *Am J Physiol – GI and Liver Physiol*. 315(4):G529-G537. doi: 10.1152/ajpgi.00133.2018.). The synthesis of chemicals was performed in Dr. Lee's laboratory by Hyunjin Lee, who wrote the chemical synthesis section for the manuscript (**Figure 6**). All biological experiments in **chapter II** (**Figures 7-13**) were designed and performed by me under the guidance of Dr. Alrefai.

The data presented in **chapter III** (**Figures 14-18**) represent experiments that were designed and performed by me, with the following exceptions. [^{3}H]-TC uptake studies (**Figures *16D*-E, 17B-C, 18B**) were performed by either Sangeeta Tyagi or Pooja Malhotra and cell surface biotinylation (**Figure 16G**) was performed by Pooja Malhotra.

TABLE OF CONTENTS

LIST OF TABLES

LIST OF FIGURES

FIGURE PAGE

LIST OF ABBREVIATIONS

2-BP	2-bromopalmitate
2BT	HEK 293 cells stably transfected with ASBT-V5
Acyl-RAC	acyl resin-assisted capture
ALA	a-linoleic acid
Alk-OA	ω-alkyne oleic acid
Alk-PA	ω-alkyne palmitic acid
AP-1	activator protein 1
APT	acyl protein thioesterase
ASBT	apical sodium-dependent bile acid transporter
AUC	area under the curve
BA	bile acid
BAD	bile acid diarrhea
BAM	bile acid malabsorption
BAS	bile acid sequestrant
BAT	bile acid transporter
BBMV	brush border membrane vesicle
BSEP	bile salt export pump
C4	7α-hydroxy-4-cholesten-3-one
CA	cholic acid
CA-SS-Luc	cholic acid-disulfide-luciferin conjugated probe
CAR	constitutive androstane receptor
CDCA	chenodeoxycholic acid
CDX	caudal-type homeobox
CFTR	cystic fibrosis transmembrane conductance regulator
CYP	cytochrome p450
DAT	dopamine transporter
DCA	deoxycholic acid
DMSO	dimethyl sulfoxide
EGCG	(-)-epigallocatechin-3-gallate
ENaC	epithelial Na^+ channel
EPA	eicosapentanoic acid
EPEC	enteropathogenic *Escherichia coli*
FA	fatty acid
FABP6	fatty acid binding protein 6
FGF15	fibroblast growth factor 15
FGF19	fibroblast growth factor 19
FGFR4	fibroblast growth factor receptor 4
FRET	fluorescence resonance energy transfer
FTF	fetoprotein transcription factor
FXR	farnesoid X receptor
GAPDH	glyceraldehyde phosphate dehydrogenase
GC	glycocholate
GCDC	glycochenodeoxycholate
GLP-1	glucagon-like peptide 1

GPBAR1	G protein-coupled bile acid receptor 1
GR	glucocorticoid receptor
HA	hydroxylamine
HEK 293	human embryonic kidney 293 cells
HNF1α	hepatocyte nuclear factor 1α
HuR	human antigen R
IBABP	ileal bile acid binding protein
IEC	intestinal epithelial cell
IL-1β	interleukin-1β
IVIS	*in vivo* imaging system
JNK	c-Jun N-terminal kinase
LCA	lithocholic acid
LDL	low density lipoprotein
LRH-1	liver receptor homolog-1
Luc^{Tg}	luciferase-expressing transgenic mice
MCA	muricholic acid
MEK1/2	mitogen-activated protein kinase kinase 1/2
MMTS	S-methyl methanethiosulfonate
MRI	magnetic resonance imaging
MTA1	metastasis-associated gene 1
NAFLD	nonalcoholic fatty liver disease
NASH	nonalcoholic steatohepatitis
NEC	necrotizing enterocolitis
NRF2	nuclear factor-E2-related factor 2
NTCP	Na^+-taurocholate co-transporting polypeptide
OA	oleic acid
OATP	organic anion transporting polypeptide
OSTα/β	organic solute transporter α/β heterodimer
PA	palmitic acid
PFIC	progressive familial intrahepatic cholestasis
PKC	protein kinase C
PMA	phorbol 12-myristate 13-acetate
PPARα	peroxisome proliferator-activated receptor α
PPT	protein palmitoyl thioesterase
PTM	post-translational modification
PTPIII	protein tyrosine phosphatase inhibitor III
PXR	pregnane X receptor
RAR	retinoic acid receptor
RIPA	radioimmunoprecipitation assay
RXR	retinoid X receptor
S1PR	sphingosine-1-phosphate receptor
SA	stearic acid
SERT	serotonin transporter
SHP	small heterodimeric partner
SIRT1	sirtuin 1
SLC10A	solute-like carrier family 10A

SREBP2	sterol regulatory element binding protein 2
T2DM	type 2 diabetes mellitus
TC	taurocholate
TCDC	taurochenodeoxycholate
TDC	taurodeoxycholate
TGR5	Takeda G protein-coupled receptor 5
THPTA	tris(3-hydroxypropyltriazolylmethyl)amine
TLCA	taurolithocholic acid
TM	transmembrane
TNF	tumor necrosis factor
UDCA	ursodeoxycholic acid
UTR	untranslated region
VDR	vitamin D receptor
zDHHC	zinc-finger aspartic acid-histidine-histidine-cysteine gene family

SUMMARY

Bile acids are a structurally diverse class of molecules that serve a wide variety of critical physiological functions. These compounds are synthesized in the liver and secreted into the small intestine, where they facilitate lipid absorption and serve as important signaling molecules. Approximately 95% of bile acids are reabsorbed in the intestine and returned to the liver, establishing their enterohepatic circulation. The ileal apical sodium-dependent bile acid transporter (ASBT) is crucial for maintaining bile acid enterohepatic circulation, as evidenced by the fact that ASBT knockout leads to a decrease in the bile acid pool size. ASBT defects or dysregulation may contribute to several disorders, including bile acid malabsorption and hypercholesterolemia. ASBT is rapidly regulated by a variety of post-translational mechanisms, including phosphorylation and modulation of its interaction with plasma membrane microdomains, which may represent adaptive responses to a rapidly changing intestinal milieu. Investigating the rapid regulation of ASBT is challenging, as traditional methods do not capture transporter activity in real time. Several recent studies have developed real time methods in order to measure various aspects of bile acid homeostasis, but none have been able to directly measure the activity of bile acid transporters such as ASBT. We hypothesized that a bioluminescence-based approach for assessing bile acid transporters would allow for real-time monitoring of transporter activity. To address this hypothesis, we designed a reporter system relying on a novel probe: cholic acid attached to luciferin via a disulfide-containing, self-immolating linker (CA-SS-Luc). We first validated its use for *in vitro* monitoring of bile acid transporter activity using HEK 293 cells transfected with ASBT or the hepatic bile acid transporter NTCP, along with firefly luciferase. We demonstrated that real-time bioluminescence production in living cells was proportional to the cellular expression of bile acid transporter. We also investigated CA-SS-Luc in mouse intestinal epithelial cells isolated from

transgenic mice expressing firefly luciferase. Ileal enterocytes displayed significantly higher luminescence compared to jejunal enterocytes, indicating a transport process mediated by ileal ASBT. These data provide evidence for the suitability of this method to assess the acute regulation of ASBT activity in real time. In this regard, rapid regulation of membrane proteins relies on post-translational modification of specific amino acid residues. Recent evidence has demonstrated that several cysteine residues present in the ASBT protein are critical for proper transport function. Cysteine residues may be subject to S-acylation, a post-translational lipid modification involving covalent binding to fatty acids, which has been shown to regulate membrane transport proteins. Therefore, we hypothesized that ASBT is subject to S-acylation, and that this modification is important for transporter function and bile acid uptake. With regard to ASBT regulation, we demonstrated that ASBT is S-acylated in native intestinal tissues from mice, as well as human organ donors. In HEK 293 cells transfected with ASBT, inhibition of S-acylation rapidly reduced ASBT activity, indicating that S-acylation is important for ASBT function. We further showed that S-acylation of ASBT by unsaturated fatty acids reduced transporter function compared to saturated fatty acids, suggesting that the fatty acid attached to ASBT is functionally important. In conclusion, these studies have established an innovative method for assessing bile acid transporters in living cells. We have also identified and characterized a novel post-translational lipid modification of ASBT that may provide important insights into the regulation of intestinal bile acid absorption and the maintenance of bile acid homeostasis.

Chapter I: Introduction

Sections A-E in this chapter were modified from:

Ticho AL, Malhotra P, Gill RK, Dudeja PK, Alrefai WA. Intestinal bile acid absorption in health and disease. *Comprehensive Physiology* 10: 21-56, 2020

Bile acids are synthesized in the liver and secreted into the small intestine, where they facilitate lipid absorption and serve as important signaling molecules. Approximately 95% of bile acids are reabsorbed in the intestine and returned to the liver, establishing their enterohepatic circulation. It has been demonstrated that the ileal apical sodium-dependent bile acid transporter (ASBT) is crucial for preserving bile acid enterohepatic circulation. Thus, maintaining proper functioning of ASBT is critical for bile acid homeostasis. In this regard, changes in ASBT function are associated with several disorders. In one respect, reduced ASBT function may lead to bile acid diarrhea, a potentially serious disease characterized by watery diarrhea. Conversely, enhanced ASBT function is associated with disorders such as necrotizing enterocolitis (NEC), progressive intrahepatic cholestasis (PFIC), and type 2 diabetes mellitus (T2DM). As such, ASBT expression and function must be tightly regulated, which is accomplished by a variety of mechanisms. Importantly, post-translational mechanisms are critical for acute postprandial regulation of ASBT. Studies have shown that ASBT is rapidly regulated by several post-translational means, including phosphorylation and modulation of its association with lipid raft microdomains. It is important to understand the mechanisms underlying the regulation of ASBT by these post-translational modifications (PTMs). However, the currently available methods for measuring ASBT activity do not fully capture rapid changes in transporter activity, necessitating the development of real-time methods for assessing bile acid transporters. Additionally, it is critical to identify novel regulatory mechanisms that may also be important for modulation of ASBT function. In this regard, recent studies have demonstrated that several ASBT cysteine residues are crucial for transport function. Cysteine residues are known to undergo S-acylation, a post-translational lipid modification that is important for the regulation and function of many transport proteins. Determining the importance of S-acylation for ASBT function and regulation is therefore critical. The objectives of these

studies were, therefore, to design a real-time method for measuring ASBT activity and to assess the functional importance of ASBT S-acylation.

In the following sections several important aspects of bile acid physiology, including bile acid structure, bile acid synthesis, the enterohepatic circulation of bile acids, and the physiological functions of bile acids will be discussed. The molecular mechanisms of intestinal bile acid absorption will then be discussed, with a focus on the structure, function, and regulation of ASBT. Finally, we will discuss post-translational lipid modifications, focusing on protein S-acylation.

A. Bile acid structure

Bile acids are one of the most structurally diverse classes of small biomolecules. Remarkably, at least 84 distinct unconjugated bile acids and 25 bile alcohols have been identified in vertebrates (108). It is important to note that subtle structural differences between bile acids dramatically affect their biological roles. During the past 100 years, much effort has been dedicated to identifying bile acid structures and their composition in humans. Because of this important basic research, we now know the structures, the relative abundance, and the basis of the structure-function relationship of these molecules in humans and other animals.

1. Structural features of bile acids

Despite their wide structural diversity, bile acids do have several defining structural features. All bile acids possess a lipophilic steroid body that is hydroxylated at one or more positions and a side chain that terminates as a carboxylic acid (108). The bile acid pool of mammals and most vertebrates is composed entirely of compounds with 24 carbon atoms, while more primitive animals may produce bile acids with up to 27 carbons. The presence of both a lipophilic

ring and hydroxyl and carboxyl moieties makes bile acids amphipathic molecules, which is necessary for their function as physiological detergents. Bile acids are necessarily hydroxylated at the 3α position (3α-OH) on steroid ring A, but many are hydroxylated at other sites as well. Indeed, the majority of bile acid diversity is the result of differential hydroxylation of the steroid ring. In addition to their hydroxylation, bile acids have a sidechain extending from C-17 on steroid ring D. The carboxylic acid moiety at the end of the side chain is conjugated to either taurine or glycine in the liver, which lowers the pKa and enhances water solubility at physiological pH.

2. Mammalian bile acid species

Of all the bile acid species that have been identified, only a few are of physiologic relevance in mammals. The chemical structures of physiologically important bile acids are shown in figure 1. Humans synthesize just two bile acids: cholic acid (CA) and chenodeoxycholic acid (CDCA). Both are produced from cholesterol in the liver and are found in all mammals, as well as many lower species. The structural difference between CA and CDCA is slight. CA is 3α-, 7α-, and 12α-hydroxylated, while CDCA is only 3α- and 7α- hydroxylated. CA and CDCA, along with the bacterial metabolite deoxycholic acid (DCA; 3α-, 12α-OH), are the major bile acid species in humans. Combined, these three bile acids and their conjugated forms account for >90% of biliary bile acids in humans (CA ~35%, CDCA ~40%, and DCA ~20%) (17, 81, 111). Additionally, several minor bile acids in humans have been identified, including lithocholic acid (LCA; 3α-OH) and ursodeoxycholic acid (UDCA; 3α-, 7β-OH). DCA and LCA are generated in the intestine by bacteria via 7α-dehydroxylation of CA and CDCA, respectively. Like CA and CDCA, DCA and LCA are found in all mammals and numerous other species. Similarly, UDCA is produced from

CDCA by intestinal bacteria via 7-OH epimerization, although it can be formed in the hepatocytes of some animals, most notably several species of bears (72, 95).

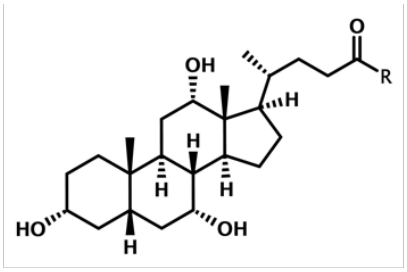

Cholic acid

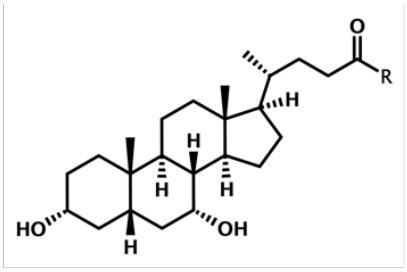

Chenodeoxycholic acid

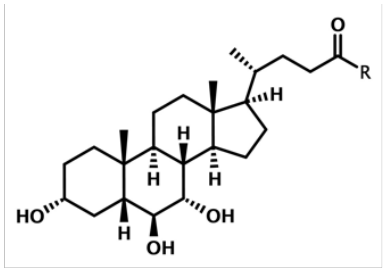

α-muricholic acid

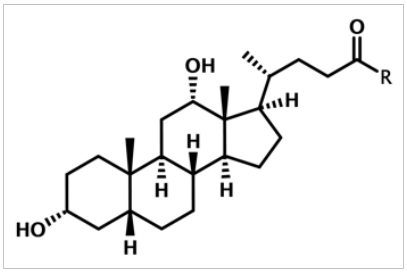

Deoxycholic acid

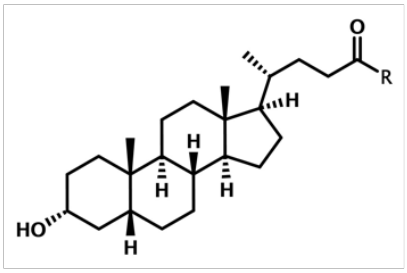

Lithocholic acid

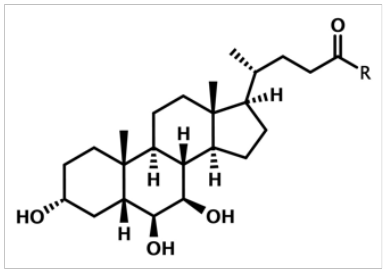

β-muricholic acid

R-group	Naming convention
-OH Acidic hydroxyl	No additional prefix or suffix (cholic acid, chenodeoxycholic acid, etc.)
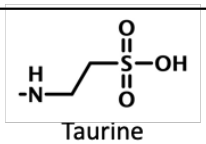 Taurine	Tauro- prefix (taurocholic acid, taurochenodeoxycholic acid, etc.)
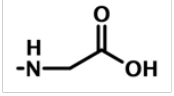 Glycine	Glyco- prefix (glycocholic acid, glycochenodeoxycholic acid, etc.)

Figure 1. Common mammalian bile acids. The structure of six common mammalian bile acids is shown. The structural variation is conferred by the number, location, and orientation of hydroxyl groups on the steroid nucleus.

Because much research in the field is conducted in mice and rats, it is critical to understand the differences between human and rodent bile acid pools. In addition to the bile acids noted above, rodents produce a group of bile acids termed muricholic acids (MCAs), which are hydroxylated at the 6-C position. The two major MCAs in mice are α-muricholic acid (α-MCA; 3α-, 6β-, 7α-OH) and β-muricholic acid (β-MCA; 3α-, 6β-, 7 β-OH). Interestingly, the MCAs constitute a majority of the rodent bile acid pool. The consequences of these different bile acid profiles are just beginning to be uncovered. However, it is clear that bile acid signaling differs greatly between human and rodents because of these chemical differences in the bile acid pool.

B. Bile acid synthesis

The primary bile acids CA and CDCA are synthesized in the liver from cholesterol at a rate of approximately 500 mg/day in humans (52, 214). Secondary bile acids, which include DCA, LCA, and UDCA, are produced by bacteria from bile acids in the intestinal lumen (111, 262). The process of primary bile acid synthesis requires at least 17 enzymes, which are located in the endoplasmic reticulum, mitochondria, peroxisomes, and cytosol. The liver is the sole organ that contains all of the enzymes required for BA biosynthesis. However, many other tissues possess enzymes that synthesize intermediate compounds, which can then be circulated to the liver for completion of the synthesis. There are two parallel pathways by which BA synthesis occurs: the classical (neutral) pathway, which accounts for up to 70% of human BA synthesis, and the alternative (acidic) pathway, which is a relatively minor route for bile acid synthesis under physiological conditions (31). Hepatic bile acids (either *de novo* synthesized or recycled from the intestine) are conjugated to the amino acids taurine or glycine by the bile acid-coenzyme A:amino acid N-acyltransferase (75, 127, 201).

The classical pathway occurs exclusively in hepatocytes and leads to production of both CA and CDCA. The first reaction in the classical pathway is catalyzed by cytochrome P450 7A1 (cholesterol 7α-hydroxylase; CYP7A1), localized to the endoplasmic reticulum. CYP7A1 hydroxylates the 7α position of cholesterol to produce 7-hydroxy cholesterol. This enzyme is rate-limiting and is critical for efficient synthesis of bile acids. Indeed, disruption of CYP7A1 by homozygous knockout of the Cyp7a1 gene in mice reduces bile acid synthesis by ~60% and bile acid pool size by ~75%, which results in increased fecal lipids, hypercholesterolemia, and poor survival (74, 122, 223, 224).

The other crucial enzyme of the classical pathway is cytochrome P450 8B1 (sterol 12α-hydroxylase; CYP8B1), which is also located in the ER. CYP8B1 is responsible for hydroxylating the 12α carbon of the steroid ring. Thus, CYP8B1 is the enzymatic branch point for the synthetic routes of cholic acid, which is 12α-hydroxylated, and chenodeoxycholic acid, which is not. As expected, Cyp8b1 knockout mice have a markedly different bile acid profile compared to wildtype animals. Whereas wildtype mice have bile acid profiles rich with CA, Cyp8b1 knockout mice are deficient in CA and DCA and have increased levels of CDCA and its derivatives, including UDCA and MCAs (159).

The alternative pathway for bile acid synthesis is a minor contributor to the total bile acid pool. In adult humans, it accounts for no more than ~30% of total bile acid synthesis (31). Unlike the classical pathway, only CDCA and not CA can be synthesized by the alternative pathway. The first and rate limiting step of the alternative pathway is the entry of cholesterol into the mitochondria, which is mediated by the steroidogenic acute regulatory protein (StAR) (197). Then, the mitochondrial sterol 27-hydroxylase (CYP27A1) oxidizes the sidechain of cholesterol. CYP27A1 is expressed in hepatocytes, as well as a variety of extrahepatic sites, including

macrophages and endothelial cells (10, 203, 206). Thus, the alternative pathway can be initiated outside of the liver. Interestingly, hepatic CYP27A1 is also critical in the classical pathway, where it oxidizes intermediates of BA synthesis. Expectedly, mice deficient in Cyp27a1 display bile acid pools ~1/3 the size of wild type mice (210).

In addition to CYP7A1, CYP8B1, and CYP27A1, which are key enzymes in bile acid synthesis, Cyp2c70 is essential for bile acid synthesis in mice. Takahashi et al. recently identified this enzyme as the bile acid 6β-hydroxylase and demonstrated that Cyp2c70 is required for the synthesis of muricholic acids (249). Mice with the Cyp2c cluster knocked out (Cyp2c ko) and Cyp2c ko mice with a human CYP2C9 transgene (hCYP2C9) were unable to synthesize MCA species and displayed a corresponding increase in CDCA. The bile acid profile in these mice more closely resembles that of humans, who do not produce MCAs. Although the implications of the different bile acid pools in mice and humans have not been fully investigated, it is clear that bile acid structure underlies the molecular basis of bile acid functions, as will be discussed in the following sections.

C. Enterohepatic circulation of bile acids

Following synthesis in hepatocytes, bile acids are excreted across the canalicular membrane by the bile salt export pump (BSEP). Biliary BAs are stored in the gallbladder and secreted into the small intestine following meals, where they act as detergents and signaling molecules. Luminal BAs travel through the small intestine and are actively reabsorbed in the distal ileum by the apical sodium-dependent bile acid transporter (ASBT). Reabsorbed BAs are shuttled from the apical to the basolateral membrane of the enterocyte and are excreted into the portal circulation by the organic solute transporter α/β heterodimer (OSTα/β). These BAs are returned to the liver via the portal vein and enter hepatocytes by the sinusoidal sodium-taurocholate

cotransporting polypeptide (NTCP), establishing the enterohepatic circulation of bile acids (Figure 2).

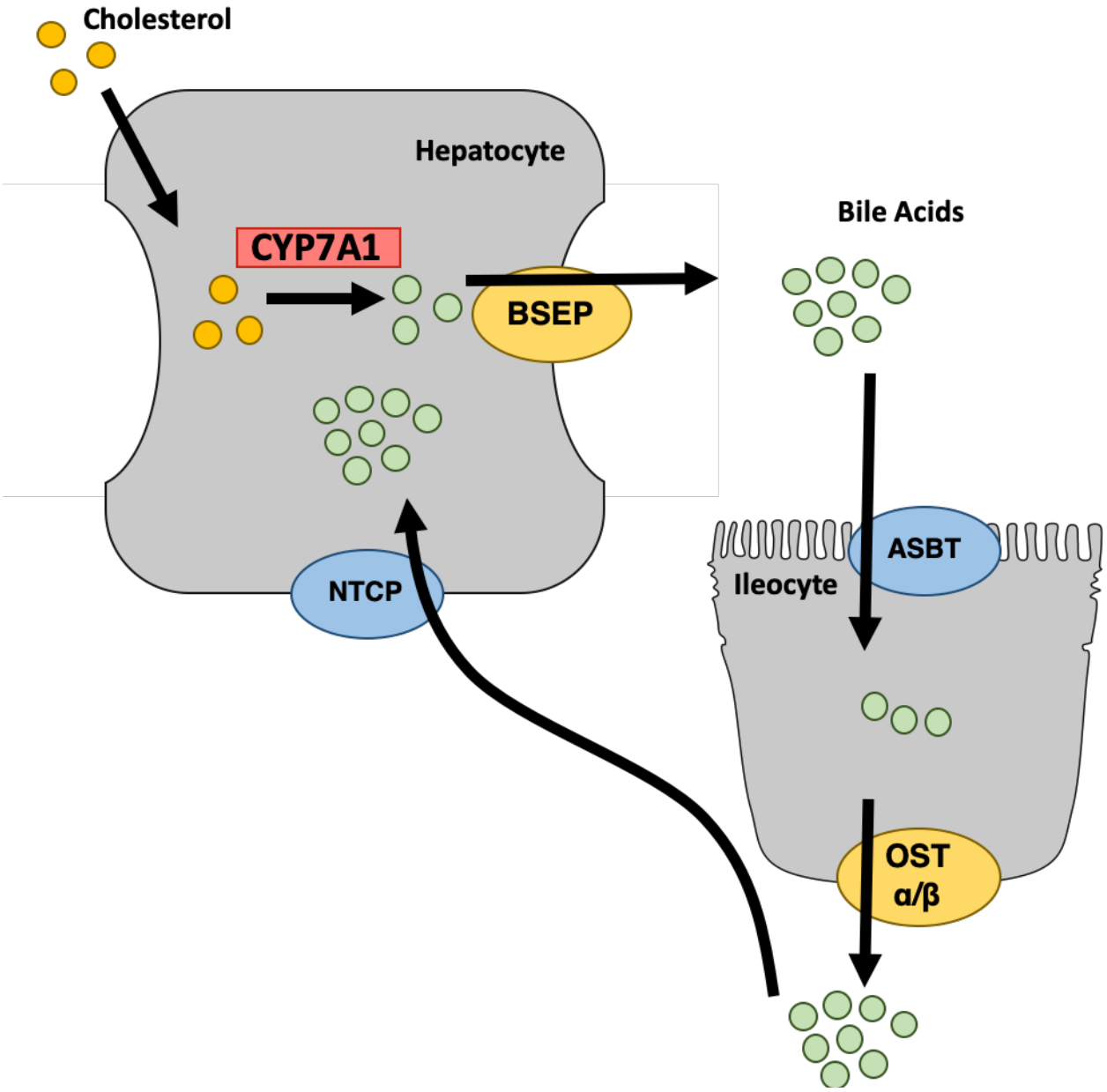

Figure 2. Enterohepatic circulation of bile acids. Bile acids are synthesized from cholesterol in the liver via a process initiated by CYP7A1 and secreted into the intestine by the bile salt export pump (BSEP). In the ileum, bile acids are taken up by enterocytes via the apical sodium-dependent bile acid transporter (ASBT) and exported into the portal circulation by the organic solute transporter α/β heterodimer (OSTα/β). These bile acids circulate to the liver, where the sodium-taurocholate cotransporting polypeptide (NTCP) is responsible for their uptake by hepatocytes.

D. Functions of bile acids

In addition to their vast structural diversity, bile acids perform a wide variety of physiological roles in the body. Some of their functions, particularly their role as detergents, have been known for more than 100 years. However, more recent research has demonstrated that bile acids also have critical signaling roles that are essential for glucose and lipid homeostasis.

1. Dietary lipid absorption

The physiological role of bile acid as detergents is historically the best-recognized of BA functions. Indeed, bile acids are of critical importance for proper lipid absorption. Bile acids are amphipathic and are present at high concentration in the intestinal lumen, allowing them to form micelles and emulsify dietary fats and cholesterol. In the gut lumen, these micelles increase lipid surface area, promoting digestion by lipases and enhancing absorption at the brush border membrane (110). In some pathological states, such as bile acid malabsorption, an insufficient bile acid pool size limits the ability to aid lipid absorption and leads to lipid malabsorption (35).

Importantly, bile acid structure greatly influences the extent to which they aid lipid absorption. Amino acid conjugation maintains high BA concentration in the lumen by preventing passive diffusion. Furthermore, bile acids in which all hydroxyl moieties are facing one side of the molecule are more hydrophobic and are thus better lipid emulsifiers. Studies performed by Wang et al. demonstrated that when mice were supplemented with CA and CDCA, cholesterol absorption was enhanced relative to non-supplemented diets (263). However, when supplemented with more hydrophilic bile acids such as MCAs, cholesterol absorption was reduced. These studies clearly illustrate the relationship between bile acid structure and function as digestive emulsifiers.

2. Bile acids as signaling molecules

While the role of bile acids in facilitating the absorption of lipids has been known for over 100 years, the effects of bile acids on other aspects of metabolism have only recently been recognized. By the early 1990s, a link between bile acid and cholesterol homeostasis was clear, but the molecular mechanisms of this interaction were not well known (73). The molecular basis underlying bile acids' importance in metabolism has started to clarify over the past 20 years. A number of studies reported bile acid interactions with cellular receptors, including the nuclear receptors farnesoid X receptor (FXR), pregnane X receptor (PXR), and vitamin D receptor (VDR), as well as the membrane G protein-coupled bile acid receptor (GPBAR1; GPCR19; TGR5) and sphingosine-1-phospate receptor (S1PR). These seminal findings identified new molecular targets for bile acid-based therapies and helped renew interest in the field of bile acid physiology. Indeed, bile acids are now understood as complex signaling molecules that exert a wide array of effects on bile acid, cholesterol, glucose, and lipid homeostasis.

E. Molecular mechanisms of bile acid absorption

1. Intestinal absorption of bile acids.

In 1936, it was reported that when concentrated bile acid solutions were injected into the small intestine of animals, bile acids were absorbed by the intestine and recovered in portal and systemic blood (129). Over the next decades, the concept of enterohepatic circulation of bile acids became well accepted, as evidence for both passive and active intestinal absorption continued to emerge (68, 139). However, the molecular mechanisms of this absorptive process remained elusive until relatively recently, when bile acid transporters were discovered.

It had long been known that at physiological pH, conjugated BAs are ionized and membrane impermeable. Therefore, their transport across epithelial cells requires membrane transport proteins (7). The hepatic sodium-taurocholate cotransporting polypeptide (NTCP; SLC10A1) facilitates bile acid uptake at the sinusoidal membrane of the hepatocyte and the bile salt export pump (BSEP) secretes bile acids into the bile canaliculi. In the ileum, this transepithelial transport is mediated by the apical sodium-dependent bile acid transporter (ASBT; SLC10A2) at the apical membrane and the organic solute transporter α/β heterodimer (OSTα/β) at the basolateral membrane (**Figure 3**, pg. 31). In addition, the ileal bile acid-binding protein (IBABP; FABP6) is important for intracellular sequestration of bile acids and may also be important for transporting bile acids from the apical to basolateral membranes during absorption (7). This process of intestinal bile acid absorption is crucial for maintaining bile acid homeostasis and enterohepatic circulation.

2. Apical sodium-dependent bile acid transporter (ASBT)

The apical sodium-dependent bile acid transporter (ASBT) is responsible for the uptake of BAs from the intestinal lumen into enterocytes and is the rate-limiting enzyme for intestinal BA absorption. Like NTCP, ASBT is a sodium-dependent bile acid cotransporter in the SLC10A gene family.

The presence of a Na^+-dependent bile acid transporter in the ileum was confirmed in 1992 in brush border membrane vesicles from pig (182) and rabbit (144) ileum. Much of the early work uncovering the role of ASBT was performed in the laboratory of Paul Dawson, who first cloned ASBT in 1994 from a hamster ileum cDNA library (270). ASBT was later identified in rat (58, 228, 229), human (60, 191, 271, 272), mouse (147, 217), and chicken (185) ileum. These early studies also showed ASBT expression in the cells of the proximal renal tubule (58, 60, 229) as

well as cholangiocytes (6, 53, 149). Recently, ASBT expression in the brain has been shown, although the functional relevance is as yet unknown (188). Within the adult intestine, ASBT is most highly expressed in villus cells of the distal ileum, with minimal expression in the colon (9, 113, 239, 265). The distribution of ASBT expression along the intestine mirrors the conjugated bile acid uptake capacity, highlighting the essential role of this transporter in bile acid absorption (239).

A great deal of evidence has supported the importance of ASBT in intestinal bile acid absorption. For instance, inactivating mutations in ASBT have been linked to some cases of primary bile acid malabsorption (PBAM), a serious condition that presents with steatorrhea and loss of bile acids in the stool (191). Additionally, mice with targeted deletion of the Slc10a2 gene display similar symptoms, with steatorrhea, loss of bile acids in the stool, decreased bile acid pool size, and enhanced bile acid synthesis (63). These lines of evidence demonstrate clearly that ASBT is critical for the intestinal absorption and enterohepatic circulation of bile acids.

a. ASBT and cholesterol metabolism

Because bile acid synthesis from cholesterol is responsible for ~50% of cholesterol elimination, ASBT-dependent recycling of bile acids is intimately related to cholesterol homeostasis. It has been known for decades that disrupting the intestinal absorption of bile acids leads to loss of bile acids in the stool and a concomitant increase in hepatic uptake of cholesterol in order to increase the synthesis of bile acids (73, 88). In this regard, it is interesting to note that patients with PBAM have low plasma LDL cholesterol levels, suggesting that loss of bile acids in the stool is protective against hypercholesterolemia (191). Indeed, ASBT knockout mice also show resistance to diet-induced and genetic models of hypercholesterolemia (65, 148).

Given that genetic ablation of ASBT reduces serum cholesterol, it is not surprising that small molecule inhibitors of ASBT have been shown to have similar antihyperlipidemic effects. Indeed, several ASBT inhibitors have been developed by pharmaceutical companies (29, 50, 136, 213). Although most are in trials for other indications (see below), they have been shown to enhance bile acid synthesis and reduce plasma cholesterol levels in several rodents (136, 157, 213, 269), ApoE knockout mice (29), pigs (116), monkeys (136), and humans (50, 232).

b. Gene structure and variants

The SLC10A2 gene is located on chromosome 13 in humans (NCBI Gene ID #6555) and chromosome 8 in mice (NCBI Gene ID #20494) (147, 272). In humans, mature ASBT mRNA consists of 6 exons comprising a 1044-nucleotide (nt) coding region, a 597-nt 5'-untranslated region, and a 2135-nt 3'-untranslated region. One splice variant has been reported, coding for a 154-aa bile acid efflux protein of unknown physiological significance that has been called t-ASBT (150).

Several genetic variants of ASBT have been reported, including some that result in altered protein function (146). The first reported variant was a single nucleotide polymorphism (SNP) resulting in a P290S mutant that abolished BA transport activity (271). Later, L243P and T262M variants that abolished transport activity were reported in a family with primary bile acid malabsorption, along with a A171S variant that did not affect transport (191). Screening approaches have since been used to identify other variants in Korean (196), German (209), and American (107) populations, though the clinical significance of many of these variants have not been fully investigated.

c. Protein structure and function

ASBT is a 348 amino acid transmembrane protein with an extracellular glycosylated N-terminus and a cytoplasmic C-terminus (**Figure 4**, pg. 39). The presence of a bile acid-binding protein with an apparent molecular weight of 43 kDa, which would later be identified as ASBT, was first discovered in 1983 by photoaffinity labeling of ileal BBMVs (140). Studies in the early 1990s similarly found a bile acid binding protein of similar molecular weight (or a ~90 kDa dimer) and noted that it was responsible for the Na^+-dependency of bile acid transport (142-144, 161, 162, 228, 231). Once ASBT was cloned, it was determined that the protein has a molecular weight of ~38 kDa, but a higher apparent molecular weight as a result of its glycosylation (271). Electrophysiological studies showed that ASBT is electrogenic with a 2:1 Na^+: BA stoichiometry (266, 267).

With respect to the structure of ASBT, the precise topology has been a matter of debate, in large part because the crystal structure of vertebrate ASBT has yet to be determined. Although initial predictions suggested that ASBT comprised 7 transmembrane (TM) domains (270), several lines of evidence supported a 9 TM model. For instance, membrane insertion scanning provided support for a 9 TM model (96) and a recent crystal structures of bacterial ASBT homologues revealed a structure consistent with 9 TM ASBT model (115, 287). However, strong evidence from dual label epitope insertion scanning mutagenesis and other methods refutes the 9 TM model in favor of a 7 TM model (23, 282).

Several laboratories, particularly that of Peter Swaan, have devoted a great deal of effort into elucidating not only the membrane topology of ASBT, but also the functional importance of the individual domains of this protein. The functions of individual domains discussed below assume a 7 TM model of ASBT (Figure 4, pg. 39). Several of the transmembrane domains are

crucial for ASBT transporter function. TM domain 1 is important for bile acid and Na^+ binding and translocation and also confers stability to the protein (62). TM domain 2 appears to be most important for Na^+ translocation via coordination with the Na^+ ion (215). The portion of TM domain 3 closest to the cytosol forms the route for bile acids as they exit ASBT and enter the cytosol (118). Additionally, the cytosolic half of TM domain 4 is another important part of the translocation pathway (135). TM domains 5 and 6 possess GxxxG motifs that are important for ASBT helix-helix interaction, conferring stability to the proteins without being directly involved with substrate translocation (177). TM domain 6 also appears important for Na^+-binding and translocation, while TM domain 7 is crucial for bile acid binding and translocation, as both of these domains line the translocation pathway (92, 117, 120, 141).

The soluble loops of ASBT have also been shown to be critical for protein function. A pair of aspartic acid residues (Asp120 and Asp122) on extracellular loop (EL) 1 are critical for Na^+-binding, and Asp124 appears to be important for binding to the 7α-OH of many bile acids (119). In addition, several other residues in this highly conserved loop are crucial for protein expression, localization, and substrate affinity (218, 220). EL 3 is also important for transporter activity via its electrostatic interactions with bile acids, which may represent the initial bile acid binding interaction site (21). Furthermore, a truncated mutant of ASBT revealed the importance of 14 amino acids in the C-terminal cytoplasmic tail in apical membrane localization of the protein (245, 246).

Of particular interest is the important role of ASBT cysteine residues. Several studies have probed the 13 cysteine residues of ASBT and noted a number of these residues that are both highly conserved between ASBT and NTCP, and are crucial for transport function, trafficking, and stability (22, 54, 216, 219, 244). Notably, mutation of the highly conserved Cys51, Cys105,

Cys132, and Cys255 to Ala or Thr nearly abolishes [^{3}H]-TC uptake (22). Mutations at other sites, such as Cys69 or Cys314, somewhat reduce [^{3}H]-TC uptake. In an effort to understand the mechanisms underlying the role of cysteine residues, a recent study concluded that cysteine residues in ASBT are likely not important for its oligomerization (54). However, the precise role of many of these important residues requires further study. It is possible that ASBT cysteine residues are modified by covalent binding to fatty acids in order to influence ASBT function. This will be the subject of the studies described in **chapter III** of this thesis.

d. Substrate specificity of ASBT

Bile acids are the only known endogenous substrates for ASBT. While ASBT is known to have a narrower substrate specificity than NTCP, it is clear that ASBT is able to efficiently transport a wide variety of bile acids, both conjugated as well as unconjugated (60, 138, 163). ASBT does not appear to have a strong preference for conjugated compared to unconjugated bile acids (60). However, CA and its conjugated derivatives appear to have a lower affinity (~15-35 μM) than CDCA and its derivatives (~3-10 μM) (60, 163, 217, 219, 270). TLCA appears to be a high affinity substrate of ASBT (163), while DCA species have an intermediate affinity between CA and CDCA (119, 270). Thus, the structural differences in bile acids determine their affinity for ASBT.

Because ASBT is an intestinal transporter that absorbs relatively large molecules, a great deal of work has been devoted to using this transport system to aid in the absorption of drugs via bile acid-conjugated prodrugs (100, 230). Bile acids are normally conjugated to taurine or glycine at 24-C, and these large conjugates serve as substrates for ASBT and other bile acid transporters. Several investigators have demonstrated that bile acids conjugated to synthetic molecules at 24-C

and other sites are substrates for ASBT and other bile acid transporters, such as NTCP (18, 165, 230). In large part because of this work, the precise structural requirements of ASBT have been meticulously elucidated. 3D-quantitative structure-activity relationship studies demonstrated that anionic sidechains at the 24-C position are preferred to neutral sidechains (25, 284). Additionally, 7-C conjugates are not efficiently transported by ASBT, although the presence of a 7α-OH moiety is not necessary for transport (138). Conversely, conjugates at the 3-C position are actively transported by ASBT (25, 138). These studies provided important details with respect to the ASBT substrate binding pocket and the substrate specificity of the transporter.

Interestingly, recent evidence has indicated an alternative transport process that ASBT may use in order to transport large molecules into the cell (3, 4). When bile acids were conjugated to a macromolecule and applied to cells expressing ASBT, vesicular endocytosis was induced and both ASBT and the macromolecule were internalized. This alternative receptor mode of ASBT-mediated uptake could be useful for designing drug delivery systems that target bile acid absorption pathways.

e. ASBT ontogeny and aging

The expression of ASBT shows distinct changes throughout an individual's lifespan. The newborn ileum shows minimal expression of ASBT, followed by a dramatic increase in expression after weaning. It appears that hormonal changes are responsible for ASBT ontogenic development. It has been demonstrated that the thyroxine hormone is critical for the induction of ASBT mRNA expression after weaning (121, 176). Additionally, the ontogeny of ASBT may be at least partially explained by its post-transcriptional regulation by RNA-binding proteins. HuR, which has been shown to stabilize ASBT, shows a pattern of ontogenic expression similar to that of ASBT.

Conversely, the destabilizing RNA-binding protein tristetraprolin shows the inverse ontogenic pattern (45, 234). Thus, the enhanced expression of ASBT after weaning could be in part the result of altered RNA-binding protein expression. Additionally, the intestinal development of ASBT expression in early life mirrors the expression of the transcription factors c-Jun and c-Fos, which are poorly expressed in mice during the neonatal period and sharply increase after weaning (42). The fact that ASBT expression is low prior to weaning is crucial for intestinal health, as the neonatal intestine is not equipped to respond to intracellular bile acids. Indeed, aberrantly high ASBT expression has been linked to neonatal necrotizing enterocolitis (99).

While it is clear that ASBT expression is enhanced after weaning, there is also evidence that aging decreases intestinal bile acid absorption. Studies by Gao et al. demonstrated that ^{3}H-TC uptake across ileum in Ussing chambers was reduced ~50% in a cohort of aged (~2-year-old) C57BL/6 mice relative to a younger (<1-year-old) cohort (87). There was a corresponding ~50% decrease in ASBT mRNA expression in the older cohort, suggesting that decreased ASBT expression in old age may be responsible for the reduced bile acid absorption in these mice. On this note, a 300-participant clinical study found that serum levels of bile acids decrease with age in men, but not women (85). Although the physiological implications of these findings were not directly investigated in either of these studies, it is reasonable to speculate that reduced intestinal bile acid absorption in older individuals may result in blunted bile acid signaling through FXR and other receptors. Future studies should focus on uncovering these functional consequences as well as the mechanisms underlying this age- and sex-related reduction in ASBT expression.

Besides age, ASBT expression also seems to be enhanced in postpartum rats. ASBT protein expression and transport function were increased in postpartum rats corresponding to an increase in food intake (179). Interestingly, ASBT mRNA expression was not affected, suggesting a

possible post-transcriptional mechanism. Although the mechanism underlying this phenomenon has not been elucidated, it is likely related to the increased energy demand during lactation (179). It is clear that the changes in ASBT expression that occur throughout the lifespan are physiologically important and warrant further study.

f. Disorders of bile acid absorption

Numerous diseases have elements of dysfunctional intestinal bile acid absorption. In some cases, disruption of intestinal BA absorption is the primary defect, while in other cases targeting BA absorption may be useful for treatment. Here, we will briefly discuss several of these disorders, including bile acid malabsorption (BAM), necrotizing enterocolitis (NEC), progressive familial cholestasis type 1 (PFIC1), type 2 diabetes mellitus (T2DM), and nonalcoholic fatty liver disease/nonalcoholic steatohepatitis (NAFLD/NASH).

i. Bile acid diarrhea (BAD)

Interruption of intestinal bile acid absorption results in bile acid accumulation in the colon, leading to watery diarrhea and bile acid loss in the stool. BAD is classified into three types depending on the underlying mechanisms of bile acid malabsorption (BAM) (35):

Type 1: Secondary to ileal resection, inflammation, or radiation

Type 2: Primary (idiopathic)

Type 3: Secondary to gastrointestinal diseases that affect absorption, such as small intestinal bacterial overgrowth or celiac disease

Type 1 BAD is bile acid malabsorption secondary to gross ileal dysfunction, such as in ileal resection, radiation enteritis, or inflammatory bowel disease (particularly Crohn's disease, as this frequently affects the distal ileum). BA malabsorption in these disorders may be caused by one or a combination of several factors. First, removal or destruction of absorptive cells in the distal ileum results in the loss of ASBT and prevents BA reabsorption. Furthermore, ileal dysfunction may cause impaired FGF19 production and disinhibition of BA synthesis, exacerbating the condition by enhancing bile acid load in the intestine (109). In addition, intestinal transit time decreases in patients with ileal resection (76), potentially leading to insufficient time to adequately absorb BAs.

In addition to impaired absorption as a result of resection or inflammation, some types of type 2 BAD are also associated with defects in intestinal bile acid absorption. As early as the 1970s, it was recognized in case reports that defective ileal bile acid absorption was a likely cause of some cases of congenital diarrhea (104, 105). After the discovery of ASBT, several inactivating mutations in this transporter were reported, including some of clinical relevance (191). Although some patients with inactivating ASBT mutations present with mild chronic diarrhea and no nutritional deficiency, many patients present in infancy with severe chronic diarrhea, steatorrhea, and fat-soluble vitamin malabsorption. Because of the large amount of bile acids lost in the stool, these patients have low FXR signaling in the gut. Thus, FGF19 production is reduced and bile acid synthesis is greatly increased, as indicated by elevated CYP7A1 expression and serum C4 (a marker of bile acid synthesis) in these patients (35, 199). Because of the compensatory overproduction of bile acids, plasma cholesterol levels remain low throughout their entire life. These patients respond well to bile acid sequestrants such as cholestyramine, which bind bile acids

in the colon and limit the severity of the diarrhea. This group of disorders highlights the importance of ASBT in maintaining sufficient intestinal bile acid absorption.

ii. Necrotizing enterocolitis

NEC is a common disease among premature infants that is characterized by severe hemorrhage and inflammatory necrosis in the distal ileum and proximal colon (98). It was noted that increased levels of hepatic pro-inflammatory cytokines were associated with exacerbated intestinal inflammation in a rat model of NEC (97). Given that the liver is the site for bile acid synthesis and the intestinal segment expressing ASBT (distal ileum) is the site predominantly affected by NEC, Halpern and colleagues postulated that disturbances in bile acid homeostasis may play a critical role in the development of NEC (98). Indeed, studies showed that luminal level of bile acids as well as the expression of ASBT were increased in an animal model of NEC and that sequestration of bile acids was protective against NEC development in this model (98). Further studies showed that ASBT deficient mice were protected against the development of NEC and that ASBT inhibitors significantly reduced the severity of the damage in a rat model of NEC (99). Since the proteins involved in key processes involved in bile acid homeostasis are not mature in newborns (20, 106, 121, 229, 241-243), the increase in ASBT leads to intracellular accumulation and toxic levels of bile acids in the ileal enterocytes, causing intestinal damage and contributing to the pathology of NEC. These studies also provide evidence for the therapeutic effects of ASBT inhibitors as potential intervention to treat NEC.

iii. Progressive familial cholestasis type 1

The obstruction of bile flow from the liver, known as cholestasis, leads to the accumulation of toxic biliary compounds, causing liver damage. The clinical features of cholestatic liver diseases are mainly jaundice and pruritus (237). Cholestasis can be categorized as either intra-hepatic and post-hepatic, depending on the location of the obstruction. Progressive familial intrahepatic cholestasis (PFIC) is a group of inherited disorders with clinical manifestations which often appear in late adolescence but may be recognized as early as infancy (237). Among these disorders, PFIC type 1 has been shown to occur due to mutations in the ATP8B1 gene, which encodes for P-type adenosine triphosphatase (FIC1 protein) that functions as aminophospholoipid flippase (82, 137). Mice harboring a homozygous, PFIC1-causing mutation exhibited an increase in intestinal bile acid absorption, suggesting that bile acid overload from the intestine may contribute to the associated cholestasis (200, 225). More extensive investigations showed that FIC1 loss-of-function leads to a decrease in FXR activity (41). Since FXR is a negative regulator of ASBT, this reduction in FXR activity causes an increase in ASBT expression. Using an siRNA-mediated approach, Chen et al showed that the knockout of ATP8B1 in intestinal epithelial Caco2 cells caused an increase in ASBT expression and promoter activity (41). They concluded that in the presence of loss-of-function mutations in ATP8B1, ASBT expression is increased. Recent studies, however, have challenged this conclusion. In this regard, van der Mark and colleagues showed that the loss of ATP8B1 in intestinal Caco2 cells did not alter ASBT expression but rather reduced its levels on the apical membrane (254). In contrast to the studies of Chen et al, these studies were performed using stable transfection of shRNA targeting FIC1, providing a more robust and chronic knockout. The decrease in ASBT surface expression implies a reduction in bile acid absorption that may explain the diarrhea associated with PFIC1. One important conclusion from these seemingly

contradictory results is that cellular ASBT expression and membrane localization is sensitive to the loss of ATP8B1 function and may contribute to pathophysiology of cholestasis or diarrhea associated with PFIC1. Further careful *in vivo* studies are warranted to examine these regulatory mechanisms and to determine the exact roles of ASBT in PFIC.

iv. Diabetes mellitus

In the United States, diabetes mellitus affects nearly 10% of the population, costing $245 billion and causing more than 250,000 deaths annually (38). While there are a large number of therapies available, the health burden of this disease warrants the investigation of novel therapeutics. In this regard, bile acid sequestrants (BASs) were first developed as LDL-cholesterol-lowering agents but have recently gained attention for their ability to improve hyperglycemia in T2DM patients. It has been shown that T2DM patients have slightly altered bile acid homeostasis compared to healthy individuals (1, 27, 33, 34, 158). While it is not clear whether changes in bile acid homeostasis are important for the pathogenesis of T2DM, it is clear that targeting BA pathways are useful for the treatment of this disease (238). The BAS colesevelam was FDA approved in 2008 for the treatment of diabetes, and in 2011 a meta-analysis confirmed that the use of colesevelam improved glycemic control in T2DM patients (101). However, the mechanisms of colesevelam's effects of glucose homeostasis are not yet fully understood. It may be dependent on alterations in intestinal FXR signaling, hepatic FXR signaling, GPBAR1 signaling, or a combination of these. It has been demonstrated that colesevelam and other BASs increase plasma levels of glucagon-like peptide 1 (GLP-1), an incretin hormone whose release is positively regulated by the GPBAR1 receptor (238, 247). This could be attributed to colonic GPBAR1 activation by bile acids, despite still being bound to BASs.

In a similar respect, inhibitors of ASBT have also gained interest for the treatment of T2DM (46, 252, 273). ASBT inhibition by luminally-restricted inhibitors has proved effective in lowering plasma glucose in preclinical models, likely via a mechanism similar to that seen with BASs (46, 273). In rodent models, plasma GLP-1 and insulin were increased, which correlated with improved glycemic control. A phase I trial showed modest benefits for T2DM even at relatively low dosage, suggesting that ASBT inhibitors may be of clinical benefit in this disease. In future studies it will be important not only to show clinical benefit, but also to delineate the mechanisms underlying the improved glycemic control when ileal bile acid absorption is inhibited.

v. Nonalcoholic fatty liver disease (NAFLD)

NAFLD is a disorder that is highly prevalent in individuals with obesity and T2DM and is thus of growing concern worldwide (202). In fact, more than 25% of the world's population and is affected by this disease. Our knowledge with respect to pathogenesis of NAFLD is constantly evolving, but it is thought to represent a progressive spectrum of liver disease beginning with simple steatosis. In a subset of this population (~10-15%), steatosis progresses to nonalcoholic steatohepatitis (NASH), which is characterized by inflammatory infiltration and can progress to liver fibrosis, cirrhosis, and hepatocellular carcinoma (26, 83, 279). As of this writing, there are no FDA approved agents for the treatment of NAFLD or NASH, though there are a number in phase II and III clinical trials.

Because bile acids are important modulators of lipid metabolism, glucose homeostasis, and energy expenditure, it is understandable that targeting bile acid pathways might be attractive for treating NALFD. Indeed, several experimental drugs for NAFLD and NASH target these pathways. The majority of BA-targeting drugs being explored for NAFLD/NASH are FXR

agonists, although there is some preclinical evidence that intestine-specific FXR antagonists may have some benefit in these disorders (91, 125). Other experimental medications target the GPBAR1 or a dual FXR/GPBAR1 agonists. These classes of drugs have been extensively reviewed elsewhere and are beyond the scope of this introduction (5, 16, 36, 51). However, we will briefly discuss the potential for inhibitors of bile acid absorption in the treatment of the NAFLD/NASH. Unlike diabetes, it appears that bile acid sequestrants may be of limited utility for NASH. Preclinical studies in rodent models have shown that colesevelam improves steatosis and hepatic inflammation (170). However, a small clinical study in NASH patients showed that colesevelam had little effect on relevant outcomes compared to placebo and may even increase hepatic steatosis (151). Finally, it should be noted that ASBT knockout mice were shown to be protected against development of diet-induced hepatic steatosis (204). Since the lack of ASBT is expected to reduce the activation of intestinal FXR, this observation is consistent with the notion that intestine-specific FXR antagonism is beneficial in treating NASH. Indeed, ASBT inhibitors may represent a promising therapeutic as they have been shown to be successful in a preclinical NASH model (204) and a phase I trial (252).

Given that modulation of ASBT may be useful for the treatment of several disorders, it is important to understand the cellular mechanisms responsible for ASBT regulation. In the following sections, the regulation of ASBT at transcriptional, post-transcriptional, and post-translational levels will be discussed.

g. Transcriptional regulation of ASBT

Transcription of ASBT mRNA is tightly regulated in order to maintain proper expression of this important transporter (**Table 1**) (64). The basal mRNA expression of ASBT is controlled

by several important transcription factors, most notably the hepatocyte nuclear factor 1α (HNF1α). Mice with deletion of the Tcf1 gene, which codes for HNF1α, completely lack ASBT expression in the ileum and kidney (226). The minimal ASBT promoter contains three HNF1α binding sites, and binding of HNF1α to the promoter has been shown to stimulate its activity as judged by electrophoretic mobility shift assays (EMSA) and luciferase reporter assays (132). Furthermore, intestinal deletion of the sirtuin 1 (SIRT1) metabolic sensor decreases HNF1α dimerization and function, with a concomitant reduction in ASBT mRNA expression (133).

The ASBT promoter also possesses two activated protein-1 (AP-1) response elements that are responsive to the c-Jun and c-Fos transcription factors (42). The upstream AP-1 site was shown to bind a c-Jun homodimer and the downstream site was shown to bind a c-Jun/c-Fos heterodimer (44). Promoter studies revealed that c-Jun activates the ASBT promoter, while c-Fos leads to repression of the promoter (186). In agreement with this model, c-Fos knockout mice display enhanced ileal ASBT expression (186). An unidentified component of human serum was also shown to stimulate ASBT mRNA expression in a manner dependent on the AP-1 response elements (69).

The expression of ASBT is thought to be regulated through a negative feedback mechanism whereby the presence of bile acids leads to a reduction in ASBT expression (Figure 3). This process occurs by several distinct mechanisms. The first mechanism appears to be an autocrine/paracrine mechanism that is initiated by FGF15/19, which is a major gene target of FXR (70, 89, 233). Much like the signaling pathway in hepatocytes, FGF15/19 binds to the FGFR4/β-klotho receptor complex. This leads to mitogen-activated protein kinase kinase 1/2 (MEK1/2) activation, c-Jun and c-Fos phosphorylation and translocation to the nucleus, which represses ASBT transcription. FXR-dependent feedback inhibition also involves three other transcription

factors: the liver receptor homologue-1 (LRH-1), the fetoprotein transcription factor (FTF), and the retinoic acid receptor/retinoid X receptor heterodimer (RAR/RXR). LRH-1 an important positive regulator of ASBT basal expression, as evidenced by the finding that LRH-1 knockout mice show reduced ASBT expression (152). Similarly, the LRH-1 orthologue FTF induces ASBT expression via direct binding to the ASBT promoter (156, 195). It appears that LRH-1 may be more important for ASBT expression in mice, while FTF may serve the same role in humans (195). Additionally, RAR/RXR contributes to ASBT basal expression through binding to retinoic acid response elements (187). These transcription factors appear to be responsible for a negative feedback regulation of ASBT whereby intracellular bile acids in the epithelium reduce ASBT expression. This important regulatory mechanism involves activation of FXR by cytosolic bile acids, which induces expression of the small heterodimer partner (SHP), an inhibitory factor. SHP impairs the activity of LRH-1 and FTF, reducing ASBT transcription (43, 156, 195). Similarly, SHP impairs RAR/RXR activity, also leading to a decrease in ASBT mRNA expression (187).

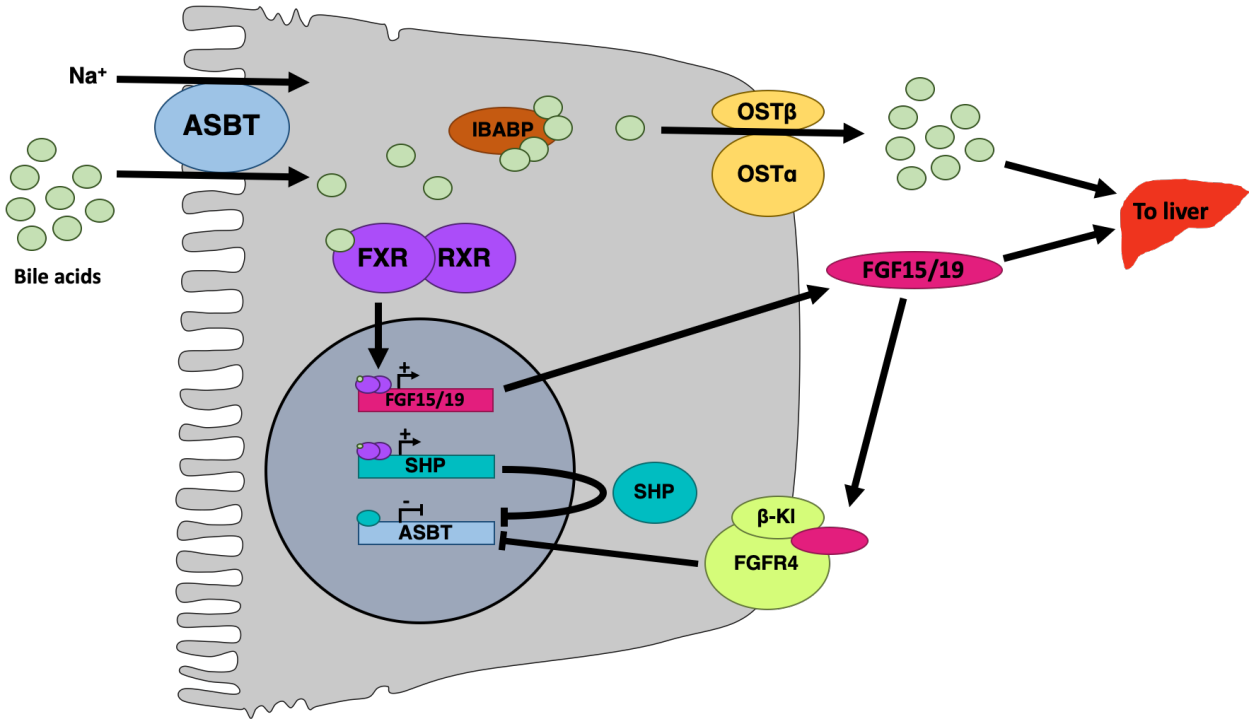

Figure 3. Mechanisms of intestinal bile acid absorption and transcriptional regulation of ASBT by bile acids. Bile acids are taken up from the intestinal lumen by ASBT, sequestered and transported intracellularly by IBABP, and exported to the portal circulation by OSTα/β. Intracellular bile acids bind FXR, which heterodimerizes with RXR and translocates to the nucleus. FXR transactivates FGF15/19 and SHP. FGF15/19 is secreted basolaterally, where it binds FGFR4/β-klotho in an autocrine/paracrine manner, activating a signaling pathway that represses ASBT transcription. SHP also negatively regulates ASBT transcription by inhibiting transcription factors that transactivate ASBT.

In addition to bile acids, ASBT transcription is affected by other steroid-like molecules, including cholesterol, glucocorticoids, and vitamin D. It has been shown that cholesterol downregulates ASBT expression and function in several model systems. In intestinal epithelial Caco2 cells and mouse models, cholesterol or 25-hydroxycholesterol administration led to a reduction in ASBT mRNA via a mechanism dependent on HNF1α and the sterol regulatory binding element protein 2 (SREBP2) and independent of FXR (8, 172, 250). SREBP2, which translocates to the nucleus in low cholesterol conditions, was shown to transactivate ASBT (250). In agreement with these data, administration of the cholesterol synthesis inhibitor atorvastatin in mice led to an increase in ileal ASBT mRNA expression (261). The glucocorticoid receptor (GR) has also been shown to bind and activate the ASBT promoter. *In vitro* promoter studies, *in vivo* studies in mice and rats, and clinical work showed that glucocorticoids induce ASBT transcription through GR-binding to glucocorticoid response elements in the ASBT promoter, increasing intestinal bile acid absorption (59, 131, 190, 192, 275). Similarly, the activation of the vitamin D receptor (VDR) was shown to transactivate ASBT (47, 56, 57).

In addition to regulation by endogenous and exogenous steroids and sterols, ASBT transcription is affected by pathological processes such as inflammation. Inflammatory processes have been shown to cause a significant reduction in ASBT expression, in part through a transcriptional mechanism. In rats with indomethacin-induced ileitis and in human Crohn's disease patients, ASBT mRNA expression has been shown to be reduced. Further studies showed that the proinflammatory cytokines interleukin-1β (IL-1β) and tumor necrosis factor (TNF) increase phosphorylation and nuclear translocation of c-Fos, leading to repression of the ASBT promoter (44, 186).

There are several other transcription factors that have been shown to regulate ASBT, though these are less well-studied than those discussed above. Positive regulators include the peroxisome proliferator-activated receptor α (PPARα) (132), the nuclear factor-E2-related factor 2 (NRF2) (264), caudal-type homeobox proteins CDX1 and CDX2 (166), and the constitutive androstane receptor (CAR) (49). Additionally, the GATA4 transcription factor was found to be a negative regulator of ASBT expression, as GATA4 knockout resulted in increased ASBT mRNA expression (28). Interestingly, it has been shown that intestinal bacteria reduce ASBT expression partially via a mechanism dependent on GATA4 (193). It has also been shown that insulin is a negative regulator of the ASBT promoter, although the molecular mechanisms are not fully understood (12). These transcriptional regulators of ASBT are crucial for maintaining proper ASBT expression and bile acid homeostasis.

Transcription factor	ASBT Transcription	References
HNF1α	↑	(132, 133, 226)
c-Jun	↑	(42, 186)
c-Fos	↓	(42, 186)
FXR	↓ (indirect)	(70, 89, 233)
LRH-1	↑	(152)
FTF	↑	(156, 195)
RAR/RXR	↑	(187)
SHP	↓	(43, 156, 187, 195)
SREBP2	↑	(8, 172, 250)
GR	↑	(59, 131, 190, 192, 275)
VDR	↑	(47, 56, 57)
PPARα	↑	(132)
NRF2	↑	(264)
CDX1, CDX2	↑	(166)
CAR	↑	(49)
GATA4	↓	(28, 193)

Table 1. Transcriptional regulators of ASBT.

h. Post-transcriptional regulation of ASBT

Although much is known about the transcriptional regulation of ASBT, relatively little research has investigated its post-transcriptional regulation. Of the few studies that have been performed in this area, most has related to the role of the 3'-untranslated region (UTR) of ASBT mRNA. The Shneider laboratory showed that a metastasis-associated gene 1 (MTA1) element within the 3'-UTR interacts with the RNA binding proteins Hu antigen R (HuR) and tristetraprolin (45, 234). They showed that HuR stabilized reporter mRNA, while tristetraprolin decreased reporter mRNA half-life. Interestingly, the overall effect of the 3'-UTR appeared to destabilize mRNA in two intestinal epithelial cell lines, which may be important for the rapid regulation of ASBT. This important post-transcriptional regulation appears to be critical in the ontogenesis of ASBT expression, as discussed earlier in the section titled "ASBT ontogeny and aging."

i. Post-translational regulation of ASBT

ASBT has been shown to be subject to rapid, post-translational modifications. It is possible that these acute regulatory mechanisms represent adaptive responses to a rapidly changing intestinal milieu. ASBT protein stability, subcellular localization, and activity have all been shown to be modulated by PTMs such as ubiquitination, glycosylation, and phosphorylation, as well as by interactions with lipids and plasma membrane microdomains.

One of the key post-translational mechanisms by which ASBT is regulated is through modulation of protein stability and degradation. It has been shown that ASBT is degraded by the ubiquitin-proteasome pathway in both cholangiocytes and ileocytes (174, 274). Interestingly, ASBT turnover is fairly rapid, as the protein has a relatively short half-life of ~6 h (184, 274). Several mechanisms have been shown to modulate the rate of ASBT proteasomal degradation. For

instance, the proinflammatory cytokine IL-1β enhances ASBT ubiquitination and degradation via a mechanism that involves c-Jun N-terminal kinase (JNK)-dependent phosphorylation of ASBT at Ser335 and Thr339 (274). Furthermore, feeding with CA, but not conjugated TC or TDC, decreased ASBT protein expression via a ubiquitin-dependent mechanism (174). Similarly, the SIRT1 activator resveratrol was shown to promote ASBT ubiquitination and proteasomal degradation, independent of Ser335/Thr339 phosphorylation (55).

ASBT is also subject to N-glycosylation at its extracellular N-terminal domain (184, 245). This glycosylation was shown to enhance ASBT protein stability, as inhibition of N-glycosylation by tunicamycin or mutation of the Asn10 glycosylation site resulted in shorter protein half-life (184). It has been found that ASBT protein expression is higher in rats with streptozotocin-induced diabetes (12). This may be partially the result of enhanced glycosylation, as *in vitro* glucose treatment promoted mature glycosylation and increased protein stability.

Phosphorylation of ASBT has also been shown to rapidly modulate ASBT function. As discussed above, Ser335/Thr339 phosphorylation was shown to promote ASBT degradation (274). In addition, activation of the protein kinase C ζ (PKCζ) pathway significantly inhibits [^{3}H]-TC uptake within 60 min of treatment with the PKC activator phorbol 12-myristate 13-acetate (PMA) (222). These studies demonstrated that treatment with PMA led to internalization of ASBT and decreased surface expression. Conversely, tyrosine phosphorylation of ASBT was shown to enhance transporter activity, although the kinase and phosphorylation site have yet to be determined (13). Interestingly, enteropathogenic E. coli (EPEC) was shown to rapidly reduce ASBT function via an effector molecule that led to tyrosine dephosphorylation and internalization of ASBT (13). Future studies should focus on further clarifying the role of phosphorylation in the regulation of ASBT function. With respect to the modulation of ASBT by enteric bacteria, an

additional report showed that reducing Enterobacteria in the gut by treatment with ampicillin resulted in a significant increase in ASBT protein levels concomitant with an increase in the levels of bile acids in the portal blood (173). The increase in ASBT was not associated with changes in the mRNA. Since the increase occurred in response to eliminating the bacteria by antibiotics, the authors concluded that Enterobacteria suppresses ASBT expression via post-transcriptional mechanisms. The studies with enteropathogenic EPEC and Enterobacteria provide strong evidence showing that ASBT protein expression and its level on the plasma membrane is sensitive to the enteric bacteria. Further investigations are warranted to determine the significance of these findings in the relation to the development of infections and to further understand the interactions between gut microbiota and intestinal absorption of bile acids.

Another critical post-translational regulatory mechanism involves the association of ASBT with plasma membrane lipid raft microdomains. Studies have demonstrated that ASBT is associated with lipid rafts, and disruption of this association reduces ASBT function (11, 14). For instance, depletion of plasma membrane cholesterol by methyl-β-cyclodextrin led to a shift of ASBT to non-raft domains of plasma membrane and was associated with reduced ASBT function without a change in its surface expression (14). Similarly, the green tea catechin (-)-epigallocatechin-3-gallate (EGCG) rapidly reduces ASBT function and is associated with a shift in ASBT into the non-raft domain of plasma membrane (11). However, the molecular mechanisms underlying ASBT association with lipid rafts have not yet been investigated.

Through these studies, it has become clear that ASBT undergoes extensive post-translational regulation that profoundly affects its function. As described above, ASBT is subject to serine and tyrosine phosphorylation, as well as glycosylation at asparagine residues (Figure 4). There is still a great deal of research that will be required in order to better understand the

molecular basis of ASBT regulation by these important post-translational modifications. As conventional methods for measuring transporter activity do not fully capture the rapid regulation of ASBT, development of real-time methods to measure transporter function is of critical importance. In addition to the PTMs described earlier, it is likely that additional modifications involving other amino acid residues, such as cysteines, may also be involved in regulating ASBT. In this regard, recent evidence has clearly demonstrated the importance of cysteine residues in ASBT function. Human and mouse ASBT have 13 cysteine residues (Figure 4), many of which have been shown necessary for full activity of the transporter, though their role in maintaining ASBT function has yet to be fully investigated (22, 54). Studies have shown that cysteine residues can be subject to covalent modification by fatty acid residues via a process known as S-acylation (39). Thus, it is possible that ASBT cysteine residues are subject to S-acylation, which may serve an important regulatory role.

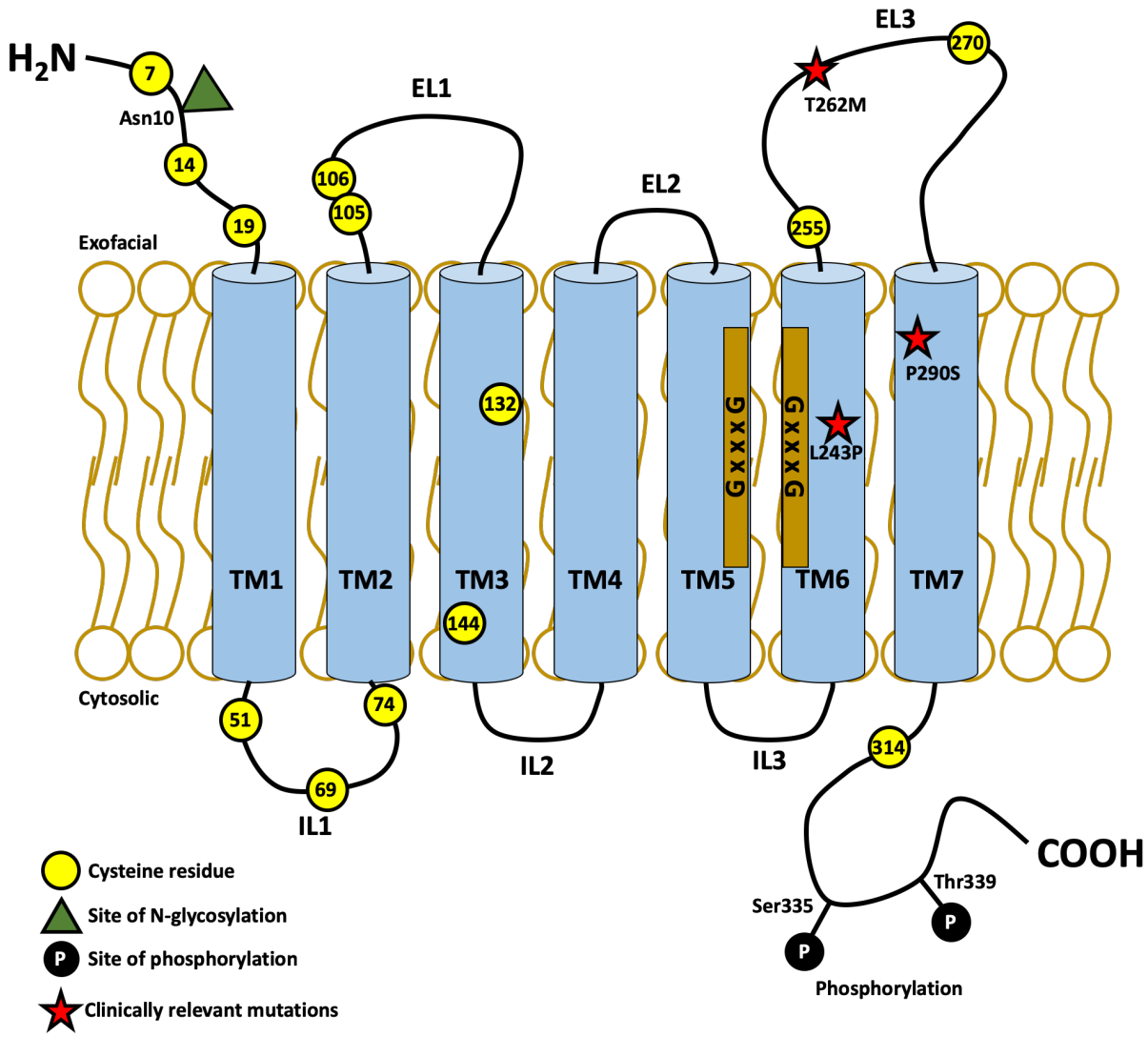

Figure 4. Topology of ASBT. A cartoon of the 7 transmembrane domain ASBT topology. Sites of post-translational modifications (glycosylation and phosphorylation) are shown, along with cysteine residues and sites of clinically relevant missense mutations.

F. Protein lipidation and S-acylation

Recently, protein lipidation has gained increasing attention as an important post-translational regulator of many transport proteins. Protein lipidation refers to a class of PTMs that mediates protein-membrane and protein-protein interactions, protein stability, as well as protein function. There are many different types of protein lipidation, as a variety of lipid molecules can be attached to different amino acid residues. Some of these modifications are stable and irreversible, whereas other are dynamic and rapidly reversible. The most common stable lipid modifications are N-terminal glycine myristoylation and cysteine prenylation. These lipids are bound to proteins via stable amide and thioether bonds, respectively.

In contrast to these stable lipid modifications, cysteine fatty acylation (S-acylation, also referred to as palmitoylation) is a reversible, covalent attachment of long-chain fatty acids to cysteine residues via a thioester linkage. S-acylation is a ubiquitous post-translational modification in eukaryotes (39, 126). A number of proteomic profiling studies have been undertaken in order to identify and characterize the cellular pool of S-acylated proteins. These studies have revealed a wide variety of transmembrane and peripheral membrane proteins that are subject to S-acylation (24, 39, 221, 280).

The primary effect of S-acylation in these proteins is to regulate the subcellular localization of proteins. For peripheral membrane proteins, S-acylation promotes stable attachment to the membrane. S-acylation of these proteins provides a long-chain lipid anchor that inserts into membranes, allowing for efficient membrane targeting. Often, these peripheral membrane proteins are subject to other forms of lipidation, including myristoylation and prenylation, in order to further promote membrane targeting. In contrast, S-acylation of transmembrane proteins has been shown to be important for plasma membrane targeting, as well as the association of plasma

membrane proteins with lipid raft microdomains. Indeed, it has been demonstrated that the majority of lipid raft-associated transmembrane proteins rely on S-acylation for their targeting to raft microdomains (155, 164). By modulating the subcellular localization of proteins, S-acylation regulates protein trafficking, stability, and interaction with other signaling pathways (39). It is crucial to recognize that S-acylation is a highly dynamic process. Indeed, the fatty acid turnover may be quite rapid, even on the order of minutes, depending on the protein (167, 211, 212). In the next section, we will briefly discuss the enzymes that mediate S-acylation and deacylation.

1. S-acyltransferases

The enzymes responsible for S-acylation of proteins belong to the zDHHC gene family. These proteins are named for their highly conserved zinc-finger aspartic acid-histidine-histidine-cysteine (zDHHC) motif. The first mammalian zDHHC enzyme with cysteine-palmitoylation activity was identified in 2004 (134). Twenty four zDHHC genes were soon identified in humans, many of which have been shown to have cysteine palmitoyl acyltransferase activity (154). All of these enzymes are polytopic transmembrane proteins with a cytosolic catalytic domain. While it is generally accepted that zDHHC proteins possess S-acyltransferase activity, relatively little is known with regards to how these enzymes identify their target proteins. Unlike many other enzymes, including those responsible for other protein lipid modifications, there are few known target consensus sequences for zDHHC enzymes (153). This has made prediction of protein S-acylation quite challenging, requiring experimental approaches in order to determine whether a protein is subject to S-acylation and which cysteine residues are involved. It is also important to note that while palmitic acid is the primary substrate for zDHHC enzymes, many of these proteins have a wide substrate specificity that includes many long chain fatty acids. Indeed, it has been

shown that the profile of fatty acids bound to proteins is dependent on the profile of fatty acids available to S-acyltransferases (130). This includes unsaturated and polyunsaturated fatty acids, which may confer different functional consequences to proteins compared with saturated palmitic acid.

2. S-acylthioesterases

Even less information is known about the enzymes responsible for deacylation of S-acylated proteins (39). The protein palmitoyl thioesterases family (PPT1 and PPT2) are localized in lysosomes and are likely responsible for deacylation during protein degradation. In contrast, cytosolic acyl protein thioesterases (APT1, APT2, and APT1-like) appear to be involved in the dynamic turnover and regulation of S-acylation. In addition, it is possible that there are other proteins with S-acylthioesterase activity that have yet to be identified.

3. S-acylation of transport proteins

S-acylation has been shown to regulate the function of a wide variety of cellular proteins, including ion and solute transporters (39, 126). Among these transport proteins, S-acylation has been shown to control plasma membrane trafficking, transport capacity, protein stability, and phosphorylation status, as well as other effects. For instance, S-acylation of the β and ɣ subunits of the epithelial sodium channel (ENaC) was shown to modulate channel gating by increasing the open probability and reducing self-inhibition of the channel (180, 181). In addition to regulation of ENaC, it was recently shown that S-acylation of the cystic fibrosis transmembrane conductance regulator (CFTR) is crucial for its trafficking from the Golgi apparatus to the plasma membrane

(168, 169). Additionally, S-acylation of the dopamine transporter (DAT; SLC6A3) was shown to regulate its phosphorylation status, transport kinetics, and stability (80, 178).

It is crucial to mention that the S-acylation of transport proteins is also implicated in the development of diseases. For instance, it has been shown that the fatty acid transporter CD36 is subject to S-acylation, which is important for its ER and Golgi processing, as well as its targeting to lipid rafts (251). Importantly, Zhao et al recently demonstrated that hepatic CD36 is hyperpalmitoylated in nonalcoholic steatohepatitis (NASH) patients, resulting in increased plasma membrane CD36 expression (283). This study also showed that blocking CD36 S-acylation in a mouse model protected against NASH development, implicating CD36 S-acylation in the pathogenesis of this disease.

It is clear from these previous studies that S-acylation is an important post-translational modification that controls the activity of numerous transport proteins. Whether ASBT is also subject to S-acylation and how this PTM regulates its function remains elusive.

G. Hypothesis and specific aims

The apical sodium-dependent bile acid transporter is rapidly regulated by a variety of post-translational mechanisms. Importantly, conventional methods to assess the function of ASBT are not sufficient to study dynamic, post-translational changes in its transport activity. These methods require cells to first be treated and then incubated with radiolabeled bile acids, washed to remove excess bile acids, lysed, and assessed by scintillation spectrometry. As this process allows for measurement of the transport function only at the end of a treatment, rapid changes in BAT function may not be fully captured by this technique, likely leading to loss of valuable information. While several real-time methods have been developed to study bile acid homeostasis, these

techniques have been unable to accurately capture ASBT function directly. **We hypothesized that a bioluminescence-based, real-time approach would allow for precise evaluation of ASBT activity.** Additionally, it had been demonstrated that cysteine residues are critical for the function of this transporter. However, the molecular basis underlying the importance of ASBT cysteine residues has not been fully investigated. Cysteine residues are known to be subject to S-acylation, which is an important PTM involved in the regulation of several transport proteins. Therefore, **we hypothesized that ASBT cysteine residues are subject to S-acylation and that this PTM is crucial for its transport function.** In order to investigate the hypotheses, the following specific aims were systematically investigated:

- **Aim 1: Establish a novel method to measure the function of bile acid transporters in real time (chapter II)**

  1a. Synthesize a luciferin-conjugated bile acid probe (CA-SS-Luc)

  1b. Examine ASBT activity in real time by CA-SS-Luc utilizing *in vitro* and *ex vivo* models

- **Aim 2: Investigate S-acylation of ASBT (chapter III)**

  2a. Examine the effect of S-acylation on ASBT function and expression

  2b. Investigate the role of different fatty acids in modulating ASBT activity

  2c. Delineate the cysteine residue(s) responsible for ASBT S-acylation

Chapter II: A novel bioluminescence-based method to investigate uptake of bile acids in living cells

The work in this chapter was modified from:

Ticho AL, Lee H, Gill RK, Dudeja PK, Saksena S, Lee D, Alrefai WA. A novel bioluminescence-based method to investigate uptake of bile acids in living cells. *Am J Physiol Gastrointest Liver Physiol* 315: G529–G537, 2018.

A. Rationale and aim

ASBT activity is subject to rapid post-translational modulation by protein tyrosine phosphatase (13), protein kinase C signaling pathways (222, 240), and changes in plasma membrane lipid rafts (14, 175). Therefore, it is essential to capture the rapid changes in ASBT and NTCP function in order to fully understand their acute regulation by cellular signaling pathways. The conventional methodology to assess the transport function of ASBT and other bile acid transporters (BATs) mainly relies on measuring the uptake of radiolabeled bile acids. Using this method to study the effect of a given treatment requires cells to first be treated and then incubated with radiolabeled bile acids, washed to remove excess bile acids, lysed, and assessed by scintillation spectrometry. As this process allows for measurement of the transport function only at the end of a treatment, rapid changes in ASBT function may not be fully captured by this technique. The delay between treatment and radioactive uptake also makes these studies impractical for measuring rapid post-translational regulation of ASBT *in vivo*. Thus, development of a real-time method for assessment of ASBT function in living systems is necessary in order to sufficiently study dynamic changes in activity.

Although several attempts have been made to monitor bile acids in real time (66, 255), none have been designed to assess ASBT function directly. Recently, bioluminescence-based methods have been used to measure the real-time function of fatty acid transporters (103, 198). **Our objective was, therefore, to develop a bioluminescence-based method for measuring bile acid transport activity in real time to precisely evaluate the rapid changes in their function**. In this study, we describe a method that relies on a novel probe: cholic acid attached to luciferin via a disulfide-containing, self-immolating linker (CA-SS-Luc). The probe is designed such that upon entry into cells expressing luciferase, the linker is cleaved to release free luciferin, generating

light that can be measured by a sensitive *in vivo* imaging system (IVIS). This quantitative approach allows for sensitive measurement of ASBT function *in vitro* and further development will confirm its *in vivo* utility.

B. Materials and methods

1. Cell culture and materials

The human embryonic kidney fibroblast cell line (HEK 293) was obtained from ATCC (Manassas, VA) and grown in plastic flasks at 37 °C in an atmosphere consisting of 5% CO_2 and 95% air. The cells were cultured in Dulbecco's modified Eagles Medium containing 4 mM L-glutamine, 4.5 g/L glucose, 1 mM sodium pyruvate, and 1.5 g/L sodium bicarbonate, supplemented with 10% fetal bovine serum, 100 units/ml penicillin, and 100 mg/ml gentamicin (Invitrogen; Carlsbad, CA). HEK 293 cells stably transfected with human ASBT-V5 (2BT) were cultured in the same media containing 7 μg/mL puromycin. All chemicals were obtained from Sigma Aldrich (St Louis, MO) unless otherwise specified.

2. Plasmid construction

Human ASBT cDNA was previously generated in our laboratory (14), and human NTCP cDNA was purchased from Origene (Rockville, MD). These cDNAs were amplified by PCR using the primers: 5'-GATTACGCGGCCGCACCATGGCCAATGATCCGAACAGC-3' and 5'-GATTACCTCGAGCTTTTCGTCAGGTTGAAATC-3' for ASBT amplification and 5'-GATTACGCGGCCGCACCATGGCCGAGGCCCACAACG-3' and 5'-GATTACCTCGAGGGCTGTGCAAGGGGAG-3' for NTCP amplification. PCR products were digested using NotI and XhoI restriction enzymes (New England Biolabs; Ipswich, MA) and

ligated into the vector pSF-CMV-Puro-COOH-TEV-V5 (Oxford Genetics; Cambridge, MA) using T4 DNA Ligase (New England Biolabs; Ipswich, MA).

3. In vitro measurement of CA-SS-Luc bioluminescence

Transfections were performed using Lipofectamine 2000 (Invitrogen) following the manufacturer's instructions. 2BT cells, which stably express ASBT-V5, were transfected with 1 μg/well pmirGLO (Promega; Madison, WI), for the expression of luciferase, and plated on 24-well TC-treated black plastic plates with glass bottoms (Perkin Elmer; Waltham, MA) at a density of 2 x 10^5 cells/well. Wild type HEK 293 cells were co-transfected with 500 ng/well pmirGLO and 1) 750 ng/well ASBT-V5 or NTCP-V5; 2) 250 ng/well ASBT-V5 or NTCP-V5 and 500 ng/well serotonin transporter (SERT-V5); or 3) 750 ng/well SERT-V5. Media was changed the next day and experiments were performed on the second day following transfection. Cells were washed twice at 25 °C with uptake buffer containing (in mM) 110 NaCl (with sodium) or choline chloride (without sodium), 4 KCl, 1 MgSO4, 1 CaCl2, 45 mannitol, 5 glucose, and 10 HEPES (pH 7.4). Cells were then incubated with the same buffer containing CA-SS-Luc (1 μM unless otherwise specified) and immediately placed into a Xenogen IVIS Spectrum *in vivo* imaging system (Caliper Life Sciences; Waltham, MA). Bioluminescence production was measured using the IVIS camera set to obtain images with 1 min exposure times unless otherwise specified. The luminescence produced from each well was quantified using Living Image software (Perkin Elmer; Waltham, MA) and reported as photon counts per minute. Images were either taken directly from this software or further processed using ImageJ (NIH).

4. Western blot analysis

Cells were lysed in cell lysis buffer (Cell Signaling Technology; Danvers, MA) supplemented with protease inhibitor cocktail (Roche; Basel, Switzerland) and 1% SDS. Protein samples were prepared in Laemmli buffer (BioRad; Des Plaines, IL) containing 2.5% 2-mercaptoethanol, subjected to SDS-PAGE on 10% polyacrylamide gel, transferred to nitrocellulose membranes, and probed with anti-V5-HRP antibodies (Invitrogen; Carlsbad, CA) or anti-mouse ASBT antibodies (a generous gift from Dr. Paul Dawson, Emory University).

5. Treatment with PTPIII

2BT cells were transfected with pmirGLO and plated as described previously. On the day of the experiment, cells were treated with protein tyrosine phosphatase inhibitor III (PTPIII; 500 μM; Sigma Aldrich) or DMSO for 60 min prior to imaging. Bioluminescence was measured as described earlier.

6. Isolation of primary intestinal epithelial cells

Transgenic mice expressing luciferase (Luc^{Tg}; FVB-Tg(CAG-luc,-GFP)L2G85Chco/J0) were obtained from Jackson Laboratory (Bar Harbor, ME) and housed in the animal facility at the Jesse Brown VA Medical Center according to approved VA and UIC IACUC protocols. At age 10-16 weeks, male and female mice were sacrificed and epithelial cells from the jejunum and ileum were isolated as previously described (12). Briefly, the small intestine was removed and flushed and the proximal (jejunum) and distal (ileum) 5 cm were cut into small pieces and washed with ice-cold PBS. The intestines from five animals were pooled for each experiment. Intestinal pieces were then washed in Ringer's solution without calcium or magnesium and supplemented with 2%

BSA and 2% glucose. Tissues were then incubated with shaking at 37 °C in Ringer's solution supplemented with 0.5 mM DTT and 1.5 mM EDTA for 15 min. Cells were collected with centrifugation at 500 *g* for 5 min and resuspended in uptake buffer containing 1 μM CA-SS-Luc and imaged by IVIS with 5 min camera exposure.

7. Statistical analysis

Results were expressed as mean ± SEM of three to four experiments performed on multiple occasions unless otherwise specified. Student's *t*-test or two-way ANOVA were used for statistical analysis. $P \leq 0.05$ was considered statistically significant.

C. Results

To develop a method for the assessment of bile acid transporter activity in real time, we have designed a reporter system relying on a novel bioluminescent probe: CA-SS-Luc. Upon entry into the cells, a two-step process initiated by intracellular glutathione results in the release of free luciferin, which will be catalyzed by luciferase expressed in the cells to generate light, as shown in Figure 5.

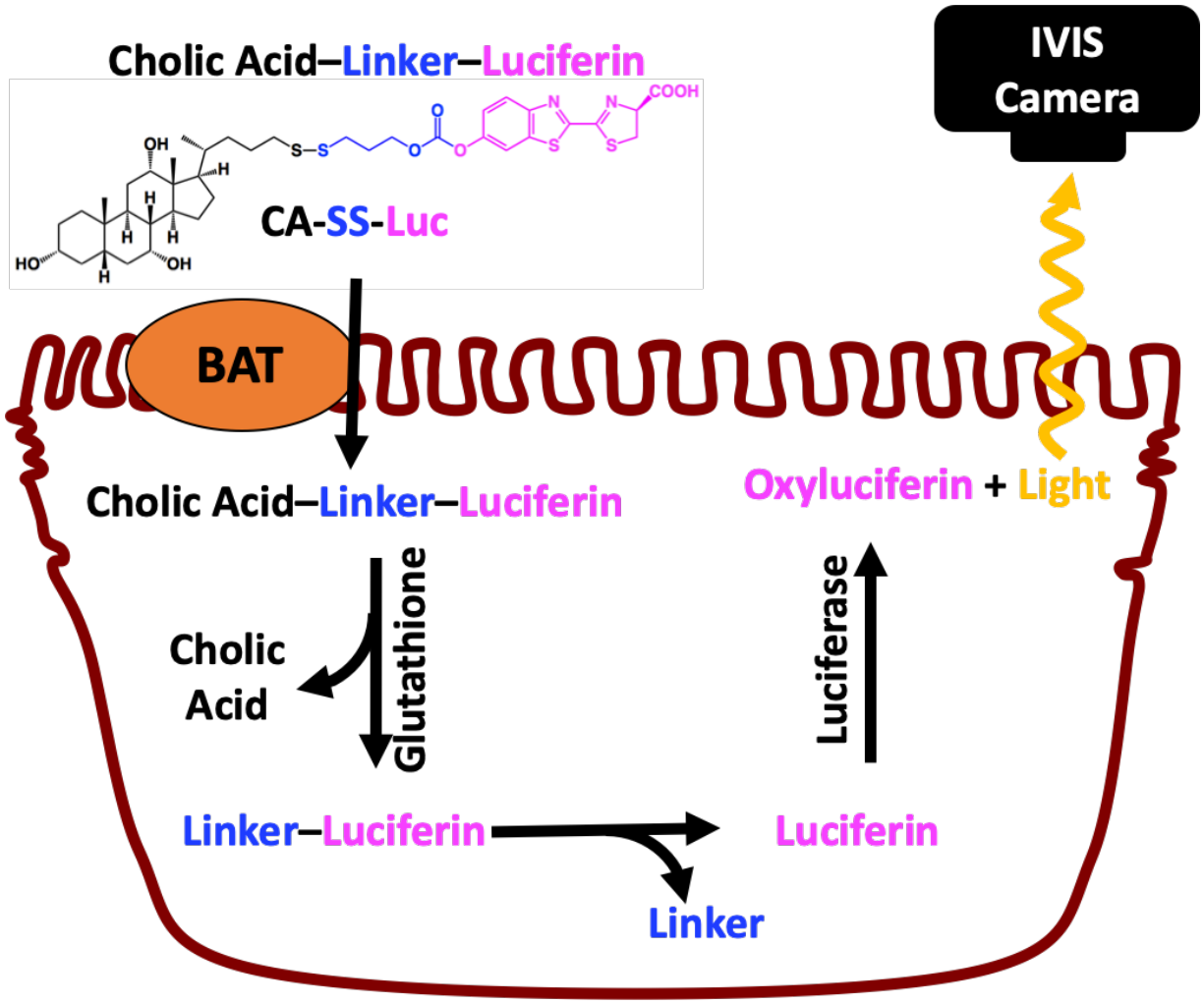

Figure 5. Schematic of luminescence production by CA-SS-Luc. CA-SS-Luc enters cells via a bile acid transporter. Intracellular glutathione cleaves the disulfide linker which self-immolates, yielding free luciferin. Luciferase oxidizes luciferin, producing light that is measured by an *in vivo* imaging system.

1. Synthesis of CA-SS-Luc

The abbreviated synthetic route for the disulfide-based probe CA-SS-Luc **7** is shown in **Figure 6**. The synthesis began with protection of three hydroxyl groups of cholic acid **1** with tert-butyldimethylsilyl (TBS) groups to generate compound **2**. Compound **2** was subjected to reduction of the carboxylic acid moiety, iodination, substitution with KSCN, and reduction of the thiocyanide moiety to generate the thiol compound **3**. Sulfide exchange of **3** with compound **4** proceeded smoothly to generate **5**. Removal of TBS groups followed by treatment of **6** with D-cysteine provided CA-SS-Luc **7**.

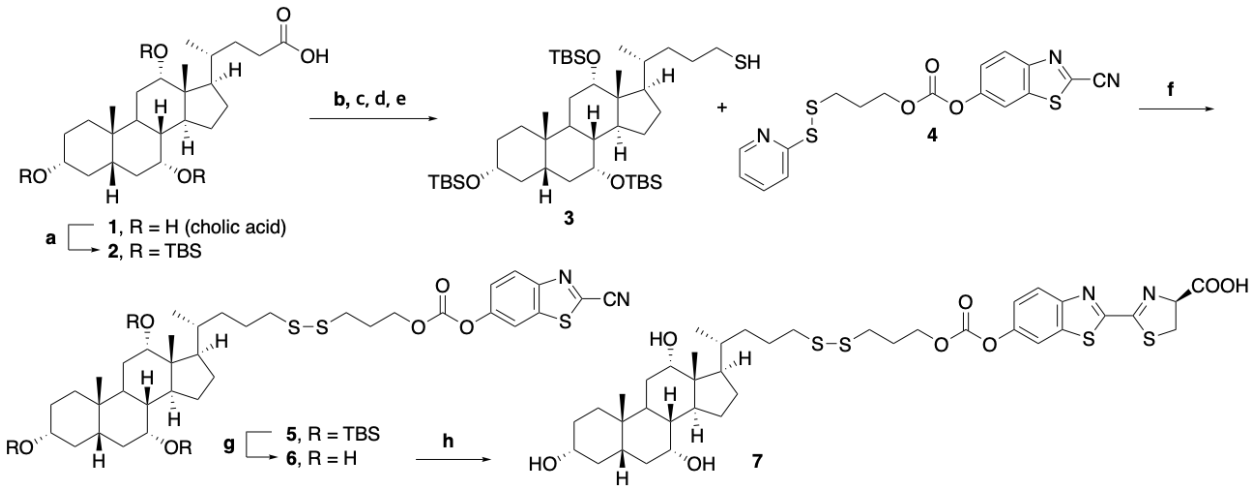

Figure 6. Synthesis of CA-SS-Luc. (a) TBSCl, imidazole, DMF, reflux 10 h. (b) $LiAlH_4$, Et_2O, 0 °C to rt, 3 h. (c) I_2, PPh_3, pyridine, CH_2Cl_2, 0 °C to rt, 1 h. (d) KSCN, acetone, rt, overnight. (e) $LiAlH_4$, Et_2O, 0 °C to rt, 5 h. (f) Et_3N, DMF, rt, 2 h. (g) *p*-TsOH, MeOH, rt, overnight. (h) D-cysteine, K_2CO_3, DCM, MeOH, H_2O, rt, 5 min. DMF = Dimethylformamide; DCM = Dichloromethane; TBSCl = *tert*-Butyldimethylsilylchloride; *p*-TsOH = *p*-Toluenesulfonic acid.

2. Transporter-dependence of CA-SS-Luc uptake

We examined the hypothesis that the putative CA-SS-Luc probe will be transported into cells specifically via a bile acid transporter, producing bioluminescence that is proportional to the amount of probe entering the cells over a given period of time. We first tested the hypothesis in HEK 293 cells stably transfected with the ileal ASBT fused to a C-terminal V5 tag (2BT cells) and transiently transfected with luciferase. 48 hours post-transfection with luciferase, these cells were incubated with different concentrations of CA-SS-Luc probe and then continuously imaged by IVIS for 45 minutes. As shown in **Figure 7**, the detected bioluminescence was found to be proportional to the concentration of CA-SS-Luc. Furthermore, the luminescent signal was time-dependent and reached equilibrium after ~20 minutes of incubation, indicating that the signal likely represents a transport activity. Since a robust signal intensity was generated by 1 μM of CA-SS-Luc, all subsequent experiments were performed using this concentration of probe.

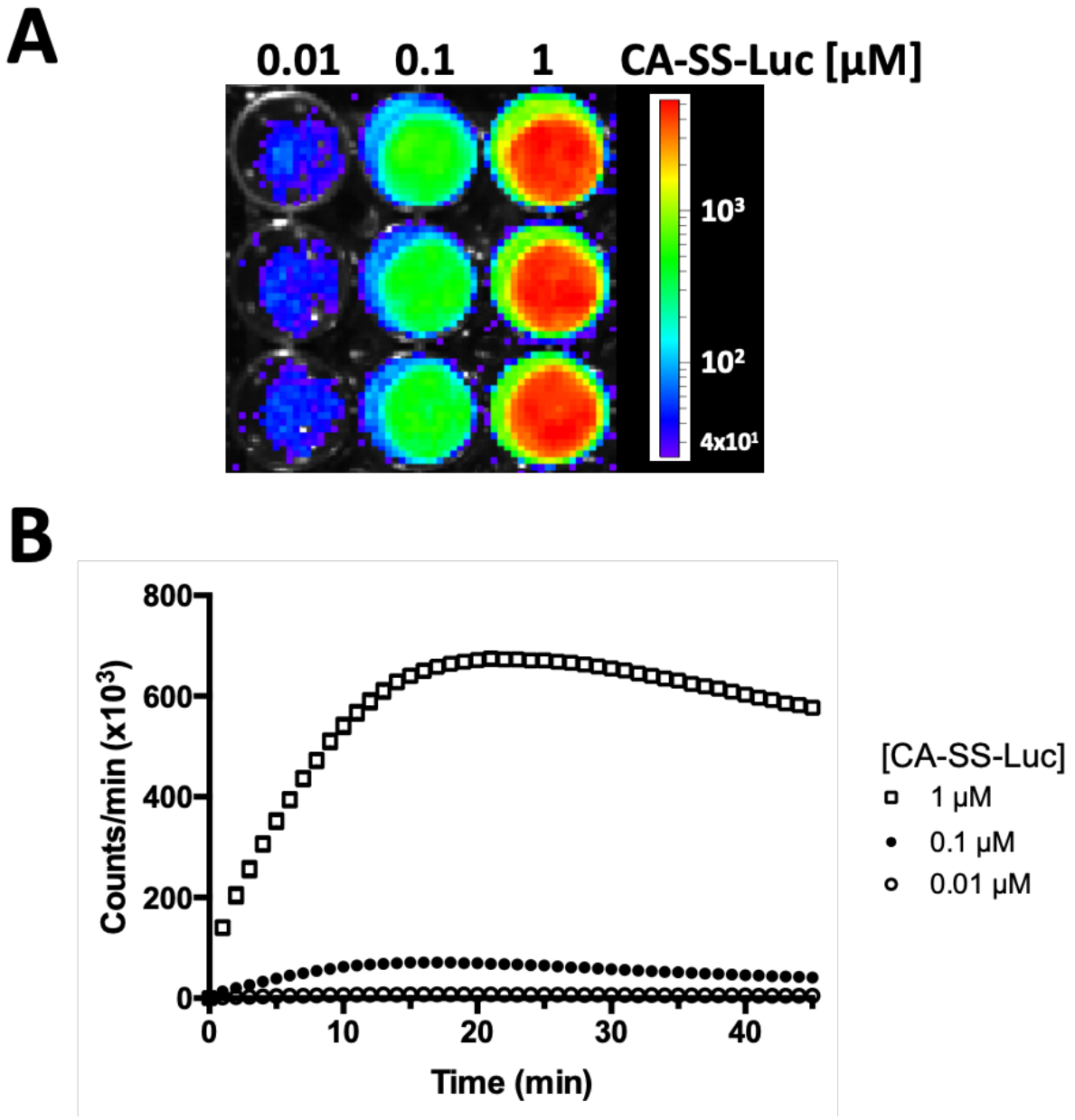

Figure 7. The bioluminescence generated by CA-SS-Luc in 2BT cells is concentration- and time-dependent. 2BT cells treated with increasing concentrations of CA-SS-Luc were imaged using IVIS. (A) a representative IVIS image following 20 min incubation. (B) Time course of luminescence production by 0.01 µM (open circles), 0.1 µM (closed circles), and 1µM (open squares) of CA-SS-Luc; n=3, Error bars representing SEM are displayed but are too small to be seen for most points. Two-way ANOVA: Time ($p < 0.0001$), Dose ($p < 0.0001$).

We next examined the dependence of the luminescence produced in the cells on cellular expression of ASBT. HEK 293 cells were transiently co-transfected with luciferase plasmid DNA (pmirGLO) and either 1) 750 ng/well of the serotonin transporter SERT-V5; 2) 250 ng/well ASBT-V5 and 500 ng/well SERT-V5; or 3) 750 ng/well ASBT-V5. Cells were imaged as above 48 hours post-transfection. As shown in **Figure 8A**, when compared to cells transfected with 750 ng/well SERT-V5, luminescence was dependent on the amount of transfected ASBT-V5. Cells transfected with 250 ng/well ASBT-V5 displayed greater luminescence than SERT-transfected cells, and this luminescence was further increased when 750 ng/well of ASBT-V5 was transfected. This corresponded to the cellular expression of ASBT-V5 as determined by western blotting (**Figure 8B**). Similar results were obtained when HEK 293 cells were transiently co-transfected with luciferase and the hepatic bile acid transporter NTCP. The bioluminescence was also significantly increased by higher levels of NTCP-V5 fusion protein in HEK 293 cells, and this luminescence was even greater than that seen in cells transfected with ASBT-V5 (**Figure 8C-D**). It is important to note that the serotonin transporter (SERT), which does not transport BAs, was used as a control plasmid in cells transfected with less than 750 ng/well of BAT. Thus, luminescence from SERT-transfected cells was minimal. To demonstrate that luminescence is the result of active uptake rather than extracellular cleavage of CA-SS-Luc followed by passive diffusion of D-luciferin, the luminescence of CA-SS-Luc was compared to that of D-luciferin. At a concentration of 1 μM, CA-SS-Luc produced several fold greater luminescence than D-luciferin for the duration of the experiment (**Figure 9**). These results suggest that extracellular hydrolysis of CA-SS-Luc is not responsible for the produced bioluminescence.

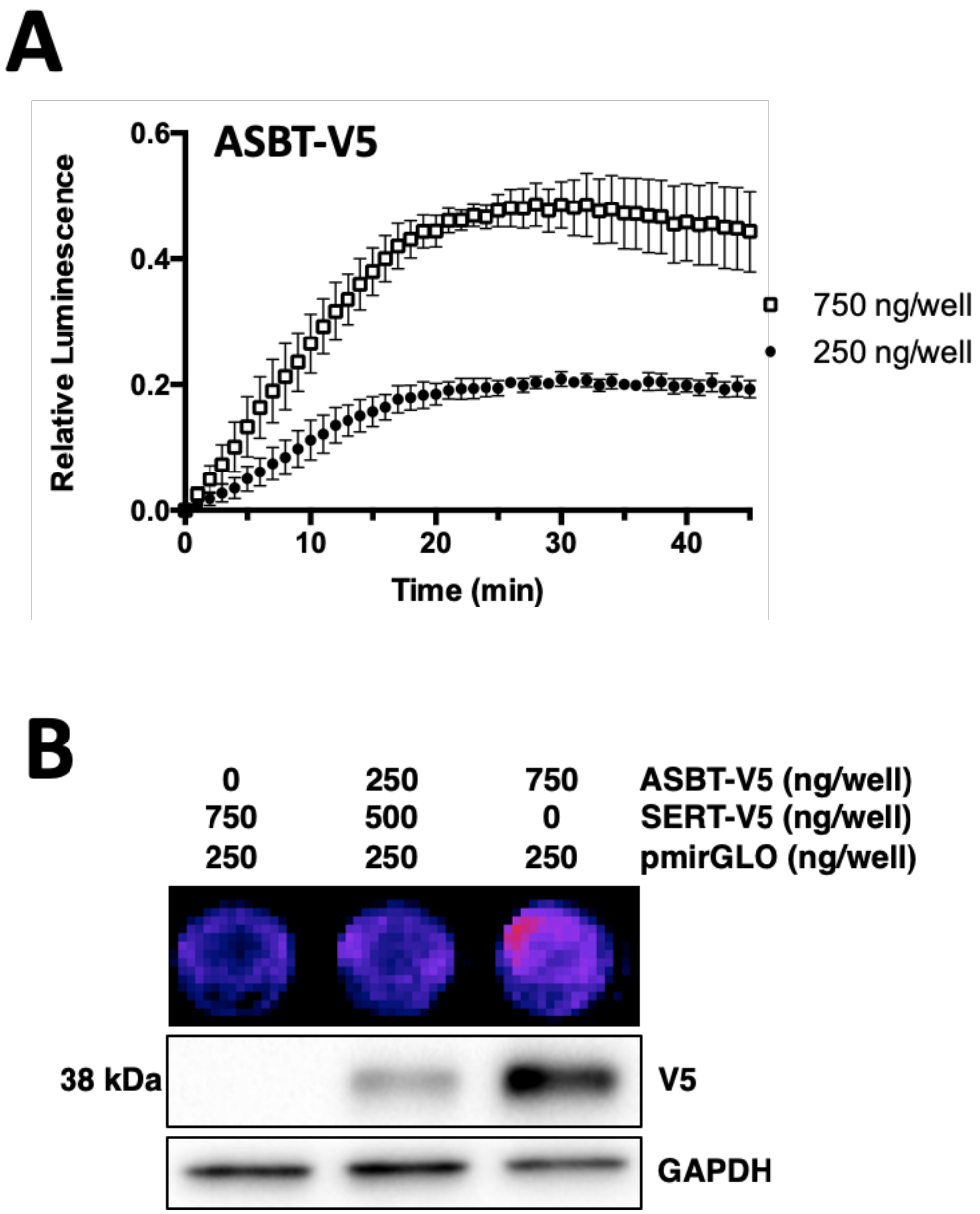
A
ASBT-V5
Relative Luminescence
0.6
0.4
0.2
0.0
0
10
20
30
40
Time (min)
750 ng/well
250 ng/well
B
0
250
750
ASBT-V5 (ng/well)
750
500
0
SERT-V5 (ng/well)
250
250
250
pmirGLO (ng/well)
38 kDa
V5
GAPDH

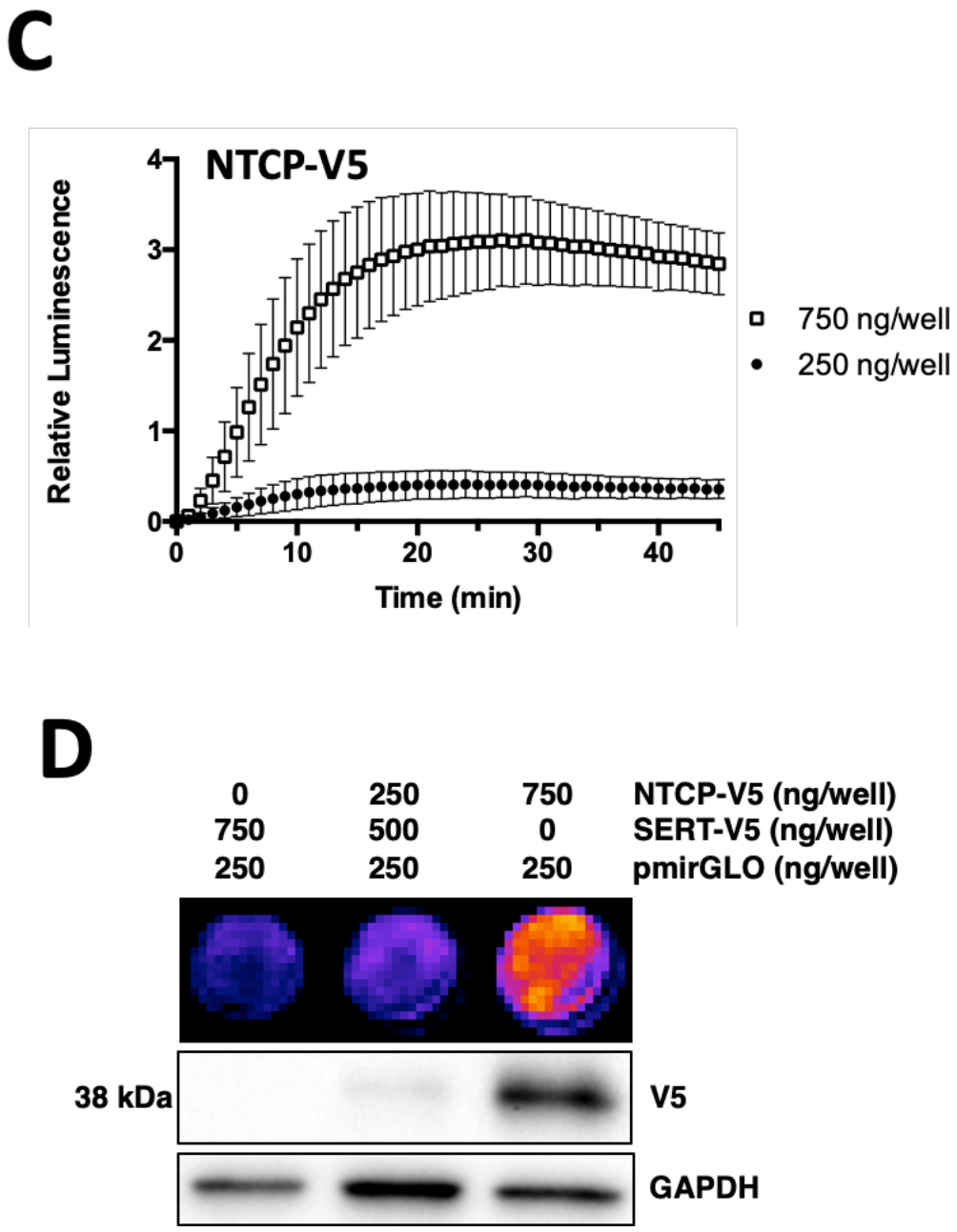

Figure 8. Bioluminescence production is dependent on cellular levels of bile acid transporters. Time course of bile acid transporter-dependent bioluminescence production in HEK 293 transiently transfected with luciferase and 250 ng/well (closed circles) or 750 ng/well (open squares) of ASBT-V5 (A) or NTCP-V5 (C) relative to cells transfected with luciferase and SERT-V5 (750 ng/well). Bioluminescence production (top) and BAT expression (middle) by increasing amounts of transfected ASBT (B) or NTCP (D); n=3. Two-way ANOVA: Time ($p < 0.0001$), Plasmid dose ($p < 0.0001$).

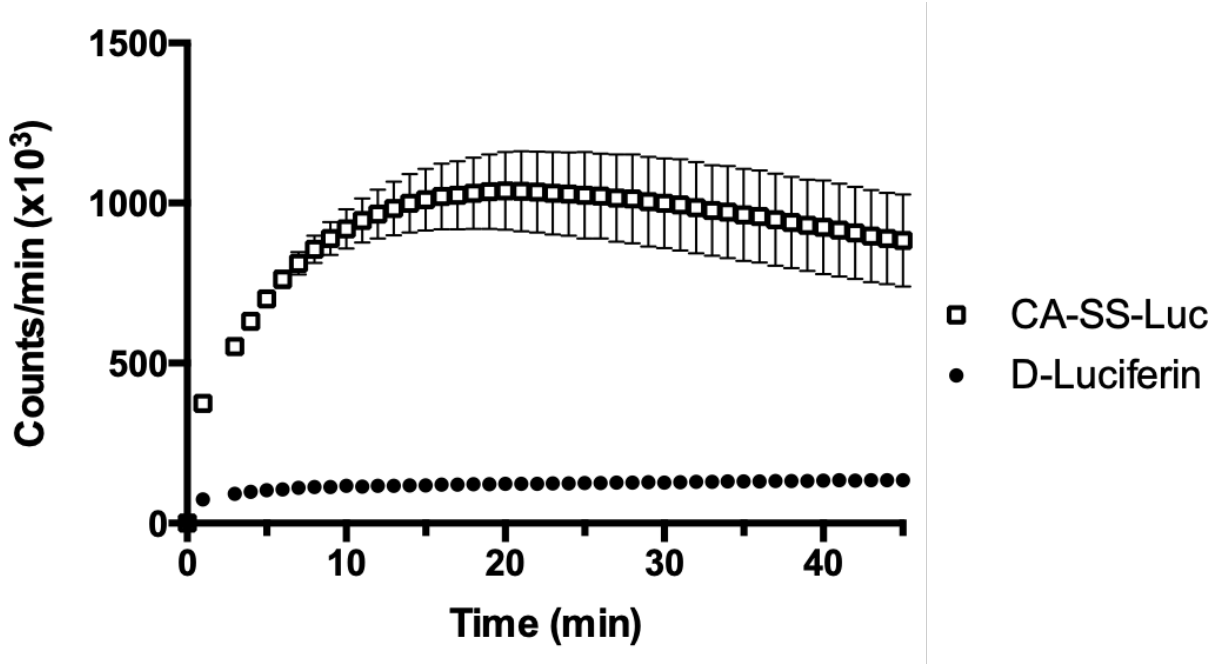

Figure 9. Incubation with CA-SS-Luc produces greater bioluminescence than D-luciferin. Luminescence production by 1 μM D-luciferin (closed circles) and 1 μM CA-SS-Luc (open squares) in 2BT cells; n=4. Two-way ANOVA: Time ($p < 0.0001$), CA-SS-Luc ($p < 0.0001$).

3. Measuring real-time changes in ASBT function

We next examined whether this assay could detect rapid changes in ASBT activity. 2BT cells stably transfected with ASBT-V5 were transiently transfected with luciferase as above. 48 hours post-transfection, cells were treated with vehicle or 500 μM tyrosine phosphatase inhibitor III (PTPIII; Millipore) for 1 h, which has previously been shown to enhance ASBT activity (13). Media containing PTPIII was removed, and cells were imaged by IVIS as above. As shown in **Figure 10A**, bioluminescence from PTPIII-treated cells increased more rapidly as compared to untreated cells in the first 10 minutes of imaging and reached a maximum ~3-fold increase in luminescence before rapidly decreasing to near control-treated luminescence. Similarly, when PTPIII was added along with CA-SS-Luc at the start of imaging, the bioluminescence signal was significantly increased compared with control (**Figure 10B**).

It is also crucial to determine the residual signal present after CA-SS-Luc is removed from the media. Given that there is an intracellular phase in which the probe decomposes to release luciferin, it is likely that this may delay the bioluminescence response to a change in ASBT activity. To address this, 2BT cells were incubated with 1 μM CA-SS-Luc as in **Figure 7**. Following 45 min imaging, we immediately washed the cells 3 times with uptake buffer that did not contain CA-SS-Luc and imaged the cells for an additional 45 min. As shown in **Figure 11**, the bioluminescence signal rapidly decreases after washout, with a calculated half-life of 8.7 ± 0.9 min.

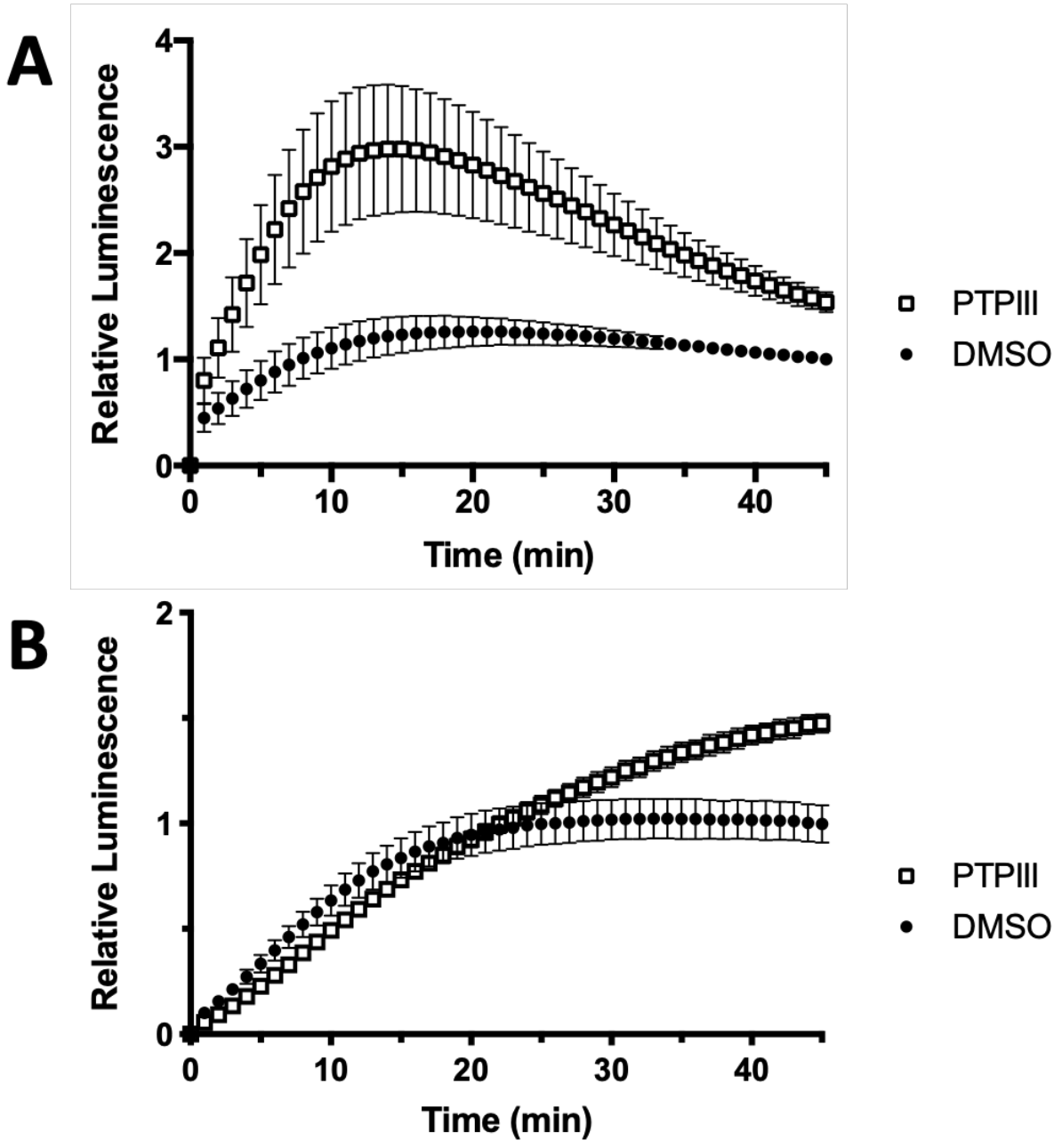

Figure 10. PTPIII enhances CA-SS-Luc bioluminescence production. (A) CA-SS-Luc luminescence in 2BT cells with 1 h pretreatment with 500 μM PTPIII (open squares) or DMSO (closed circles); n=6. Two-way ANOVA: Time ($p < 0.0001$), PTPIII ($p < 0.0001$). (B) CA-SS-Luc luminescence in 2BT cells treated at the start of imaging with 500 μM PTPIII (open squares) or DMSO (closed circles); n=3. Two-way ANOVA: Time ($p < 0.0001$), PTPIII ($p < 0.0001$)

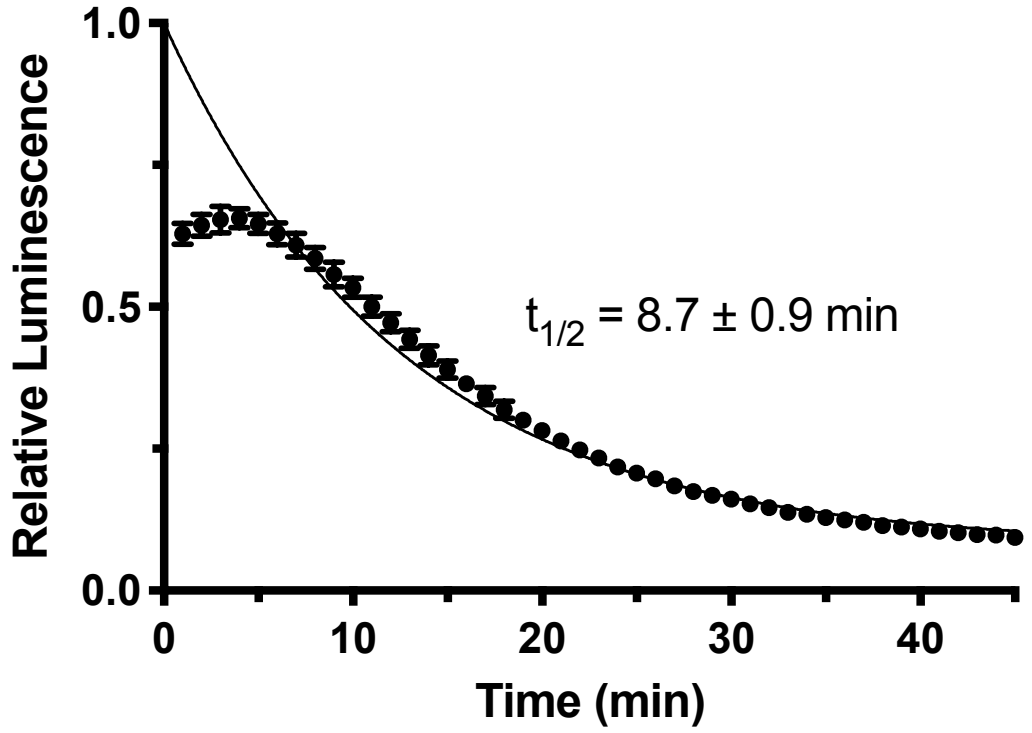

Figure 11. CA-SS-Luc bioluminescence rapidly decreases after washout. Bioluminescence in 2BT cells incubated for 45 min with 1 μM CA-SS-Luc followed by washout and further imaging for 45 min. Data are normalized to CA-SS-Luc bioluminescence at the end of the initial 45 min imaging and were fit to a single-phase decay equation; n=3

4. Induction of the bioluminescence by co-incubation with natural bile acids

We then examined whether co-incubation of CA-SS-Luc with excess of natural bile acids could compete with CA-SS-Luc for entry into the cell. Interestingly, addition of 100 μM taurocholate (TC) to the uptake solution enhanced the luminescence by ~1.5 fold in HEK 293 cells transiently transfected with either ASBT-V5 (**Figure 12A**) or NTCP-V5 (**Figure 12B**), but not in cells transfected with SERT, which does not transport BAs (**Figure 12C**). It should be noted that bioluminescence is observed in cells expressing SERT-V5. However, the raw luminescence signal is significantly less than cells expressing bile acid transporters (**Figure 8**) and likely represents a background bioluminescence that is not further induced by the addition of exogenous bile acids. Similar results were seen with the bile acids taurodeoxycholate (TDC), glycocholate (GC), and glycochenodeoxycholate (GCDC), demonstrating that natural bile acids enhance CA-SS-Luc bioluminescence in a bile acid transporter-dependent manner (**Figure 12D**).

We further investigated BA-dependent luminescence induction in the presence of different BA concentrations. As seen in **Figure 12E**, concentrations of TC as low as 5 μM resulted in enhanced luminescence and was further increased with TC concentrations up to 100 μM in stable 2BT cells transiently expressing luciferase. Interestingly, addition of taurochenodeoxycholate (TCDC) enhanced CA-SS-Luc luminescence to a greater extent and at lower concentrations than TC (**Figure 12F**). We then plotted the bile acid-dependent increase in luminescence at 15 minutes against the concentration of bile acid (5, 25, 50 100, and 300 μM) with a plotted curve that resembled classic kinetics (**Figure 12G**). Based on the Michaelis-Menten equation, the apparent K_m of TC was calculated as 53.1 ± 10.7 μM and the apparent K_m of TCDC was calculated as 10.0 ± 2.6 μM.

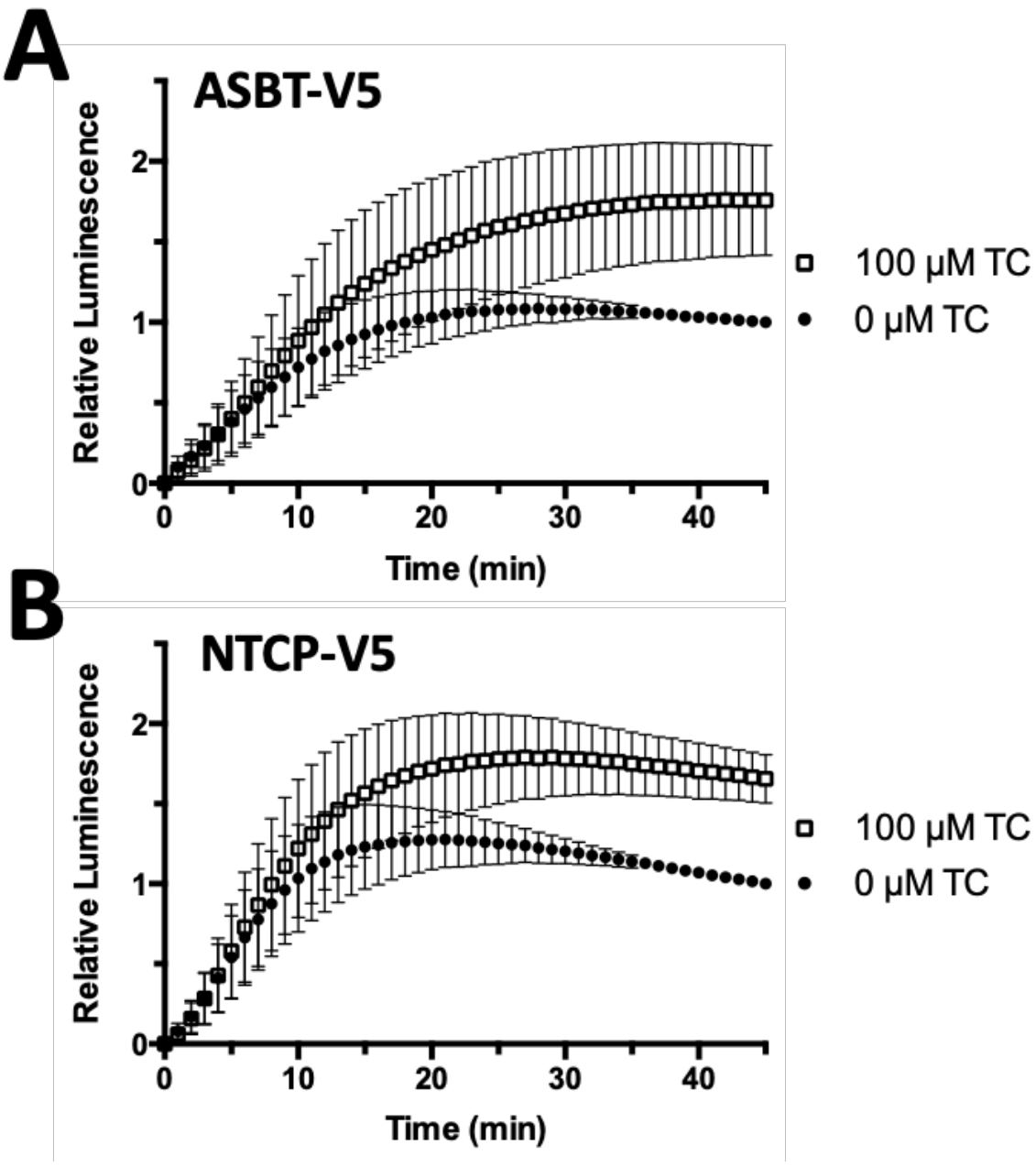
A
ASBT-V5
Relative Luminescence
0
1
2
0
10
20
30
40
Time (min)
100 µM TC
0 µM TC
B
NTCP-V5
Relative Luminescence
0
1
2
0
10
20
30
40
Time (min)
100 µM TC
0 µM TC

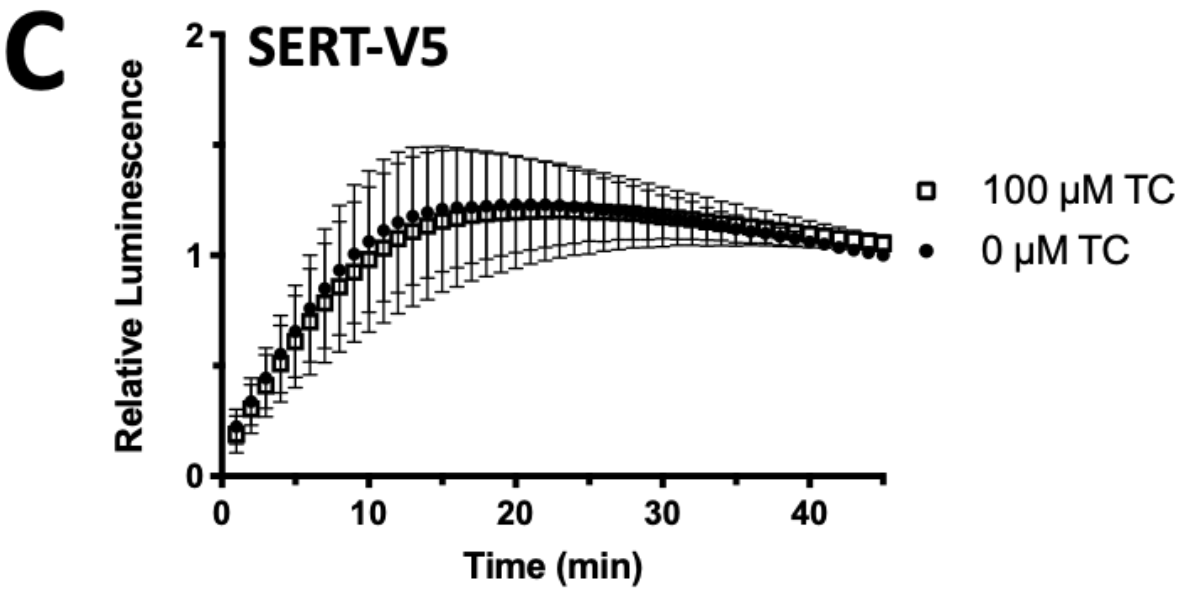
C
SERT-V5
Relative Luminescence
Time (min)
100 µM TC
0 µM TC

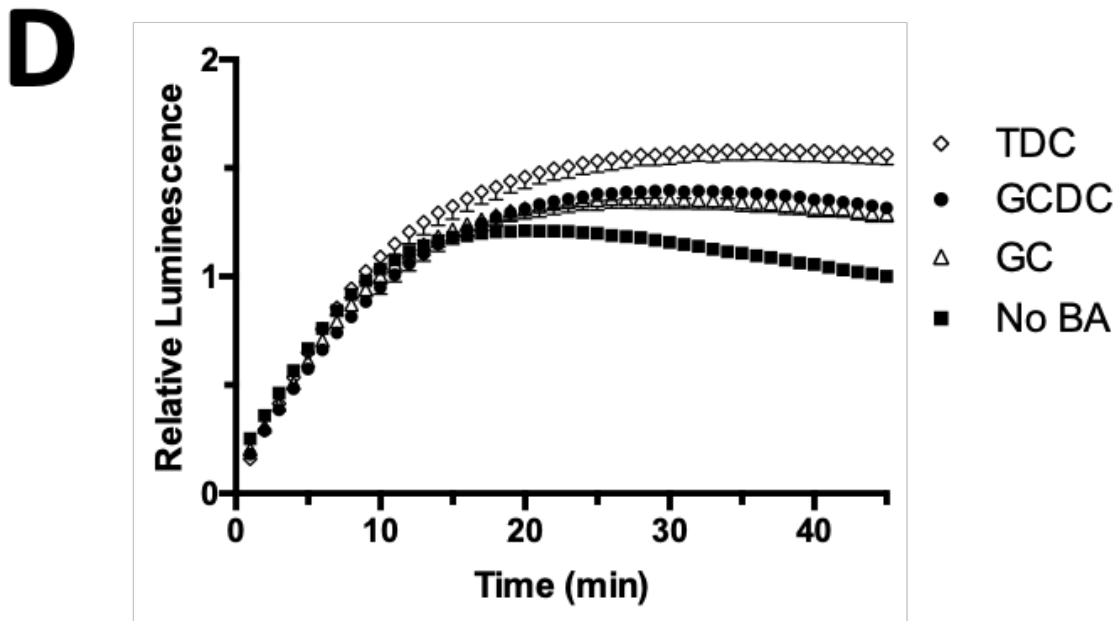
D
Relative Luminescence
Time (min)
TDC
GCDC
GC
No BA

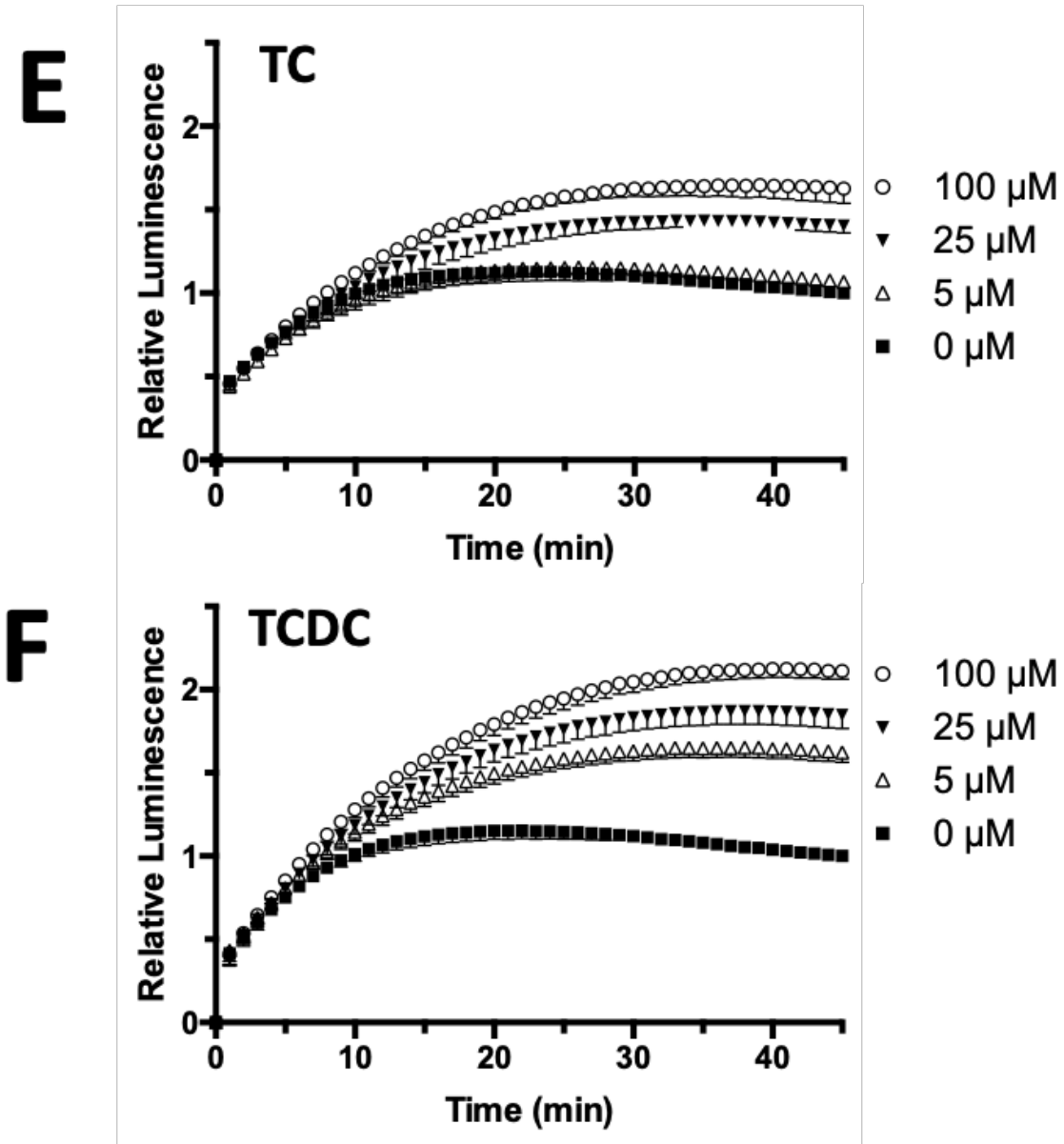
E
TC
Relative Luminescence
0
1
2
0
10
20
30
40
Time (min)
100 µM
25 µM
5 µM
0 µM
F
TCDC
Relative Luminescence
0
1
2
0
10
20
30
40
Time (min)
100 µM
25 µM
5 µM
0 µM

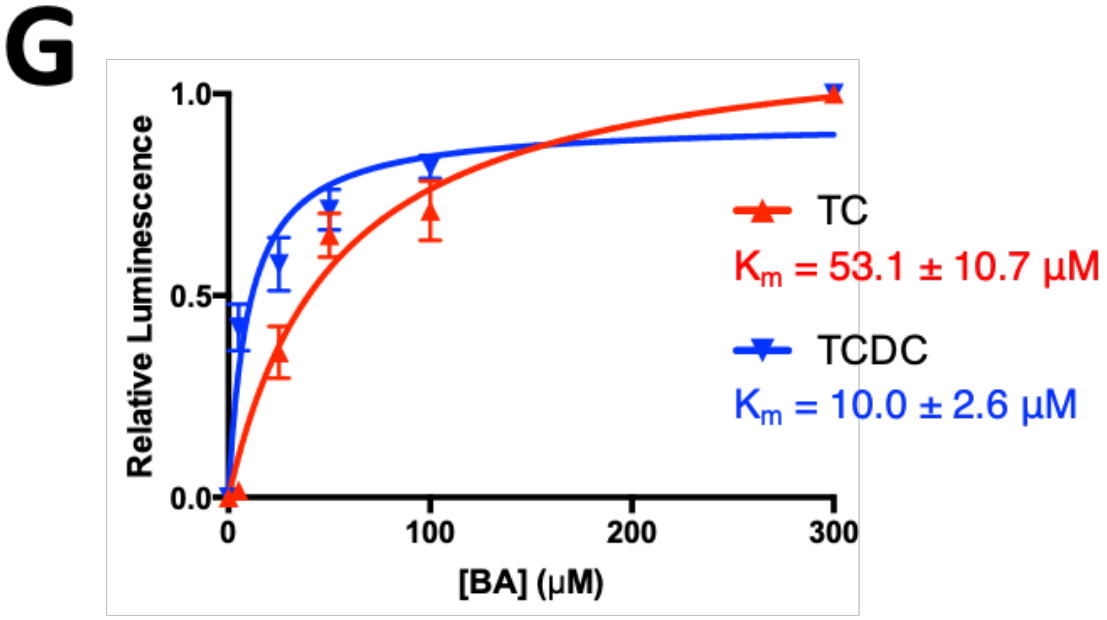

Figure 12. Natural bile acids enhance CA-SS-Luc bioluminescence. (A-C) Relative bioluminescence production by CA-SS-Luc co-treated with 100 μM TC (open squares) or 0 μM TC (closed circles) in HEK cells transiently expressing ASBT (A), NTCP (B), or SERT (C); n=3. Two-way ANOVA: Time (A-C: $p < 0.0001$), TC (A-B: $p < 0.0001$; C: ns). (D) Induction of CA-SS-Luc luminescence by 0 BA (closed squares) or 50 μM of either GC (open triangles), GCDC (closed circles), or TDC (open diamonds). (E-F) Induction of CA-SS-Luc luminescence by 0 μM (closed squares), 5 μM (open triangles), 25 μM (closed triangles), and 100 μM (open circles) TC (D) and TCDC (E) in 2BT cells; n=4. Two-way ANOVA: Time ($p < 0.0001$), Dose ($p < 0.0001$). (G) Luminescence induction normalized to 300 μM BA by different concentrations of TC (red) or TCDC (blue). Curve fit to the Michaelis-Menten equation and apparent K_m calculation by GraphPad Prism 6.0; n=4, $p < 0.05$.

5. CA-SS-Luc uptake in isolated intestinal epithelial cells

Because our *in vitro* studies indicated that luminescence generated by CA-SS-Luc likely represents bile acid transport activity, we hypothesized that CA-SS-Luc could be used to measure ASBT activity in native ileal enterocytes. Intestinal epithelial cells (IECs) were isolated from the jejunum and ileum of transgenic mice expressing luciferase (Luc^{Tg}). Viability of these IECs was approximately 70% following the isolation, as determined by trypan blue staining. Isolated IECs were immediately incubated with 1 μM CA-SS-Luc in uptake buffer and imaged by IVIS with a single 5 min exposure time. The bioluminescence generated by ileal IECs was significantly higher than that generated by an equal number of jejunal IECs, which corresponds to ASBT protein expression as determined by western blot (**Figure 13**). These data demonstrate that CA-SS-Luc luminescence from IECs is enhanced in ileal cells, consistent with the localization and mechanism of ASBT.

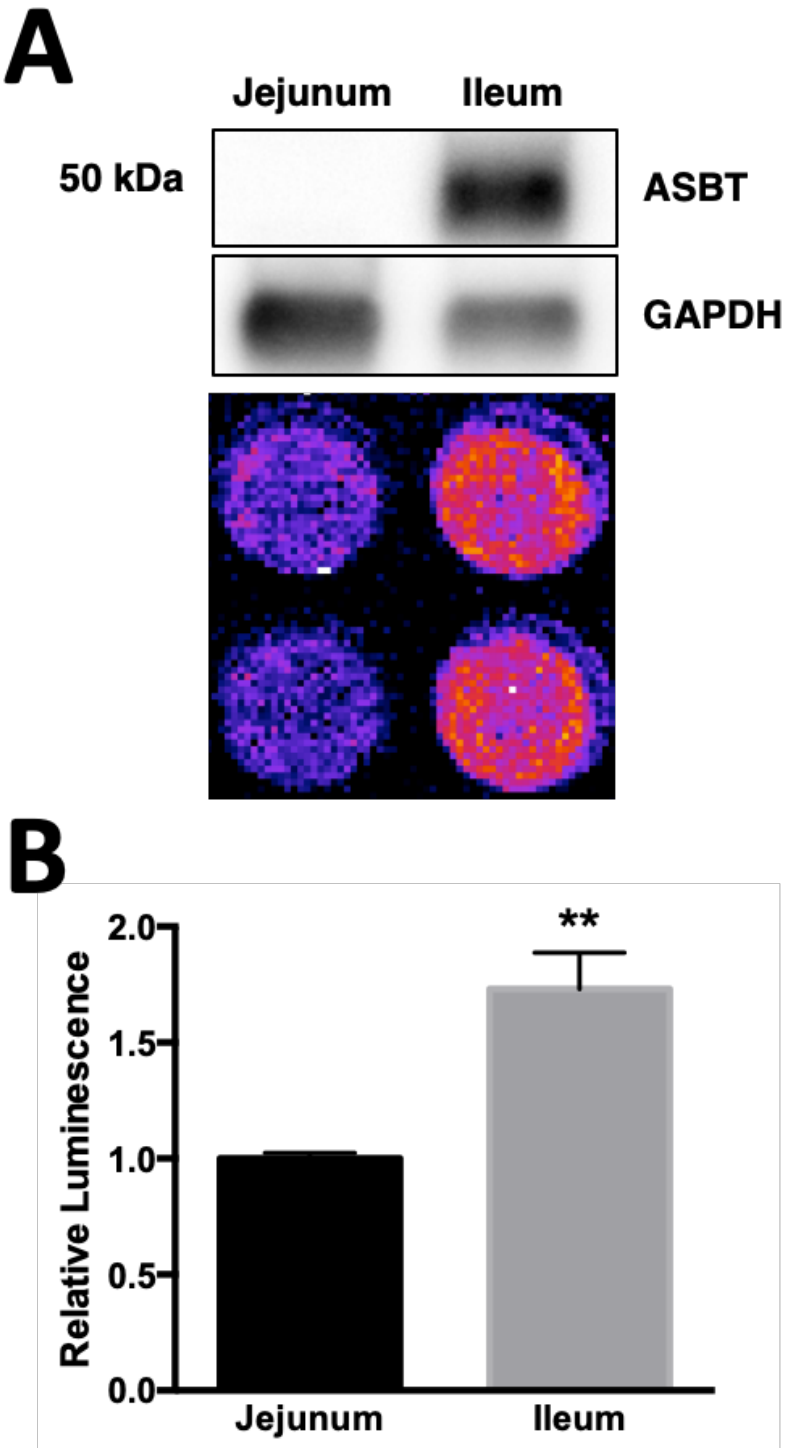

Figure 13. CA-SS-Luc uptake is enhanced in ileal intestinal epithelial cells. (A) ASBT protein expression in jejunal and ileal IECs from Luc^{Tg} mice (representative western blot from n=3 mice) corresponds to CA-SS-Luc bioluminescence production. (B) CA-SS-Luc luminescence relative to jejunal IECs; n=4, **$p < 0.01$

D. Discussion

We have developed a novel, bioluminescence-based method for assessing the cellular uptake of bile acids, and real-time monitoring of the transport activity of ileal ASBT and hepatic NTCP. Recent work in the field has focused on developing methods for real-time imaging of bile acids. Specifically, taurocholic acid has been conjugated to fluorophores and ^{19}F-labeled lysine to generate probes to trace bile acid translocation within the enterohepatic system (66, 259). While these labelled probes could be used as tracers, they are not suitable to directly measure the function of BATs in real time.

The traditional methods for directly assessing BAT activity, which rely on radiolabeled uptake, are unable to sufficiently assess rapid functional changes in these transporters. Recently, bioluminescence-based methods have become increasingly useful tools for measuring real-time transporter activity and other cellular processes (103, 194, 198). In our study, we designed a novel method that relies on a small molecule probe, designated as CA-SS-Luc, which is composed of a cholic acid moiety conjugated to firefly luciferin via a cleavable disulfide linker. The use of a bile acid-based probe is an attractive method for measuring BAT function because these transporters have a fairly broad substrate specificity. ASBT and NTCP have been shown to transport bile acids conjugated to synthetic molecules, a property that has also led to interest in using BATs as prodrug targets (230). We designed CA-SS-Luc to adhere to known structural requirements for ASBT substrates because ASBT has a narrower substrate specificity compared to NTCP (15). Studies showed that many high affinity substrates for ASBT contain the bile acid ring structure conjugated to other molecules at the terminus of the C-24 sidechain (15). Also, a negatively charged C-24 side chain improves translocation of substrates via ASBT (19). The structure of CA-SS-Luc is consistent with all of these parameters, making it a likely substrate for BATs. It will be interesting

to determine in future studies whether probes with luciferin attached to other sites of the bile acid, such as the 3-hydroxy moiety, have different affinity and transport properties compared to CA-SS-Luc. The previously-described self-immolating linker was designed such that upon CA-SS-Luc entry into the cell, glutathione cleaves the disulfide bond, releasing free luciferin and leading to luminescence in cells expressing firefly luciferase (128). Notably, because CA-SS-Luc itself is not a substrate for luciferase, light is only generated after cellular uptake and free luciferin release. This allows for real-time measurement of uptake with minimal extracellular background, which provides an advantage over fluorescence- or MRI-based methods, whose extracellular signal prevents a direct measurement of cellular uptake (66, 259).

In this study, we demonstrate that CA-SS-Luc is useful for the measurement of BAT function in a cell culture model. In HEK 293 cells expressing luciferase and either ASBT or NTCP, CA-SS-Luc bioluminescence is both concentration- and time-dependent. It is important to note that incubation with 15 μM CA-SS-Luc produced significantly higher bioluminescence that saturated the signal collected by IVIS (data not shown), indicating that at the CA-SS-Luc concentrations used in this manuscript, neither intracellular glutathione nor luciferase expression were limiting. The bioluminescence signal, which represents a velocity of the transport activity, increases linearly for ~20 minutes and then reaches a plateau representing a steady-state consistent with a transporter-mediated process for CA-SS-Luc cellular entry. Importantly, bioluminescence is dependent on the levels of BAT expression but not expression of other transport proteins that are not involved in bile acid transport, such as SERT. This provides strong evidence that the bioluminescence signal generated by CA-SS-Luc is specifically induced by BATs. It was also interesting that the relative luminescence in cells transfected with NTCP-V5 was considerably higher than the luminescence in cells transfected with an equal amount of ASBT-V5 plasmid DNA.

This may simply be the result of different expression levels of these transporters at the plasma membrane of transfected cells, different levels of expression from plasmid DNA, or different transfection efficiency. Future studies will test the utility of this system to measure bile acid transport via other BATs, such as the hepatic bile salt export pump (BSEP) and organic anion transporting polypeptide (OATP), as well as the ileal organic solute transporter α/β (OST α/β). Notably, this method was also able to measure rapid changes in ASBT activity. We have previously shown that ASBT-dependent ^{3}H-TC uptake was significantly increased by 30 min incubation with the phosphatase inhibitor PTPIII (13). Here, we show that CA-SS-Luc bioluminescence rapidly increased in the presence of PTPIII. Additionally, we demonstrated that CA-SS-Luc bioluminescence rapidly decreases following washout, suggesting that the intracellular phase of bioluminescence production is rapid. Taken together, these data provide strong evidence for the ability of CA-SS-Luc to assess rapid changes in ASBT function in real time. This observation will be further tested using other compounds known to rapidly modulate BAT function (222, 273).

Interestingly, co-incubation with natural bile acids to compete with CA-SS-Luc for cellular uptake instead caused a significant increase in the luminescence signal. This induction was sodium-dependent and occurred in cells expressing BATs, but not in cells expressing other transporters, such as SERT. Additionally, co-incubation with TCDC produced greater induction than with TC. Since ASBT was previously shown to have more affinity for TCDC as compared to TC, we considered that the observed enhanced luminescence is directly related to the transport activity of ASBT. When the enhancement of CA-SS-Luc luminescence by increasing concentrations (5-300 μM) of TC or TCDC was fit to the Michaelis-Menten equation, we calculated the apparent K_m of TC as 53.1 ± 10.7 μM and the apparent K_m of TCDC as 10.0 ± 2.6

μM. Interestingly, these values are consistent with those previously measured by radioactive uptake (6, 53, 60, 145, 244). It should be noted that the induction of the bioluminescence by co-incubation with higher levels of natural bile acids is unexpected, as previous data from our laboratory has demonstrated that the uptake of radiolabeled tracer ^{3}H-TC is decreased in the presence of higher concentrations of unlabeled TC. The TC-dependent induction of bioluminescence in our system is not the result of increased ASBT expression, as the induction occurs within minutes and expression of ASBT is driven by a constitutive CMV promoter from transfected plasmid DNA. It is possible that the presence of extracellular BAs increases luminescence either by disrupting membrane integrity and allowing passive diffusion or by promoting extracellular cleavage of CA-SS-Luc, leading to diffusion of free luciferin. However, both of these possibilities are unlikely as: i) the BA-dependent increase in luminescence occurred only in cells expressing ASBT or NTCP and not cells expressing other transporters; and ii) our results showed that incubating the cells with D-luciferin alone produced minimal signal as compared to CA-SS-Luc. Another possibility is that intracellular BAs increase luminescence, potentially through enhancing the intracellular cleavage of CA-SS-Luc. This also is quite unlikely, as intracellular bile acid accumulation tends to produce oxidative stress (189) and could reduce intracellular glutathione, which would instead be expected to decrease the cleavage of CA-SS-Luc and thus decrease luminescence. A likely explanation for this increased luminescence is that CA-SS-Luc and natural bile acids bind to distinct sites on ASBT and NTCP and, hence, are not competitors. Rather, the binding and transport of natural bile acids appears to enhance the transport of CA-SS-Luc. Delineating the molecular basis for this speculation will be the subject of future studies.

It is important to mention that in the absence of exogenous BAs, the bioluminescence production from CA-SS-Luc is predominantly sodium-independent. This is a particularly interesting finding given that the signal is clearly dependent on the expression of BATs and would thus be expected to display sodium dependence. The possibility of multiple binding sites may explain both the induction of bioluminescence by exogenous bile acids, as well as the sodium-independent bioluminescence that is produced in the absence of exogenous BAs.

While investigating the different binding sites for CA-SS-Luc on ASBT and NTCP, it is important to note that both ASBT and NTCP form functional dimers (30, 54). It should also be mentioned that ASBT has been recently shown to exhibit a second functional mode, acting as a receptor for large compounds behaving as ligands and leading to their rapid internalization. It is possible, therefore, that the co-presence of CA-SS-Luc and natural bile acids stimulate a functional transport mechanism distinct from the transport of individual bile acids. Nevertheless, we provide here strong evidence that this novel method in the presence of natural bile acids faithfully capture BAT function.

It is of particular importance that our method can be used to assess ASBT activity in native intestinal epithelial cells, a more complex and physiologically relevant model. Our present data demonstrate that in primary IECs isolated from Luc^{Tg} mice, CA-SS-Luc bioluminescence is significantly higher in cells isolated from the ileum, the intestinal segment where ASBT is expressed. This indicates that in native mouse intestinal cells, CA-SS-Luc uptake is dependent on ASBT expression. Furthermore, preliminary data from live Luc^{Tg} mice and excised intestines suggest that luminescence from CA-SS-Luc is predominantly produced from the ileum. However, further study is required in order to confirm these finding and to identify the precise location where luminescence is produced. This method provides an advantage over the recently described

fluorescence resonance energy transfer (FRET)-based biosensor that measures intracellular bile acid concentrations (255). This FRET-based method allows for efficient, real-time measurement of bile acid concentration at subcellular resolution *in vitro*. Although the FRET-based method provides an attractive approach to assess the intracellular concentrations in a single cell, the application of such an approach to animal models may be challenging. On the other hand, our novel luciferase-based method may offer an *in vivo* approach to evaluate the function of intestinal and hepatic bile acid transporters in living animals, as well as from primary cells isolated from Luc^{Tg} mice. However, it is important to note that this method will not allow for the measurement of BAT activity in human patients, as it does require expression of luciferase in intestinal epithelial cells. Thus, its utility is limited to *in vitro* and *in vivo* preclinical models. Ongoing studies in our laboratory are focusing on developing novel methods to measure bile acid transport and distribution in humans.

In conclusion, we have developed a method for assessing BAT activity in real time using a novel bioluminescent probe. This method will be applied to develop assays to identify compounds that modulate BAT activity, as well as pursuing the *in vivo* use of CA-SS-Luc. Future *in vivo* studies will not only allow for real-time measurement of BAT activity in the intestine and liver, but also may identify novel bile acid transport processes in other organ systems.

Chapter III: A novel role of S-acylation in the modulation of ileal apical sodium-dependent bile acid transporter function

The work in this chapter was modified from:

Ticho AL, Malhotra P, Manzella CR, Dudeja PK, Saksena S, Gill RK, Alrefai WA. S-acylation modulates the function of the apical sodium-dependent bile acid transporter in human cells. Journal of Biological Chemistry 295: 4488-4497, 2020.

A. Rationale and aim

ASBT function is tightly regulated by several post-translational mechanisms, including ubiquitination, glycosylation, phosphorylation, and association with plasma membrane microdomains. In this regard, protein S-acylation, a post-translational lipid modification, has been shown to be responsible for regulating several membrane transport proteins by controlling plasma membrane trafficking, transport capacity, protein stability, phosphorylation status, and lipid raft targeting (39, 80, 126, 168, 169, 178, 180, 181, 251, 283). S-acylation is the reversible attachment of long chain fatty acids (FAs) to cysteine residues of transmembrane and cytosolic proteins via a covalent thioester bond. The attachment of FAs is catalyzed by the zDHHC family of palmitoyl acyltransferases, which are transmembrane proteins that contain a zinc-finger Asp-His-His-Cys catalytic domain on their cytosolic face (153, 154). Deacylation is performed by a smaller family of acylthioesterases (40, 281). While palmitic acid (PA) is the most common lipid in S-acylated proteins, many other long chain FAs can be used, including unsaturated FAs such as oleic acid (OA) (130, 153).

To date, the potential regulation of ASBT by S-acylation has not been examined. In the present study, **we aimed to investigate the role that S-acylation plays in regulating ASBT function**. Our data demonstrated that S-acylation is crucial for ASBT activity and may serve an important regulatory role in bile acid homeostasis.

B. Materials and methods

1. Cell culture, materials, and western blot analysis

Wild type HEK 293 and 2BT cells were maintained and transfected as described in **chapter II**. All chemicals and reagents were purchased from Sigma Aldrich (St Louis, MO) unless

otherwise specified. Western blotting was performed as in **chapter II** using antibodies against V5 (Invitrogen; Carlsbad, CA), hASBT (previously generated in our laboratory) (14), mASBT (a generous gift from Dr. Paul Dawson, Emory Universiry), flotillin-1 (Abcam; Cambridge, MA), or claudin-2 (Invitrogen; Carlsbad, CA)

2. Plasmid construction

Human ASBT cDNA was generated as described in **chapter II**. Site mutagenesis was performed using the Quikchange II XL kit (Agilent; Wood Dale, IL) per the manufacturer's instructions with the primers listed in **Table 2**.

C7S	5’-TGTTGCATTGTCCACACTGCTGTTCGGATCATTCA-3’
	5’-TGAATGATCCGAACAGCAGTGTGGACAATGCAACA-3’
C51S	5’-TGATTTCCACGTTGCTTCCCATGGAGAACATCAC-3’
	5’-GTGATGTTCTCCATGGGAAGCAACGTGGAAATCA-3’
C69S	5’-GGCCGTGGGGCATTAGTGTTGGCTTCCT-3’
	5’-AGGAAGCCAACACTAATGCCCCACGGCC-3’
C74S	5’-GCATGATTCCAAACTGACTGAGGAAGCCAACACAAAT-3’
	5’-ATTTGTGTTGGCTTCCTCAGTCAGTTTGGAATCATGC-3’
C105S	5’-CTCCAGGGCAGCTTCCTATAATGAGCACCACTACG-3’
	5’-CGTAGTGGTGCTCATTATAGGAAGCTGCCCTGGAG-3’
CC105/	5’-TCCTCCAGGGCTGCTTCCTATAATGAGCACCACTAC-3’
106SS	5’-GTAGTGGTGCTCATTATAGGAAGCAGCCCTGGAGGA-3’
C106S	5’-GCAGTTCCTCCAGGGCTGCATCCTATAATGAGC-3’
	5’-GCTCATTATAGGATGCAGCCCTGGAGGAACTGC-3’
C144S	5’-GTATAGATAAGGAGGCTCAGCGGCATCATTCCG-3’
	5’-CGGAATGATGCCGCTGAGCCTCCTTATCTATAC-3’
C255S	5’-GCAACCGTTCGGCTCCTGTACCAGGGT-3’
	5’-ACCCTGGTACAGGAGCCGAACGGTTGC-3’
C314S	5’-TCTGCCTTGTTTTTTCCATGACTTTTCTTGTATGCCACATAAAATC-3’
	5’-GATTTTATGTGGCATACAAGAAAAGTCATGGAAAAAACAAGGCAGA-3’

Table 2. Primers for ASBT cysteine mutants.

3. Isolation of mouse ileal intestinal epithelial cells (IECs)

8-14 week old C57BL/6J mice (Jackson Labs; Bar Harbor, ME) were sacrificed and the distal 5 cm of ileum were dissected. Ileal IECs were prepared as in **chapter II** and used for acyl resin-assisted capture (acyl-RAC) analysis (see below).

4. Preparation of human donor ileal brush border membrane vesicles (BBMVs)

Small intestine from healthy adult organ donors were obtained from Gift of Hope immediately after harvest of organs for transplantation. The small intestine was divided into 3 segments of equal length and the distal segment was designated as the ileum. The intestine was cleaned, and mucosa scraped from the seromuscular layer and stored at -80°C. Purified BBMVs were prepared from frozen samples by the $CaCl_2$ precipitation method as previously described (14, 71, 90, 102). Purified BBMVs were suspended in buffer containing 25 mM HEPES (pH 7.4), 25 mM NaCl, 1 mM EDTA, and 1% Triton X-100 for acyl-RAC analysis (see below).

5. Acyl resin-assisted capture (acyl-RAC)

Acyl-RAC was performed on crude membrane preparations as previously described (**Figure 14A**) (79, 268). Briefly, cells were harvested in detergent-free buffer containing 25 mM HEPES (pH 7.4), 25 mM NaCl, and 1 mM EDTA. Lysates were subjected to ultracentrifugation at 136000 x g for 1 h to prepare crude membranes, which were then solubilized in the lysis buffer supplemented with 1% Triton X-100. Membranes were subjected to thiol blocking by 1.5% S-methyl methanethiosulfonate (MMTS) in a buffer containing 100 mM HEPES (pH 7.4), 1 mM EDTA, and 2% SDS for 4 h at 40°C. Blocked proteins were precipitated in acetone, washed several times, and resuspended in buffer containing 100 mM HEPES (pH 7.4), 1 mM EDTA, and 1% SDS.

Hydrated thiopropyl sepharose 6B resin was added to these proteins and mixed with hydroxylamine (HA; pH 7.5) at a final concentration of 0.5 M. As a negative control, a separate reaction was prepared with HA replaced by Tris-HCl. This solution was incubated overnight at room temperature with end-over-end mixing. The following day, supernatant (unbound fraction) was collected, the resin was washed several times, and bound proteins were eluted by boiling in Laemmli buffer supplemented with 2.5% β-mercaptoethanol for 10 min. Laemmli buffer was added to bound fractions to equalize the volume to unbound fractions. Samples were then subjected to SDS-PAGE followed by western blotting.

6. Metabolic labeling with alkyne-fatty acids

Metabolic labeling with 100 μM alkyne-palmitic acid (alk-PA; palmitic acid 15-yne; Avanti Polar Lipids) or μM alkyne-oleic acid (alk-OA; oleic acid 17-yne; Avanti Polar Lipids; Alabaster, AL) was performed in DMEM supplemented with 0.25% fatty acid-free BSA. To prepare these solutions, 200 mM DMSO stocks of either unlabeled PA, alk-PA, or alk-OA were added to 20% fatty acid-free BSA to a concentration of 8 mM. 50 mM 2-bromopalmitate or vehicle were also added to a concentration of 2 mM. These solutions were sonicated briefly and incubated at 37℃ until the fatty acids had fully dissolved, followed by 80x dilution in 37℃ DMEM. These solutions were added to cells and incubated at 37℃ for 15 h to allow for incorporation of fatty acids. Following incubation, cells were lysed in buffer containing 150 mM NaCl, 50 mM HEPES, 2 mM $MgCl_2$, 0.1% Triton X-100, 1% SDS, and 1X EDTA-free protease inhibitor. Up to 200 μg of protein lysate was subjected to copper-catalyzed azide-alkyne cycloaddition with azido-PEG_3-biotin as previously described (112). Briefly, lysates were incubated for 1 h at room temperature with 50 μM azido-PEG_3-biotin in a solution containing 100 μM $CuSO_4$, 500 μM tris(3-

hydroxypropyltriazolylmethyl)amine (THPTA), and 1.5 mM sodium ascorbate. Proteins were precipitated in methanol and chloroform. The precipitate was then washed with methanol and resuspended in radioimmunoprecipitation assay (RIPA) buffer (Cell Signaling Technologies, Danvers, MA) supplemented with 1% SDS. Proteins were then incubated with NeutrAvidin agarose beads (Thermo; Waltham, MA) overnight at 4°C with end-over-end mixing. The following day, supernatant (unbound fraction) was collected, the resin was washed several times, and bound proteins were eluted by boiling in Laemmli buffer supplemented with β-mercaptoethanol for 10 min. Samples were then subjected to SDS-PAGE followed by western blotting.

7. Preparation of detergent soluble and insoluble membrane fractions

2BT cells were treated with DMSO or 2-bromopalmitate (2-BP; 1-25 μM) in DMEM supplemented with 0.25% fatty acid-free BSA for 15 h. Detergent soluble (DS) and detergent insoluble (DI) membrane fractions were prepared as previously described (14). Briefly, crude membranes were prepared by lysing cells in a buffer containing 25 mM HEPES (pH 7.4), 25 mM NaCl, and 1 mM EDTA, followed by ultracentrifugation of lysates at 136000 x g for 30 min at 4°C. Membranes were incubated for 30 min at 4°C in a buffer containing 50 mM MES (pH 6.5), 60 mM NaCl, 3 mM EGTA, 5 mM $MgCl_2$, 1% Triton X-100. Following incubation, membranes were centrifuged again at 136000 x g for 30 min at 4°C. The supernatant was designated as the DS fraction and the pellet was resuspended in an equal volume of RIPA buffer and designated as the DI fraction. An equal volume of DS and DI fractions were subjected to SDS-PAGE followed by western blotting.

8. Cell surface biotinylation

Cell surface biotinylation was performed as previously described (2, 14). Briefly, cells were incubated with sulfo-NHS-SS-biotin (0.5 mg/ml; Thermo) in borate buffer (154 mM NaCl, 7.2 mM KCl, 1.8 mM $CaCl_2$, and 10 mM H_3BO_3, pH 9.0) for 1 h at 4°C to minimize endocytosis. Cells were lysed and biotinylated proteins were precipitated with NeutrAvidin agarose beads. Biotinylated proteins were eluted by boiling in Laemmli buffer supplemented with β-mercaptoethanol for 10 min, followed by SDS-PAGE and western blotting.

9. Supplementation with fatty acids

Fatty acid supplementation of 2BT cells with either 100 μM palmitic acid (PA; 16:0), stearic acid (SA; 18:0), oleic acid (OA; 18:1); α-linolenic acid (ALA; 18:3), or eicosapentanoic acid (EPA; 20:5) was performed in DMEM supplemented with 0.25% fatty acid-free BSA prepared as above. ASBT function was then assessed as described below. For FA replacement experiments, after 15 h of treatment with OA or ALA, media was either replenished with the same unsaturated FA (control) or replaced with 100 μM PA for 24 h.

10. Assessment of ASBT function by [^{3}H]-taurocholate (TC) uptake

Following treatment with FAs or 2-BP, assessment of ASBT activity by [^{3}H]-TC uptake was performed as previously described (14). Briefly, cells were washed twice at room temperature with uptake buffer containing 110 mM NaCl (with sodium) or choline chloride (without sodium), 4 mM KCl, 1 mM $MgSO_4$, 1 mM $CaCl_2$, 45 mM mannitol, 5 mM glucose, and 10 mM HEPES (pH 7.4). Cells were then incubated with uptake buffer containing 1 μCi/mL of [^{3}H]-TC and 10 μM cold taurocholate (TC) at room temperature for 5 min, washed with ice-cold PBS, and lysed

in 0.5 M NaOH. Radioactivity was measured by liquid scintillation counting (Packard Tri-CARB 1600-TR, Packard Instruments) and total protein was measured by the method of Bradford (32). Results were calculated as pmol • mg protein^{-1} • 5 min^{-1} and normalized to control.

11. Assessment of ASBT function by bioluminescent bile acid tracer (CA-SS-Luc) uptake

Assessment of ASBT activity by CA-SS-Luc uptake was performed as described in **chapter II**. For cotreatment with 2-BP, either 25 μM 2-BP or DMSO vehicle was added along with CA-SS-Luc. The luminescence produced from each well was quantified using Living Image software (Perkin Elmer; Waltham, MA).

12. Statistical analysis

Results were expressed as mean ± SEM of at least three experiments. Statistical analysis was performed by Student's t-test when comparing two groups and one-way ANOVA when comparing multiple groups (GraphPad Prism; San Diego, CA). $P \leq 0.05$ was considered statistically significant.

C. Results

1. ASBT is acylated in native intestinal epithelial cells and cultured 2BT cells

S-acylation is a crucial mechanism by which the localization and function of membrane proteins are regulated. We first aimed to determine whether ASBT protein was S-acylated in native intestinal tissues from mice and from human donors. We used acyl resin-assisted capture (acyl-RAC) to quantify the proportion of ASBT that was S-acylated. In this method, proteins are treated with MMTS, which blocks free (non-acylated) thiols. Blocked proteins are then treated with

hydroxylamine (HA), which cleaves the thioester bonds of S-acylated residues. Thus, cysteine residues that were initially non-acylated are blocked by MMTS, while residues that were initially acylated are cleaved to form free thiols. Proteins are then precipitated using thiopropyl sepharose 6B resin, which binds to the initially acylated free thiols. This method results in S-acylated proteins binding to the resin, while non-acylated proteins remain unbound in the supernatant (79, 268) (**Figure 14A**). For these experiments, treatment with Tris was used as a negative control for the HA reaction, such that in samples treated with Tris, no protein should bind to the resin as acyl groups are not cleaved.

To investigate the acylation of ASBT in mice, intestinal epithelial cells were isolated from the distal 5 cm of ileum and membranes preparations were performed as previously described. These membranes were subjected to acyl-RAC, and western blotting was performed for ASBT. The results demonstrate that ~80% of ASBT from native mouse ileocytes is present in the bound fraction of HA-treated proteins, compared to <5% with Tris treatment (**Figure 14B**). Claudin-2, which has previously been shown to be acylated (257), displayed a similar pattern to ASBT. These data indicate that the majority of ASBT is acylated in mouse ileum. Similarly, when acyl-RAC was performed on brush border membrane vesicles from human donor ileum, the majority of ASBT and Flotillin-1 (a well-known S-acylated membrane protein (123)) were found in the bound fraction of HA-treated samples (**Figure 14C**). These data strongly indicate that the majority of ASBT is acylated in both mouse and human intestine.

We next investigated whether ASBT is acylated in HEK 293 cells stably transfected with an ASBT-V5 fusion protein (2BT cells). We have previously shown that ASBT-V5 in 2BT cells is functional and regulated in a similar manner to native ASBT (12, 14). When acyl-RAC was

performed in these cells, ~80% of ASBT-V5 bound to the resin, similar to what was seen in native tissues (**Figure 15**).

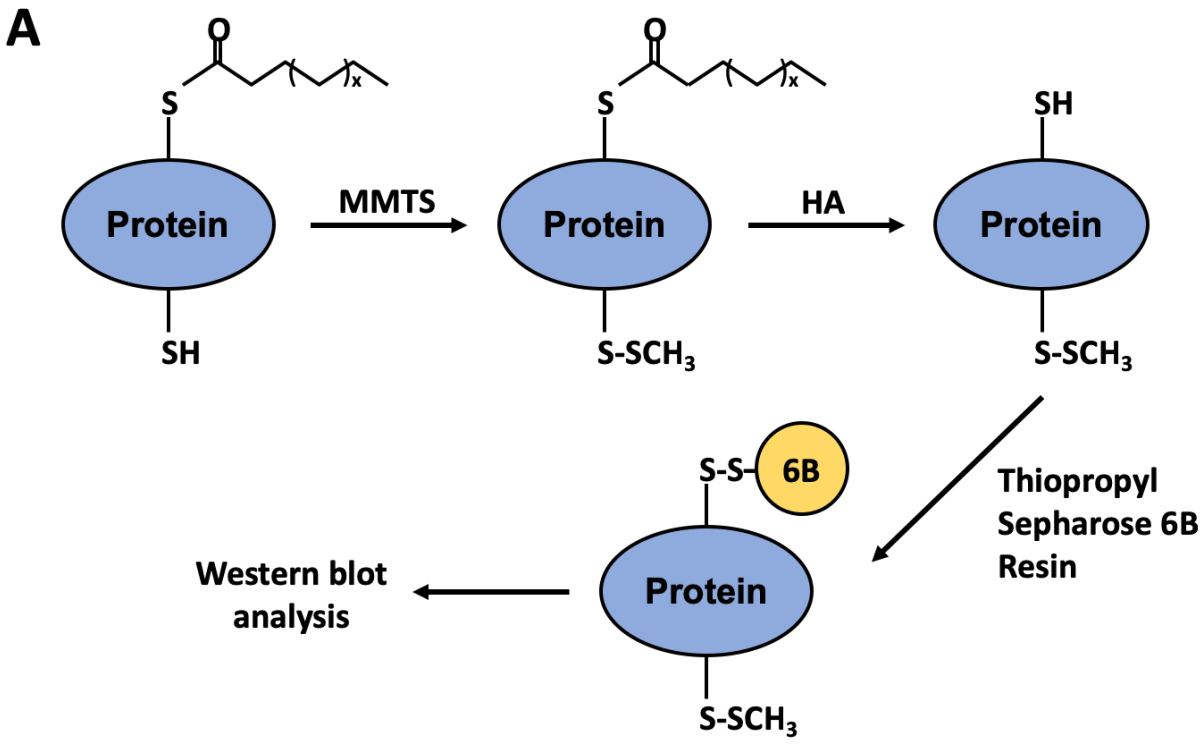
A
O
S
x
Protein
SH
MMTS
S-SCH3
HA
Thiopropyl
Sepharose 6B
Resin
S-S-
6B
Western blot
analysis

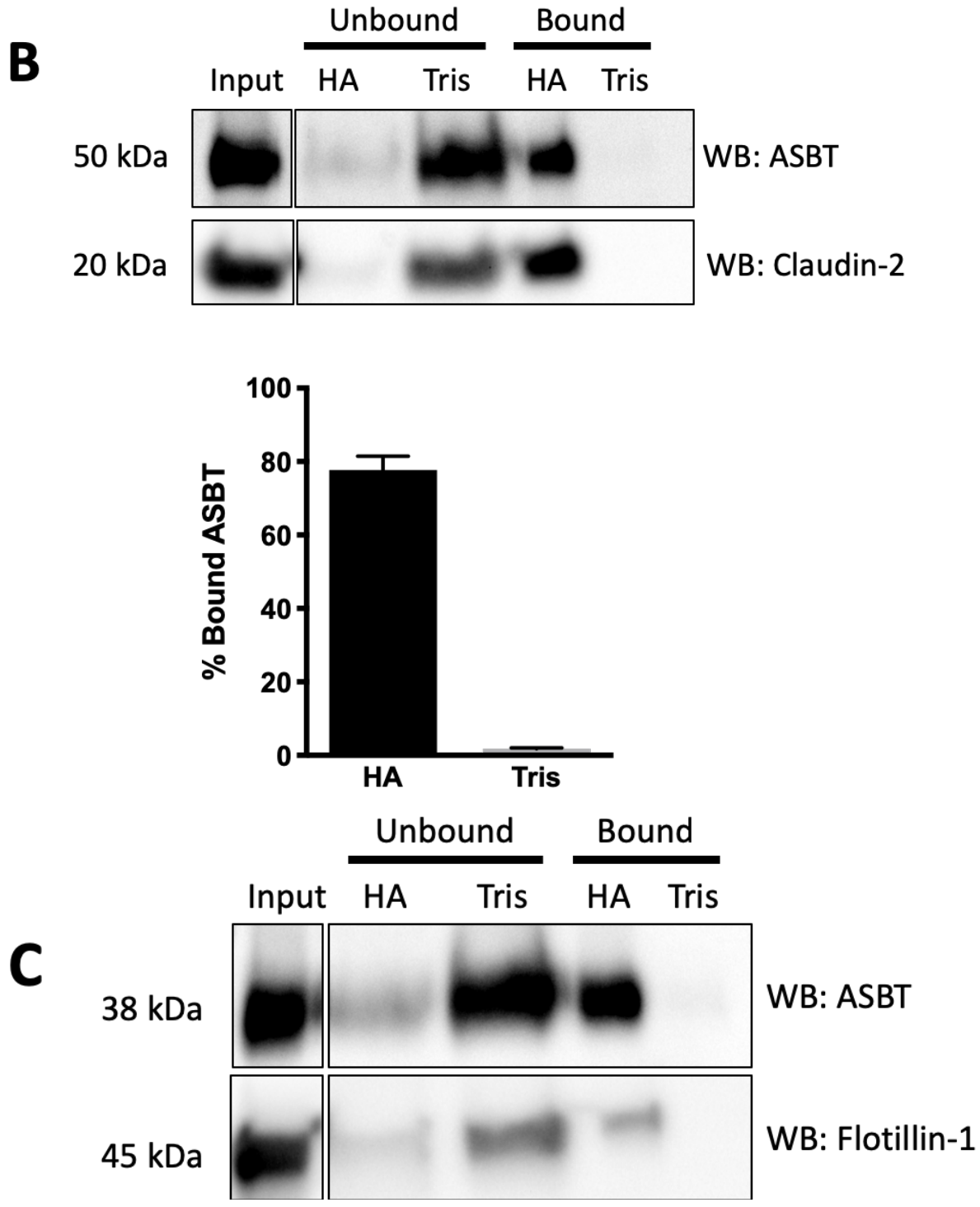

Figure 14. ASBT is S-acylated in native intestine. (A) Schematic of acyl-RAC method. Free cysteines are blocked with MMTS, followed by cleavage of thioesters with hydroxylamine. Acylated proteins are precipitated with thiopropyl sepharose 6B resin. (B) ASBT acyl-RAC in mouse ileal intestinal epithelial cells; n=3. (C) ASBT acyl-RAC in human ileal brush border membrane vesicles (representative western blot from 3 different donors with similar results).

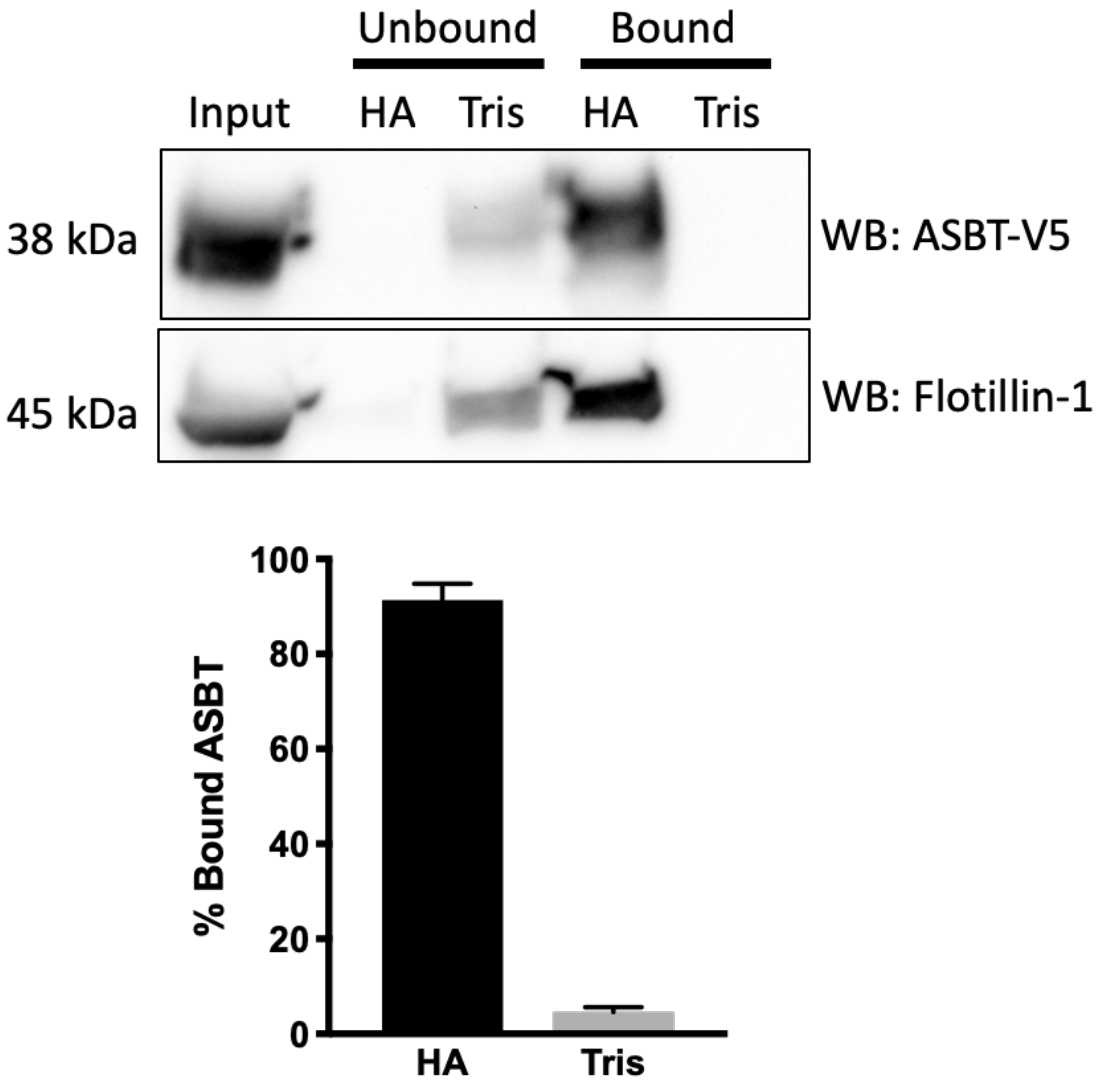

Figure 15. ASBT is S-acylated in cultured 2BT cells. ASBT acyl-RAC in HEK 293 cells stably transfected with ASBT-V5; n=4.

2. 2-bromopalmitate reduces ASBT acylation and function

To further confirm that ASBT is acylated in 2BT cells, we performed metabolic labeling by incorporating alkyne-palmitic acid (alk-PA) into acylated proteins, allowing for detection by click chemistry-based approaches. To incorporate alk-PA, cells were deprived of lipids for 6 h in media containing 0.25% fatty acid-free bovine serum albumin (FA-free BSA), followed by 15 h incubation with either 100 μM palmitic acid (PA) or 100 μM alk-PA in the presence or absence of 25 μM 2-BP, an inhibitor of acyltransferases. Protein lysates were prepared, and alkyne-palmitoylated proteins were conjugated to azido-PEG3-biotin via Huisgen cycloaddition, also known as "click chemistry" (86, 278). Biotin-conjugated proteins were precipitated with NeutrAvidin agarose beads, followed by SDS-PAGE and western blotting (**Figure 16A**). As shown in **Figure 16B**, cells treated with PA did not show ASBT-V5 in the bound fraction (as expected), while those treated with alk-PA did, indicating that alk-PA was incorporated into ASBT-V5. The incorporation of alk-PA in ASBT-V5 was ~50% reduced by treatment with the acyltransferase inhibitor 2-BP (**Figure 16B-C**), suggesting enzyme-dependent acylation of ASBT in 2BT cells. In addition to reducing ASBT acylation, short-term treatment (30 min) with 25 μM 2-BP was able to produce a robust ~50% decrease in [^{3}H]-TC uptake (**Figure 16D**). 15 h incubation with 2-BP reduced [^{3}H]-TC uptake, with a maximal decrease of nearly 90% when treated with 25 μM 2-BP (**Figure 16E**). These findings were confirmed by measuring real-time CA-SS-Luc luminescence when 2BT cells were treated with 2-BP at the same time that CA-SS-Luc was added. Under these conditions, the rate of CA-SS-Luc luminescence generation was markedly reduced when cells were treated with 10 or 25 μM 2-BP (**Figure 16F**). The area under the curve (AUC) measurement, which represents total CA-SS-Luc uptake, was ~70% reduced by 10 μM 2-BP and nearly eliminated by 25 μM 2-BP. To investigate the potential mechanism(s) by

which 2-BP reduces ASBT function, we examined ASBT plasma membrane expression by cell surface biotinylation. As shown in **Figure 16G**, 30 min treatment with 25 μM 2-BP reduced ASBT surface expression by ~40%, suggesting that S-acylation may be important for targeting ASBT to the plasma membrane. Furthermore, preliminary experiments (n=1) indicate that 15 h 2-BP treatment may also reduce the proportion of ASBT present in detergent insoluble lipid raft membrane fractions without disrupting the distribution of the raft protein flotillin-1 (**Figure 16H**). These data suggest that reduced acylation by 2-BP may rapidly lead to decreased ASBT plasma membrane expression and lipid raft association, with a corresponding decrease in ASBT function.

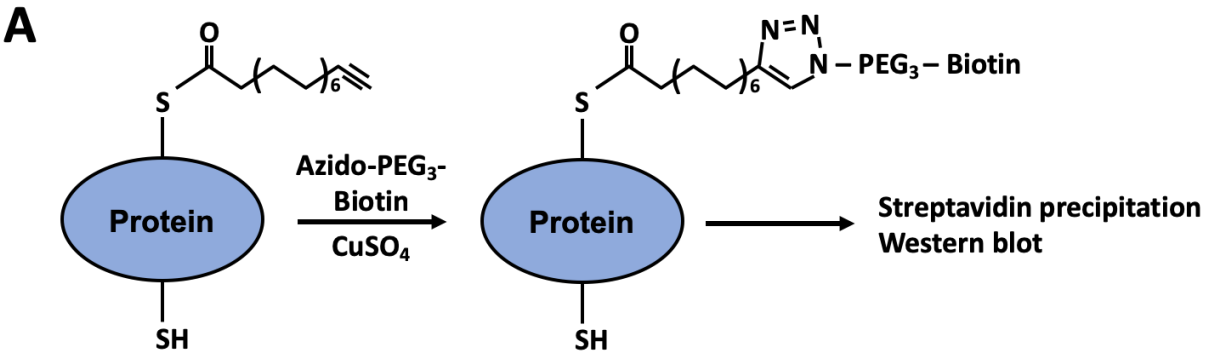
A
O
S
6
Protein
SH
Azido-PEG3-
Biotin
CuSO4
N=N
N – PEG3 – Biotin
Streptavidin precipitation
Western blot

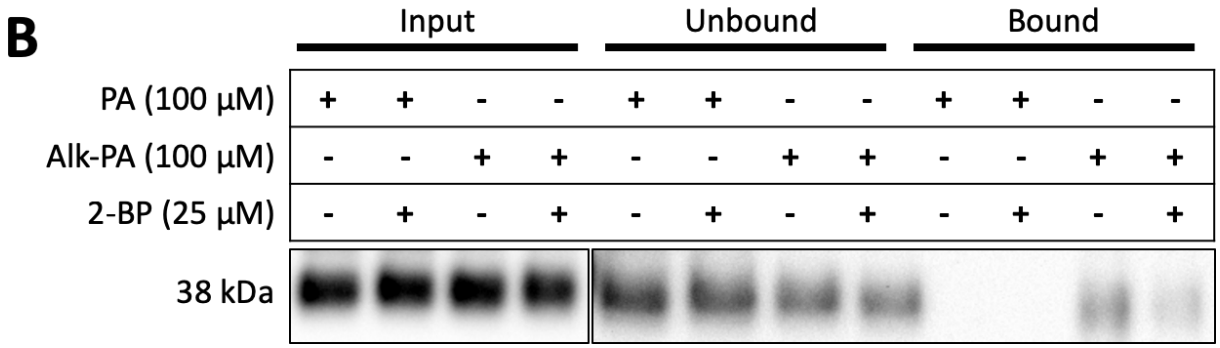
B
Input
Unbound
Bound
PA (100 µM)
Alk-PA (100 µM)
2-BP (25 µM)
38 kDa

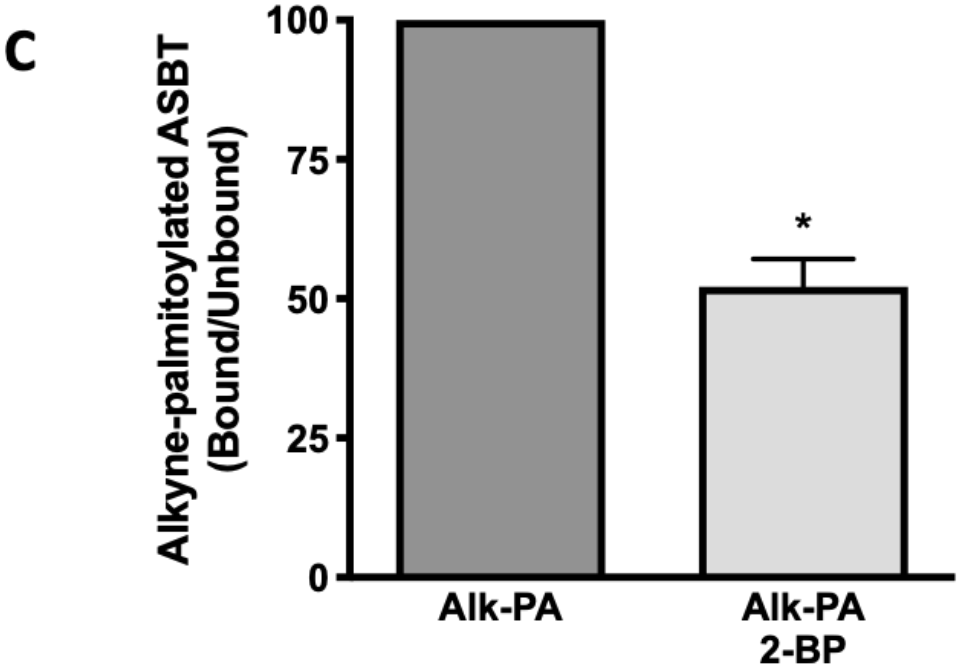
C
Alkyne-palmitoylated ASBT
(Bound/Unbound)
100
75
50
25
0
*
Alk-PA
Alk-PA
2-BP

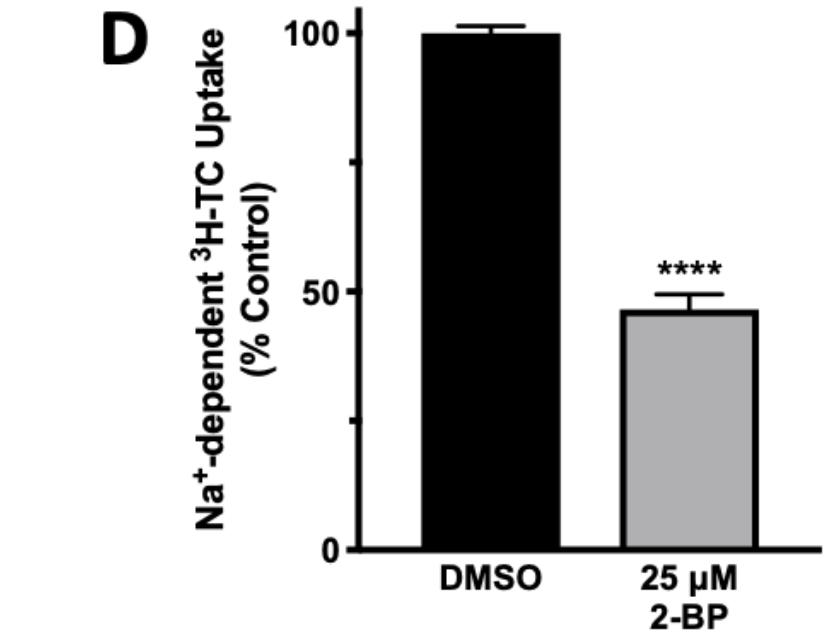
D
Na+-dependent 3H-TC Uptake
(% Control)
100
50
0
****
DMSO
25 µM
2-BP

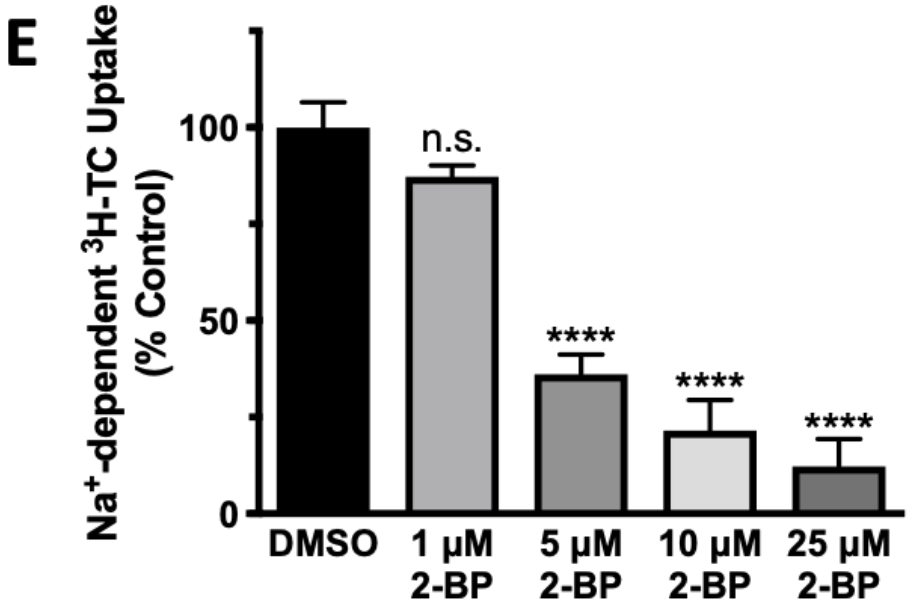
E
Na+-dependent 3H-TC Uptake
(% Control)
100
50
0
n.s.
****
****
****
DMSO
1 µM
2-BP
5 µM
2-BP
10 µM
2-BP
25 µM
2-BP

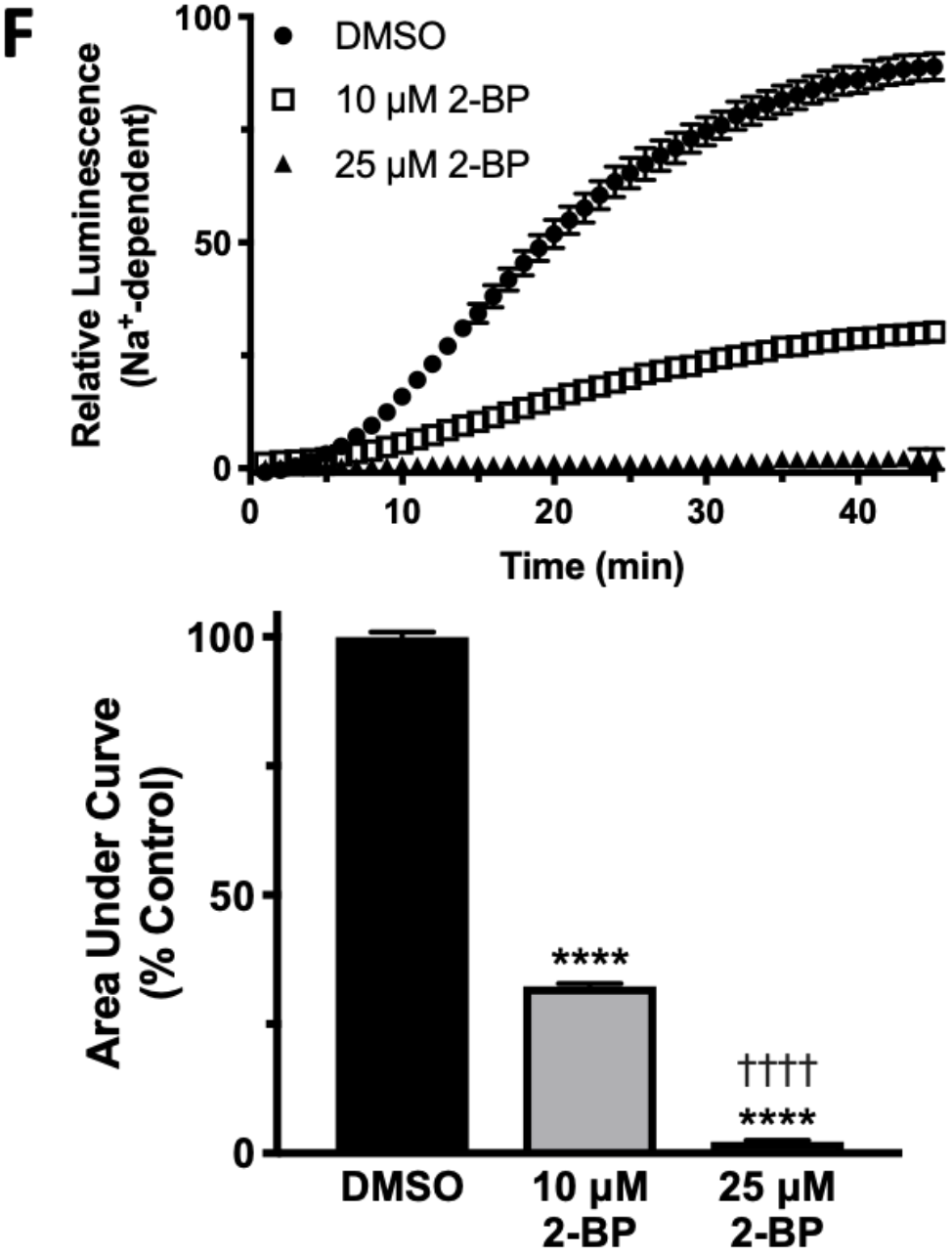
F
100
50
0
DMSO
10 μM 2-BP
25 μM 2-BP
Relative Luminescence
(Na+-dependent)
0
10
20
30
40
Time (min)
100
50
0
Area Under Curve
(% Control)
****
††††
****
DMSO
10 μM
2-BP
25 μM
2-BP

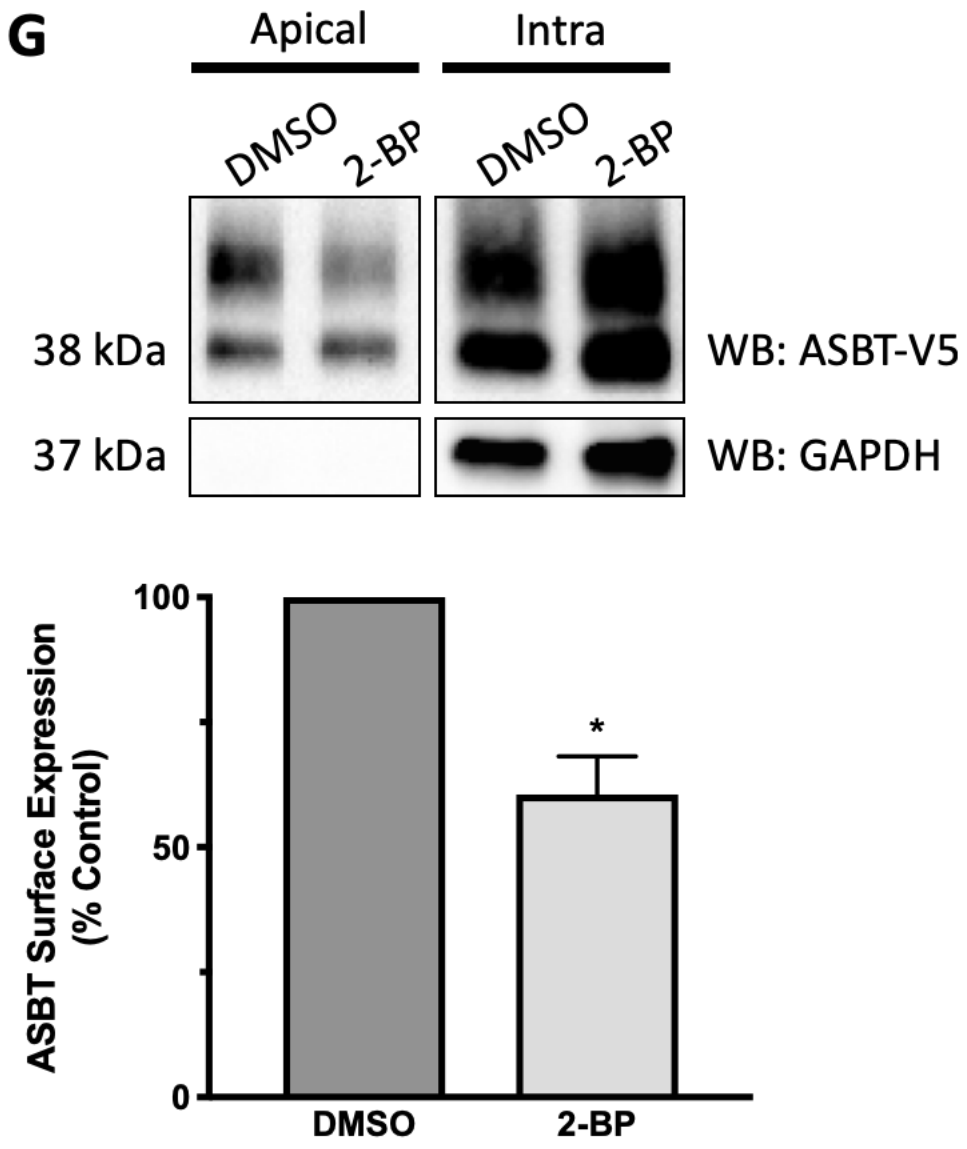
G
Apical
Intra
DMSO
2-BP
DMSO
2-BP
38 kDa
WB: ASBT-V5
37 kDa
WB: GAPDH
ASBT Surface Expression
(% Control)
100
50
0
*
DMSO
2-BP

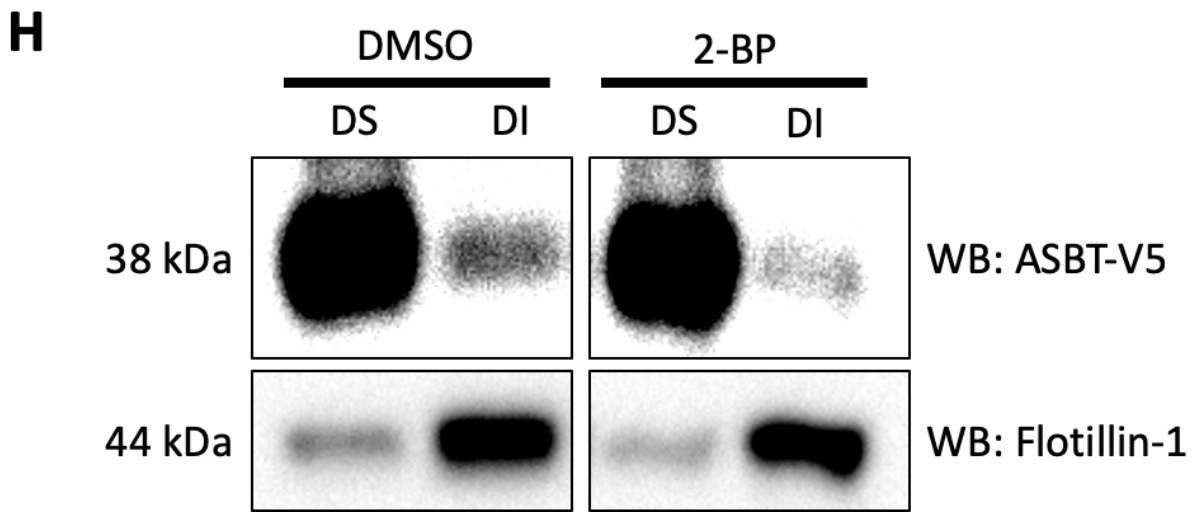

Figure 16. 2-bromopalmitate decreases ASBT acylation and transporter activity. (A) Schematic of metabolic labeling by alkyne-palmitic acid (alk-PA) in 2BT cells. Alk-PA incorporates into acylated proteins and is conjugated to biotin by click chemistry. Biotinylated proteins are precipitated with streptavidin agarose resin. (B,C) Incorporation of alk-PA in ASBT in the presence or absence of 25 μM 2-BP; n=3, *$p < 0.05$. (D) [^{3}H]-taurocholate uptake in 2BT cells treated with 25 μM 2-BP for 30 min; n=6, ****$p < 0.0001$. (E) [^{3}H]-taurocholate uptake in 2BT cells treated with 25 μM 2-BP for 15 h; n=6, ****$p < 0.0001$ compared to control. (F) Bioluminescence and area under the curve calculations from 2BT cells treated with 1 μM CA-SS-Luc and 100 μM TC added simultaneously with either 10 μM or 25 μM 2-BP and imaged in real time; n=4, ****$p < 0.0001$ compared to DMSO, †††† $p < 0.0001$ compared to 10 μM 2-BP. (G) Cell surface biotinylation of 2BT cells treated with 25 μM 2-BP for 30 min; n=4, *$p < 0.05$. (H) Distribution of ASBT in lipid raft microdomains in 2BT cells treated with 25 μM 2-BP for 15 h; n=1.

3. Incubation with unsaturated fatty acids decreases ASBT function

Although palmitic acid (PA) is the most common fatty acid seen in S-acylated proteins, other types of fatty acids can be incorporated into proteins (130, 153). In order to determine whether other fatty acids can be incorporated into ASBT, we performed metabolic labeling with alkyne-oleic acid (alk-OA). As shown in **Figure 17A**, alk-OA was incorporated into ASBT, indicating that oleic acid and other unsaturated fatty acids may S-acylate ASBT. Interestingly, the type of fatty acyl moiety has been shown to affect the function of acylated proteins (37, 160, 227). We hypothesized that incubation with fatty acids other than PA would result in altered ASBT function. 2BT cells were incubated for 15 h with fatty acid-free BSA (FA-free) or 100 μM either palmitic acid (PA; 16:0), stearic acid (SA; 18:0), oleic acid (18:1); α-linolenic acid (ALA; 18:3), or eicosapentanoic acid (EPA; 20:5). Following incubation, [^{3}H]-taurocholate (TC) uptake was performed and results were normalized to FA-free incubation. Treatment with saturated fatty acids PA and SA did not significantly change [^{3}H]-TC uptake. However, incubation with 18:1 unsaturated OA decreased uptake by ~50%. Both ALA (18:3) and EPA (20:5) further decreased [^{3}H]-TC uptake to ~10% and ~25% of control, respectively (**Figure 17B**). In order to demonstrate that these cells remain viable after OA or ALA treatment, we incubated 2BT cells with 100 μM either OA or ALA for 15 h, followed by additional 24 h of either replenishment with the same fatty acid or replacement with 100 μM PA. As shown in **Figure 17C**, replacement with PA was able to reverse the effect of OA and ALA, supporting the viability of these cells. Using the CA-SS-Luc bioluminescence approach from measuring ASBT function, PA incubation significantly increased bioluminescence by ~30% compared to DMSO control, while OA incubation reduced bioluminescence by ~75% after 45 minutes of imaging (**Figure 17D**). These studies indicate that

unsaturated fatty acids may decrease ASBT function via a mechanism dependent on ASBT acylation.

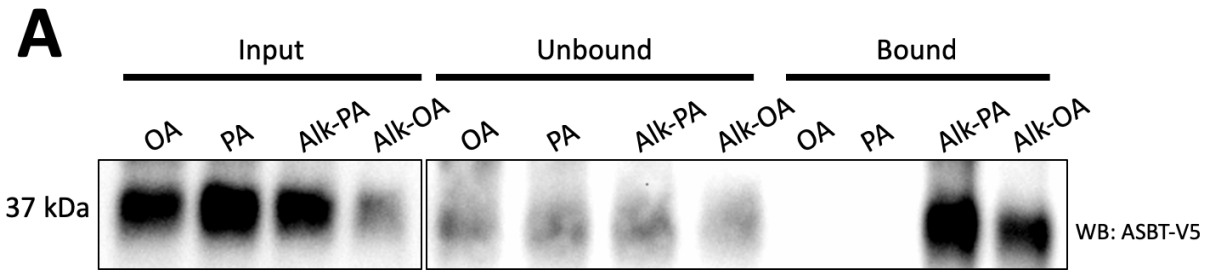
A
Input
Unbound
Bound
OA
PA
Alk-PA
Alk-OA
OA
PA
Alk-PA
Alk-OA
OA
PA
Alk-PA
Alk-OA
37 kDa
WB: ASBT-V5

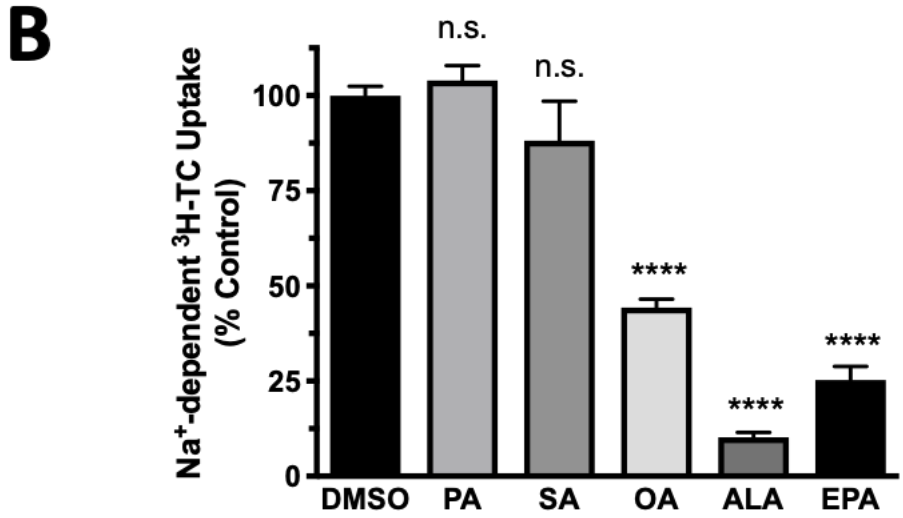
B
n.s.
n.s.
****
****
****
Na+-dependent 3H-TC Uptake
(% Control)
100
75
50
25
0
DMSO
PA
SA
OA
ALA
EPA

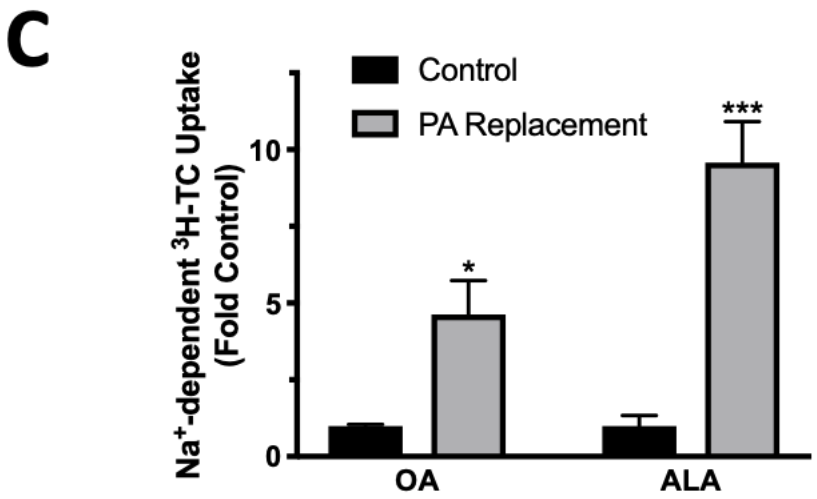
C
Control
PA Replacement
***
*
Na+-dependent 3H-TC Uptake
(Fold Control)
10
5
0
OA
ALA

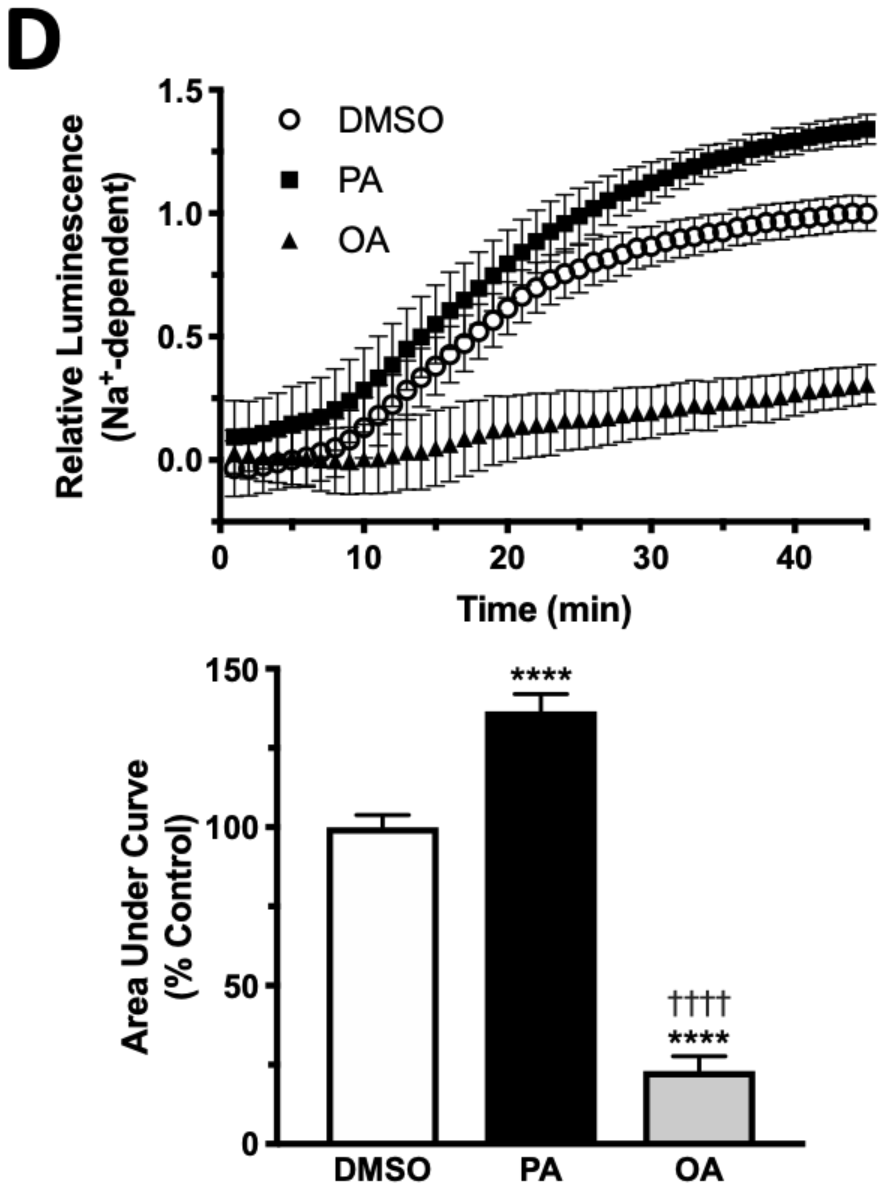

Figure 17. Incubation with unsaturated fatty acids decreases ASBT function. (A) Metabolic labeling of ASBT by alkyne-oleic acid (alk-OA) in 2BT cells (representative western blot of 3 separate experiments) (B) [^{3}H]-taurocholate uptake in 2BT cells treated with DMSO or either 100 µM palmitic acid (PA), stearic acid (SA), oleic acid (OA), α-linolenic acid (ALA), or eicosapentanoic acid (EPA) for 15 h; n=6, ****$p < 0.0001$ compared to control. (C) [^{3}H]-taurocholate uptake in 2BT cells treated with 100 µM either OA or ALA for 15 h, followed by additional 24 h of either replenishment with the same fatty acid or replacement with 100 µM PA; n=6, *$p < 0.05$, ***$p < 0.001$ compared to control. (D) Real-time uptake (left) and area under the curve calculation (right) of bioluminescent bile acid tracer CA-SS-Luc in 2BT cells treated with DMSO, 100 µM PA, or 100 µM OA; n=4, ****$p < 0.001$ compared to DMSO, †††† $p < 0.001$ compared to PA.

4. Cysteine 314 is important for ASBT S-acylation and transport function

In order to determine which cysteine residue(s) are important for ASBT S-acylation, we generated 10 ASBT-V5 plasmids with cysteine to serine point mutations (**Table 2**, pg.75). 9 of the 13 cysteine residues were mutated, as well as one double mutant (CC105/106SS). These plasmids were transfected in HEK 293 cells and western blotting and [^{3}H]-TC uptake was performed. As shown in **Figure 18A**, all of the mutants retained expression in these cells. However, many showed significantly decreased function relative to wild-type ASBT (**Figure 18B)**. Of particular note for these studies are the four constructs with mutated cysteine residues located in the cytosolic loops of ASBT (C51S, C69S, C74S, and C314S). These residues are the best candidate sites for S-acylation, as the catalytic site for zDHHC acyltransferases is cytosolic. These four mutants all showed significantly reduced transport function. Indeed, [^{3}H]-TC uptake was almost completely abolished in C51S, C69S, and C74S, and was reduced by >50% in the C314S mutant (**Figure 18B**). To further investigate these cytosolic cysteine mutants, we transfected HEK 293 cells and performed acyl-RAC as described earlier. Interestingly, the C314S mutant showed significantly lower acylation compared with wild-type ASBT, while the other mutants did not show any change in acylation (**Figure 18C)**. These data indicate that C314 is acylated under basal conditions and that blocking acylation at this site may contribute to the reduction in ASBT transport function. However, as can be seen in **Figure 18C**, there is a population of ASBT C314S that remains acylated, suggesting the involvement of additional cysteine residues.

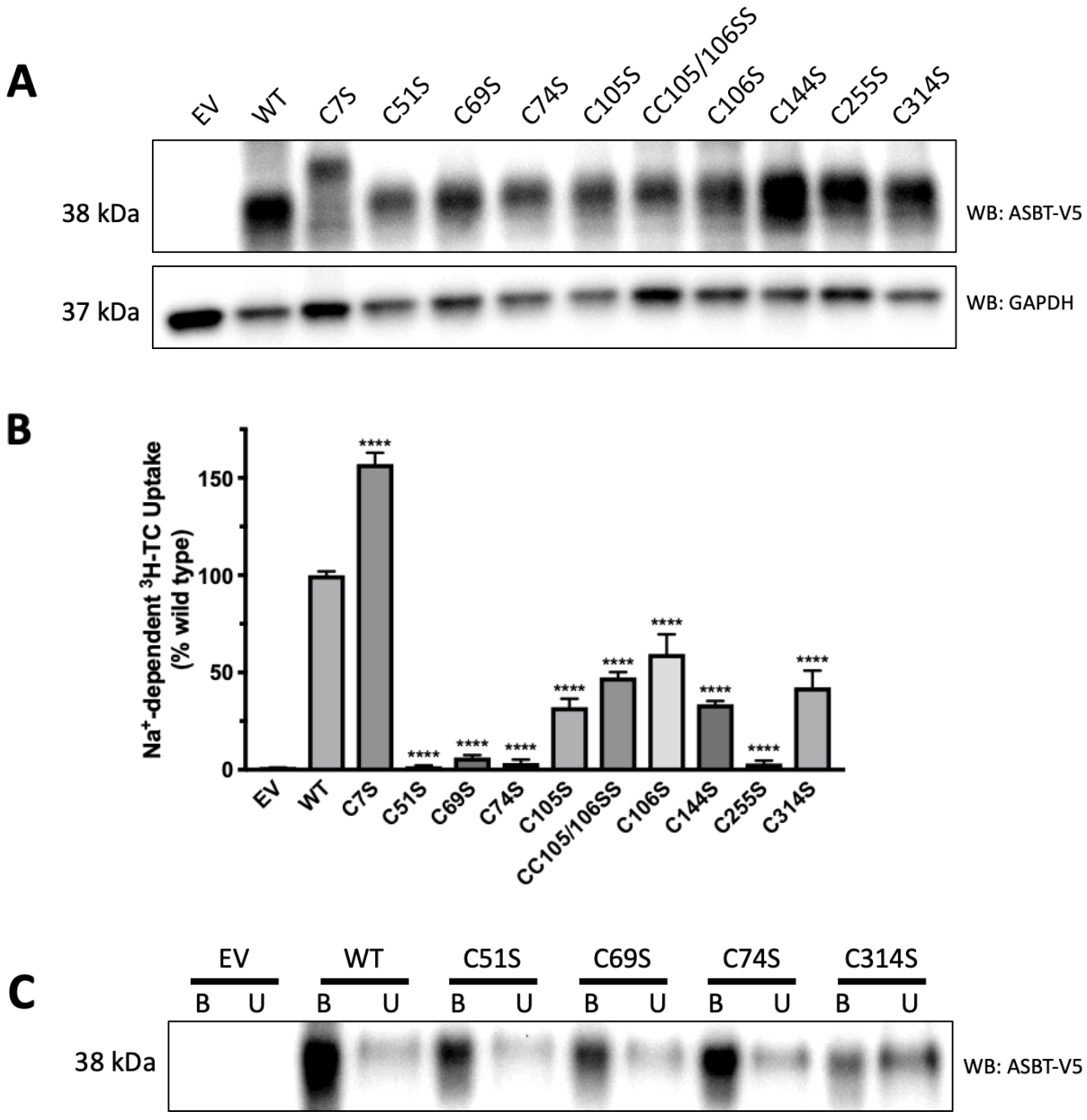

Figure 18. Cys314 is important for ASBT S-acylation and transport function. Cellular expression (A) and [^{3}H]-taurocholate uptake (B) in HEK 293 cells transfected with ASBT-V5 cysteine mutants; n=3, ****p < 0.0001 compared wo wild type. (C) Acyl-RAC of select ASBT-V5 cysteine mutants (representative of 3 western blots with similar results).

D. Discussion

In this chapter, we have demonstrated that S-acylation is an important post-translational regulatory mechanism that modulates ASBT function. It is important to note that unlike many other PTMs, there are no known sequence motifs that are useful for predicting which proteins are likely to be S-acylated. There are some prediction tools available (114, 207, 276, 286), but it remains necessary to empirically identify S-acylated proteins. To date, no studies examining the global pool of S-acylated proteins in the intestine have been performed. Thus, ASBT had not yet been identified as an S-acylated protein. In the present study, we demonstrated by acyl-RAC that ASBT is S-acylated in human and mouse ileum under basal conditions, as well as in human embryonic kidney (HEK) 293 cells that overexpress ASBT-V5 (2BT cells). Furthermore, studies in 2BT cells showed that alk-PA incorporation into ASBT is reduced ~50% by the competitive acyltransferase inhibitor 2-bromopalmitiate (2-BP), providing further evidence that ASBT is a substrate for zDHHC palmitoyl acyltransferases. Interestingly, incubation with 2-BP not only reduced ASBT acylation, but also reduced ASBT plasma membrane expression. Furthermore, preliminary evidence indicates that 2-BP causes a reduction in ASBT association with lipid rafts. These data suggest that S-acylation may contribute to targeting ASBT to plasma membranes, as well as promoting ASBT association lipid raft microdomains. Importantly, these experiments also demonstrate that ASBT acylation is functionally relevant. Indeed, 2-BP treatment for 15 h drastically decreased transport function (~90% inhibition at 25 μM). Even short-term treatment with 2-BP significantly reduced ASBT function. 30 min treatment with 25 μM 2-BP reduced [^{3}H]-TC uptake by ~50%, suggesting that ASBT S-acylation may be subject to rapid turnover. Similarly, real-time measurement of CA-SS-Luc bioluminescence was reduced by ~70% by 10 μM 2-BP and almost completely abolished be 25 μM 2-BP over the course of 45 min imaging.

Interestingly, recent evidence has indicated that the effects of S-acylation may vary depending on the specific fatty acid bound to a protein. Originally, palmitic acid was thought to be the principal fatty acid attached to cysteine residues, which is why this PTM has traditionally been called palmitoylation. However, it has become understood that other fatty acids can also be substrates for S-acylation. Indeed, studies from the Laposata laboratory used gas chromatography/mass spectrometry to show that in human platelets, ~74% of the pool of S-acylated fatty acids were palmitic acid, ~22% were stearic acid, and ~4% were oleic acid (183). Importantly, they did note that intersubject variability was high, and that the composition of this pool could be altered by exogenous supplementation of fatty acids. These studies highlight the potential role of non-palmitic fatty acids in regulating proteins via S-acylation. Other studies have demonstrated that zDHHC enzymes, which are the acyltransferases responsible for S-acylation, have a relatively broad substrate specificity that allows PA, OA, and long chain polyunsaturated fatty acids to act as substrates for S-acylation (94, 285). Indeed, numerous studies have identified distinct functional effects depending on the fatty acyl moiety attached to a protein (227). For example, studies demonstrated that polyunsaturated FAs can be attached to cysteine residues in order to reduce association with lipid rafts and affect protein function (37, 160). In the present study, we showed that 15 h incubation of 2BT cells with saturated PA increased ASBT function, while incubation with unsaturated OA and polyunsaturated ALA and EPA decreased transporter activity. Using click chemistry-based metabolic labeling, we also showed that alkyne-oleic acid incorporates into ASBT, indicating that the effects of unsaturated FAs on ASBT function may be dependent on S-acylation.

Given that ASBT S-acylation is important for association with lipid rafts and protein function, it was important to identify which cysteine residue(s) are subject to this PTM. We

generated 10 ASBT constructs with Cys to Ser point mutations and found that while all proteins were expressed in transfected HEK 293 cells, several displayed significantly reduced transport function. Of particular note were the mutants C51S, C69S, C74S, and C314S. These mutated residues are present in cytosolic domains of ASBT, where S-acylation is likely to occur (22, 40). Of these, C314 showed ~60% decreased function, while the others were unable to transport [^{3}H]-TC. The effect of these mutations on the function of ASBT is consistent with previous studies from the Swaan laboratory, who had mutated each cysteine residue to either alanine or threonine (22). However, whether these cysteine residues were subject to S-acylation was not explored in those studies. We examined these cytosolic cysteine mutants by performing acyl-RAC and found that a smaller pool of C314S ASBT was S-acylated compared to wild type ASBT, whereas the other mutants did not show decreased acylation. This indicates that Cys314 is subject to S-acylation, but the fact that a sizeable pool of ASBT C314S remains acylated suggests the involvement of additional acylation sites. Further study will be necessary in order to determine which other cysteine residues are subject to S-acylation and also which acyltransferases and thioesterases are involved in ASBT acylation.

It will be interesting in future studies to determine whether ASBT S-acylation is important in the pathology of diseases in which ASBT is implicated. It has been shown that several disease states, including obesity and metabolic syndrome, are associated with alterations in the global pool of S-acylated proteins, often referred to as the palmitoylome (208, 221). It is interesting to note that dietary lipids, insulin signaling, and ethanol metabolism can also alter the palmitoylome (84, 235, 236, 277). For instance, feeding of a high-fat diet (~60% calories from saturated FAs) was associated with hyper-palmitoylation and dysregulation of AMPA glutamate receptor subunit GluA1 in the brain (236). These studies strongly suggest that consumption of FAs affects global

S-acylation. However, it is not known whether changing the composition of dietary FAs will affect the fatty acyl moieties attached to proteins, which could be expected to show functional changes. Therefore, it will be important in future studies to examine the effects of individual dietary compounds as well as disease states on ASBT acylation status and transport function, both in cell culture and *in vivo* models.

In conclusion, we have discovered that ASBT function is dependent on its S-acylation. Inhibiting acylation with 2-BP or incubation with unsaturated FAs decrease ASBT function, while incubation with saturated PA increases ASBT function. We identified Cys314 as a potential site of S-acylation, but there are likely other sites that remain unidentified. Future studies should focus on the role of ASBT S-acylation in the pathophysiology of diseases in which ASBT is implicated.

Chapter IV: Conclusions and future directions

It has been demonstrated that the activity of ASBT is regulated on a rapid time-scale by a variety of post-translational mechanisms and that this regulation is not fully captured by traditional methods of assessing transporter activity. The goal of this dissertation was to develop a new method for measuring the activity of ASBT and other BATs that would allow these rapid changes in function to be fully revealed. Additionally, we sought to elucidate the role of S-acylation in the post-translational regulation of ASBT. In **chapter II**, we presented evidence that a novel cholic acid-luciferin conjugate probe (CA-SS-Luc) is suitable for real-time assessment of bile acid transporter activity. This method has been examined using *in vitro* and *ex vivo* models. In **chapter III**, we demonstrated that ASBT is subject to S-acylation, an important post-translational modification. Additionally, we showed that ASBT S-acylation has an important regulatory role in the function and subcellular localization of ASBT.

A. Bioluminescent method for measuring BAT activity

In **chapter II**, we present a method for real-time assessment of bile acid transporter activity. This method was based on a similar approach that was developed to measure fatty acid uptake in real time and in living systems (103). Our approach, shown in **Figure 5**, relies on a novel molecular probe comprising a cholic acid moiety conjugated to firefly luciferin via a cleavable, self-immolating disulfide linker (CA-SS-Luc). Upon entry into cells, CA-SS-Luc is broken down, releasing free D-luciferin. D-luciferin is then oxidized by firefly luciferase, producing visible light. Thus, luminescence production is expected to be proportional to the amount of CA-SS-Luc taken into the cell.

To synthesize CA-SS-Luc, we generated a cholic acid analogue, where the carboxylic acid moiety is replaced by a thiol moiety (**Figure 6**). This allows for disulfide conjugation to firefly D-

luciferin via a multi-step synthesis. We first tested CA-SS-Luc in HEK 293 cells transfected with a BAT, either ASBT or NTCP. This model system was chosen because bile acid transport in ASBT-transfected HEK 293 cells is regulated in a similar manner to native intestinal cells (12, 14). Additionally, the technical ease of this model system makes it attractive for high throughput assays, which are a potential application for this method. In HEK 293 cells transfected with ASBT (2BT cells), we first demonstrated that the luminescence generated by CA-SS-Luc is dependent on both the concentration of probe added to the cells, as well as the incubation time (**Figure 7**). Both of these findings are expected for a transporter-dependent uptake process, as increasing the concentration of substrate and incubation time will increase uptake. Importantly, we showed that CA-SS-Luc bioluminescence was dependent on the protein expression of the transporter (**Figure 8**). When increasing amounts of either ASBT or NTCP were transfected, luminescence was correspondingly higher, representing increased uptake of CA-SS-Luc. Furthermore, we found that the luminescence from CA-SS-Luc is greater than the luminescence generated by the same concentration of D-luciferin (**Figure 9**). This important finding demonstrated that the uptake of CA-SS-Luc is an active process, as the rate of uptake is faster than the diffusion rate of D-luciferin. Most importantly, we demonstrated that this method was able to capture dynamic changes in ASBT function. Treatment with protein tyrosine phosphatase inhibitor III (PTPIII), which has previously been shown to enhance ASBT function, increased CA-SS-Luc luminescence both when cells were pretreated with PTPIII and when cells were treated with PTPIII at the initiation of luminescence imaging (**Figure 10**). We also showed that bioluminescence rapidly decreased with CA-SS-Luc washout (**Figure 11**). These findings established conclusively that our method indeed is able to measure real-time changes in ASBT function. This was further confirmed in **chapter III**, when we showed that treatment with the palmitoyl acyltransferase inhibitor 2-bromopalmitate (2-

BP) decreased ASBT function as measured by both [^{3}H]-TC uptake and CA-SS-Luc bioluminescence (**Figure 16**). Interestingly, we also found that coincubation of CA-SS-Luc with natural BAs enhanced CA-SS-Luc luminescence in cells expressing ASBT or NTCP, but not cells expressing the serotonin transporter (**Figure 12**). This phenomenon was dose- and sodium-dependent and was reproducible with all the bile acids we tested, suggesting that it indeed represented a bile acid transport process. This was initially a somewhat puzzling observation, as we expected natural BAs to compete for BAT-dependent uptake. However, there are several indications that this finding may represent an activation of transport activity by these endogenous ligands. First, we expect that CA-SS-Luc is a relatively low affinity substrate for these transporters, given that other synthetic bile acid C-24 conjugates have been shown to have lower affinity than natural substrates (230, 248). Also, recent evidence has indicated that ASBT and NTCP both function as homodimers (30, 54). This suggested to us that the presence of a high affinity natural ligand may enhance the activity of the transporter for lower affinity ligands, such as CA-SS-Luc. This could be mediated through a cooperativity between BAT monomers or might be an inherent property of the transporters. Identifying the molecular basis behind the enhanced CA-SS-Luc luminescence in the presence of endogenous BAs will be important for future studies, as it may reveal new information about the transport mechanism of SLC10A transporters. It will also be interesting in the future to examine whether this phenomenon in BATs that are not in the SLC10A family, such as OSTα/β.

It is important to discuss several advantages that our method presents over other methods for measuring BAT function. First, traditional methods that rely on measuring radioactive uptake do not provide crucial minute-to-minute resolution of ASBT function. In order to assess the effect of a given treatment on ASBT function, one must add the treatment to cells, wait a predetermined

amount of time, washout the treatment, equilibrate cells in a bile acid uptake buffer, add [^{3}H]-TC, and allow uptake for several minutes, followed by washing, cell lysis, and scintillation counting. This provides few options for measuring the effect of short-term treatments, as equilibration and uptake necessitates at least a 15-minute delay. Even if the equilibration step were eliminated in order to reduce this delay, this method is severely limited by the fact that only one treatment time point can be measured. In contrast, the bioluminescence-based method allows for transport calculations immediately after initiating a given treatment and at each successive minute for at least 45 minutes.

It is important to note that we are not the first to recognize that traditional radioactive uptake methods are insufficient for understanding the intricacies of enterohepatic bile acid homeostasis. Indeed, there have been several other methods for measuring bile acid homeostasis in real time. For instance, a tri-fluorinated synthetic bile acid has been developed in order to use [^{19}F]-magnetic resonance imaging (MRI) to assess bile acid malabsorption in human patients, a disease with limited diagnostic testing options (48, 77, 171, 205, 258-260). This method has been extensively validated in animal models, demonstrating its ability to effectively measure intestinal bile acid absorption and transport through the portal circulation to the liver and gallbladder. While this approach addresses a key unmet clinical need, it is critical to mention that this method is unable to directly measure bile acid transporter activity in real time. Rather, this probe serves as a tracer that may be suitable for global assessment of the physiological processes by which bile acids are moved from the intestinal lumen to the liver and gallbladder. In addition to the [^{19}F]-MRI approach, there has been one other important method for measuring real time bile acid homeostasis. The van de Graaf laboratory recently developed a fluorescence resonance energy transfer (FRET)-based biosensor with the capacity to measure the intracellular concentration of

bile acids with subcellular resolution (253, 256). The exquisitely designed biosensor, which is based on the endogenous bile acid sensor FXR, allows for the monitoring of bile acid dynamics in single cells. However, as this sensor is designed to measure intracellular BA concentrations, it is not able to provide a true measurement of transporter activity. This approach efficiently measures rapid changes in BA homeostasis, eventually settling at a stable FRET value that represents the steady state BA concentration under a given set of conditions. Thus, the measurement will represent a combination of BA uptake, BA export, and intracellular BA availability (which may be reduced by the presence of bile acid-binding proteins). Additionally, the dynamic range of this technique is relatively small (~1-30 μM), as it depends on the affinity of the sensor for BAs.

In contrast to the approaches described above, the method presented in this thesis is designed to precisely measure uptake activity of bile acid transporters, given that it relies on intracellular cleavage of a disulfide bond. Thus, when CA-SS-Luc is introduced to a cell, it will be taken into the cytosol via a BAT and light will be produced. In this way, our method is designed to specifically assess the function of bile acid uptake transporters and not to assess global bile acid absorption. Additionally, the dynamic range of this approach is considerably larger as it depends on the intracellular glutathione concentration and luciferase activity, which are expected to be high capacity (78, 93). It is particularly interesting to note that this method allows for real-time measurement of the relative rate of bile acid uptake. For every CA-SS-Luc molecule that is transported into a cell and cleaved to D-luciferin, one photon is released. Thus, when an image with a one-minute exposure is captured, the resulting luminescence is directly proportional to the number of CA-SS-Luc molecules transported during that minute. The fact that this measurement represents a transport rate may allow for nontraditional assessment of transporter activity that could provide unique insights into the regulation of BATs. At the most basic level, when looking

at a plot of luminescence vs. time, integration of the resulting curve will provide a value directly proportional to the total number of CA-SS-Luc molecules that have entered a cell. Indeed, this is the measurement that most closely represents traditional radioactive [^{3}H]-TC uptake studies, with the additional benefit that these measurements can be calculated each minute, rather than only at the conclusion of the experiment. In addition to integrating the curve, measuring the slope may also provide useful information, particularly during perfusion experiments when solutions could be changed during the course of an experiment. This might allow for calculation of how a given treatment changes transport kinetics in real time, as well as how quickly this change occurs.

One of the most exiting applications of this method relates to its feasibility for *in vivo* use. Currently available *in vivo* methods for assessing bile acid homeostasis rely on either [^{3}H]-TC or [^{19}F]-MRI. Despite their utility, these methods have several practical and technical limitations, necessitating the development of additional methods. As discussed earlier, these approaches are useful in that they can provide a global assessment of bile acid homeostasis. Whereas approaches depending on radiolabeled BAs are destructive methods that require sacrifice of the animal, the [^{19}F]-MRI method has a major advantage in that it can be performed in live animals. Unlike the CA-SS-Luc method that requires transgenic luciferase expression, the [^{3}H]-TC and [^{19}F]-MRI techniques can be used in any research animal, and the [^{19}F]-MRI approach may even be useful in the clinic. Nevertheless, neither the [^{3}H]-TC nor [^{19}F]-MRI methods are able to directly assess cellular uptake of bile acids *in vivo*, as they are confounded by the presence of bile acid export proteins. As shown in **Figure 13**, the method we developed appears to be dependent on ASBT expression in IECs isolated from transgenic mice that express luciferase (Luc^{Tg} mice). Given the availability of these mice, validating our approach *in vivo* could provide an attractive and technically simple method to study *in vivo* bile acid homeostasis.

In order to apply this method to *in vivo* models, it will be crucial to ensure that when mice are gavaged with CA-SS-Luc, the bioluminescence signal generated is dependent on ASBT. Thus, these studies should be performed in $ASBT^{-/-}$ mice crossbred with Luc^{Tg} mice, as well as in Luc^{Tg} mice fed with an ASBT inhibitor. Once a method for *in vivo* measurement of real-time ASBT activity is optimized, a wide array of critical studies could be undertaken. Most importantly, this technique will allow for direct assessment of ASBT function in the context of disease models and therapeutic interventions. For instance, there is evidence that ASBT function contributes to metabolic syndrome. However, direct evidence of this is somewhat limited. It would be of great interest to compare ASBT activity in diabetic, obese, and/or hyperlipidemic mice. A major advantage of such an approach is that the same mouse could serve as its own control, so the effect of a given treatment or diet could be studied in the same animal. Also, this method could be used to study the activity of bile acid transporters throughout the lifetime of an animal. A great deal of evidence has shown that ASBT expression is low in the neonatal period and is enhanced after weaning (58, 61, 176). A recent study also showed that ileal ASBT expression and [^{3}H]-TC uptake was markedly reduced in 2-year-old mice. However, it would be interesting to further examine these findings in live animals over the course of their lifetime. It will also be interesting to us CA-SS-Luc to explore bile acid uptake in other tissues. Injection of CA-SS-Luc into the tail vein of Luc^{Tg} mice could show bile acid uptake in organs previously not known to transport BAs, which may provide clues with respect to the role of BAs outside of the enterohepatic system. Furthermore, recent studies have demonstrated that ASBT is expressed in the brain. It is possible that cerebrospinal fluid infusion of CA-SS-Luc would provide an interesting way to study the relatively unexplored field of bile acid physiology in the brain. Undoubtedly, once the *in vivo* use

of CA-SS-Luc is optimized, it will be an exceptionally powerful tool to study bile acid transporters throughout the body.

B. Regulation of ASBT by S-acylation

In **chapter III**, we present a series of studies that demonstrate a novel mechanism by which ASBT activity and subcellular localization can be regulated. A vast array of evidence has demonstrated that ion channels and transport proteins are commonly subject to S-acylation. Indeed, more than 50 ion channel subunits and many other transporters are S-acylated (39, 227). In these proteins, S-acylation has been shown to regulate quaternary structure assembly, subcellular trafficking, transport kinetics, protein stability, and modification by other PTMs such as phosphorylation (39). In this way, S-acylation can be involved in virtually every aspect of channel and transporter biology. In these studies, we demonstrated that ASBT is subject to S-acylation, and that this important PTM regulates protein function and subcellular localization. We first showed that ASBT is S-acylated in native intestinal tissues from mice and human donor samples using acyl resin-assisted capture (acyl-RAC) and further showed its S-acylation in 2BT cells by acyl-RAC and metabolic labeling with alkyne-palmitic acid (alk-PA) (**Figures 14-15**). These data demonstrated that ASBT S-acylation is well-conserved between species and model systems. We further demonstrated that ASBT S-acylation can be inhibited using the palmitoyl acyltransferase inhibitor 2-BP (25 μM, 15 h, **Figure 16**). It will be interesting in future studies to identify which zDHHC acyltransferase is responsible for ASBT S-acylation. Currently, identifying which enzymes are involved is technically challenging, as there are no specific inhibitors for individual zDHHC enzymes. Thus, these studies would likely need to be performed by overexpression and siRNA knockdown strategies. Overexpression and knockdown of these

enzymes must be confirmed by RT-PCR and western blotting, and ASBT S-acylation would be measured by alk-PA labeling. These experiments would be further complicated by the fact that many of these zDHHC enzymes display some redundancy (124). Thus, it may be necessary to perform combined siRNA knockdowns before an effect on ASBT S-acylation is observed. These experiments will be important in order to fully understand how ASBT S-acylation is regulated, as well as for targeting this pathway therapeutically.

After demonstrating that ASBT is S-acylated and that this process can be inhibited by 2-BP, we showed that ASBT S-acylation is important for ASBT function and subcellular localization (**Figure 16**). 15 h treatment with 2-BP significantly reduced ASBT-dependent [^{3}H]-TC uptake in 2BT cells, which was accompanied by a shift of ASBT out of detergent-insoluble lipid raft membrane fractions. These data indicate that S-acylation is important for targeting of ASBT to lipid raft domains, which has previously been shown critical for the function of this transporter (14). Interestingly, there was also a short-term effect of 2-BP treatment. 30 min incubation with 2-BP was sufficient to decrease ASBT-dependent [^{3}H]-TC uptake and reduce its plasma membrane expression, suggesting that ASBT S-acylation is also important for plasma membrane targeting. Importantly, this was further confirmed using real-time CA-SS-Luc-based imaging. When 2-BP treatment and CA-SS-Luc imaging were performed simultaneously, the rate of CA-SS-Luc luminescence production was significantly reduced compared to control at exceptionally early time points (<10 min). It is interesting that an effect of 2-BP could be observed within only a few minutes, which leads to questions about the mechanism underlying this rapid decrease in ASBT activity. If such a rapid effect is indeed the result of direct inhibition of ASBT acylation, that would first require deacylation of ASBT by acylthioesterases, as we have shown that the majority of ASBT is S-acylated at baseline. After this deacylation occurs, 2-BP inhibition of acyltransferases

would then result in the decreased activity seen in our studies. This is a reasonable hypothesis, as it has been shown that many S-acylated proteins are subject to rapid fatty acid turnover (167, 211, 212). Nevertheless, it is possible that the short-term effect of 2-BP on ASBT function is not dependent on the direct acylation of ASBT, but rather may involve other intermediates or signaling pathways. In order to elucidate this mechanism, it will be important to quantify ASBT S-acylation following short-term 2-BP treatment using acyl-RAC and metabolic labeling approaches. Additionally, it will be useful to measure ASBT lipid raft and cell surface localization to determine whether short-term 2-BP treatment changes the subcellular distribution of ASBT. It should be noted that typical metabolic labeling studies cannot be performed at such short treatment time points, necessitating other approaches to measure the short-term effect of 2-BP on ASBT acylation. Instead of cotreating cells for 15 h with 2-BP and alk-PA, it may be useful to first label cells for 15 h with alk-PA, followed by a short-term treatment with 2-BP and subsequent measurement of alkyne-palmitoylated ASBT. If short-term 2-BP treatment does reduce ASBT acylation, this would provide strong evidence that ASBT S-acylation is rapidly and dynamically regulated. It is key to mention that these findings highlight a major advantage of real time approaches for measuring bile acid transport activity. By comparing the two methods for measuring ASBT transport activity shown in **Figure 16**, it is clear that the real time method is a more sensitive method for detecting changes in transport function. At 30 min of treatment with 25 μM 2-BP, [^{3}H]-TC uptake was reduced by ~50%. In contrast, the rate of CA-SS-Luc luminescence production after 30 min of treatment was ~90% lower than control cells.

It was especially interesting to find that not only is ASBT S-acylation important for transport function, but that the specific fatty acid attached to ASBT also dramatically affects ASBT activity. We showed in **Figure 17** that when 2BT cells were incubated for 15 h with 100 μM of

unsaturated OA, [^{3}H]-TC uptake was reduced by >50%. Incubation with polyunsaturated fatty acids ALA and EPA further reduced [^{3}H]-TC uptake by as much as 90%. However, incubation with saturated PA or SA did not significantly change [^{3}H]-TC uptake. When confirming these findings by CA-SS-Luc luminescence, we found that OA incubation reduced AUC by ~75%, while PA incubation actually increased AUC by ~30%. Using alk-OA metabolic labeling, we demonstrated that alk-OA incorporates into ASBT, indicating that reduced ASBT function may be the result of changes in the S-acylated fatty acid.

These studies provide cause for interesting speculation with respect to the role of diet in bile acid homeostasis. It is known that the proportion of S-acylated fatty acids is dependent at least in part on the relative availability of each fatty acid species (183). It is likely that diets high in unsaturated fatty acids lead to increased availability of these fatty acids within intestinal epithelial cells. It is then possible that S-acylation of ASBT by unsaturated fatty acids will be increased, resulting in reduced ASBT function, reduced intestinal bile acid absorption, and increased fecal bile acid excretion. This could have a variety of downstream effects that might be similar to the medications that target bile acid absorption, such as reduced intestinal FXR activation, enhanced hepatic bile acid synthesis genes, and reduced plasma LDL cholesterol (LDL-C). Interestingly, it is well-known that diets high in unsaturated fatty acids can reduce LDL-C. For instance, a Mediterranean diet has been shown to reduce LDL-C as well as the rate of cardiovascular events (67). The fatty acid composition of a prototypical Mediterranean diet comprises up to 10% polyunsaturated fatty acids and >80% monounsaturated fatty acids (67). It is therefore possible that incorporation of unsaturated fatty acids into ASBT is partly responsible for the cardioprotective effect of these diets.

Unfortunately, relatively little is known with respect to the role of dietary fatty acids on bile acid homeostasis. In order to elucidate the effect of dietary fats on bile acid homeostasis, it will be useful to look closely at how they affect the activity of ASBT and other bile acid transporters. Once an *in vivo* method for measuring real-time ASBT function using CA-SS-Luc has been developed and optimized, this will be an indispensable tool for studying the effect of diet on bile acid transporter activity. Such studies could involve feeding of a diet high in either saturated or unsaturated fatty acids, followed by *in vivo* measurement of ASBT activity. As an additional control, ASBT function could also be measured prior to initiation of the diet. If a change in ASBT function is observed with either diet, it would also be important to demonstrate that the dietary fatty acids were incorporated into ASBT at higher levels than in control animals. This could be accomplished by immunoprecipitating ASBT from ileal protein lysates, followed by cleavage of thioester bonds by hydroxylamine and mass spectrometric analysis of the released fatty acids.

In addition to showing that the S-acylation of different fatty acids can affect ASBT function, it was also important for us to identify the precise cysteine residues that are subject to S-acylation. We generated cysteine to serine mutants for nine individual cysteine residues, as well as one double mutant (**Figure 18**). All mutants showed cellular expression in HEK 293 cells, but several showed reduced [^{3}H]-TC uptake compared to wild type ASBT. We identified five mutants with mutations present in the cytosolic domains of ASBT as the most likely sites of S-acylation, given that zDHHC palmitoyl acyltransferases have a cytosolic catalytic site. All five of these mutants displayed reduced [^{3}H]-TC uptake, but only Cys314Ser showed reduced (but not abolished) S-acylation as measured by acyl-RAC. Future studies should aim to identify any other potential sites of S-acylation using a combination of acyl-RAC and metabolic labeling approaches. Furthermore, it will be important to determine whether nonacylated mutants have improper

subcellular localization. Such a defect could cause either poor lipid raft localization or could impair plasma membrane trafficking, which could provide crucial insight into the molecular mechanisms underlying ASBT regulation by S-acylation.

In conclusion, our studies have established an innovative tool for assessing bile acid transporters, which has important *in vitro* and *in vivo* applications. We have also identified and characterized a novel post-translational lipid modification of ASBT that may be crucial for modulating bile acid absorption and homeostasis.

Chapter V: Cited Literature

1. **Abrams JJ**, **Ginsberg H**, **Grundy SM**. Metabolism of cholesterol and plasma triglycerides in nonketotic diabetes mellitus. *Diabetes* 31: 903–910, 1982.

2. **Akhter S**, **Cavet ME**, **Tse CM**, **Donowitz M**. C-terminal domains of Na(+)/H(+) exchanger isoform 3 are involved in the basal and serum-stimulated membrane trafficking of the exchanger. *Biochemistry* 39: 1990–2000, 2000.

3. **Al-Hilal TA**, **Chung SW**, **Alam F**, **Park J**, **Lee KE**, **Jeon H**, **Kim K**, **Kwon IC**, **Kim I-S**, **Kim SY**, **Byun Y**. Functional transformations of bile acid transporters induced by high-affinity macromolecules. *Sci Rep* 4: 4163, 2014.

4. **Al-Hilal TA**, **Park J**, **Alam F**, **Chung SW**, **Park JW**, **Kim K**, **Kwon IC**, **Kim I-S**, **Kim SY**, **Byun Y**. Oligomeric bile acid-mediated oral delivery of low molecular weight heparin. *J Control Release* 175: 17–24, 2014.

5. **Ali AH**, **Carey EJ**, **Lindor KD**. Recent advances in the development of farnesoid X receptor agonists. *Ann Transl Med* 3: 5, 2015.

6. **Alpini G**, **Glaser SS**, **Rodgers R**, **Phinizy JL**, **Robertson WE**, **Lasater J**, **Caligiuri A**, **Tretjak Z**, **LeSage GD**. Functional expression of the apical Na+-dependent bile acid transporter in large but not small rat cholangiocytes. *Gastroenterology* 113: 1734–1740, 1997.

7. **Alrefai WA**, **Gill RK**. Bile acid transporters: structure, function, regulation and pathophysiological implications. *Pharm Res* 24: 1803–1823, 2007.

8. **Alrefai WA**, **Sarwar Z**, **Tyagi S**, **Saksena S**, **Dudeja PK**, **Gill RK**. Cholesterol modulates human intestinal sodium-dependent bile acid transporter. *Am J Physiol Gastrointest Liver Physiol* 288: G978–85, 2005.

9. **Anderle P**, **Sengstag T**, **Mutch DM**, **Rumbo M**, **Praz V**, **Mansourian R**, **Delorenzi M**, **Williamson G**, **Roberts M-A**. Changes in the transcriptional profile of transporters in the intestine along the anterior-posterior and crypt-villus axes. *BMC Genomics* 6: 69, 2005.

10. **Andersson S**, **Davis DL**, **Dahlbäck H**, **Jörnvall H**, **Russell DW**. Cloning, structure, and expression of the mitochondrial cytochrome P-450 sterol 26-hydroxylase, a bile acid biosynthetic enzyme. *J Biol Chem* 264: 8222–8229, 1989.

11. **Annaba F**, **Kumar P**, **Dudeja AK**, **Saksena S**, **Gill RK**, **Alrefai WA**. Green tea catechin EGCG inhibits ileal apical sodium bile acid transporter ASBT. *Am J Physiol Gastrointest Liver Physiol* 298: G467–73, 2010.

12. **Annaba F**, **Ma K**, **Kumar P**, **Dudeja AK**, **Kineman RD**, **Shneider BL**, **Saksena S**, **Gill RK**, **Alrefai WA**. Ileal apical Na+-dependent bile acid transporter ASBT is upregulated in rats with diabetes mellitus induced by low doses of streptozotocin. *Am J Physiol Gastrointest Liver Physiol* 299: G898–906, 2010.

13. **Annaba F**, **Sarwar Z**, **Gill RK**, **Ghosh A**, **Saksena S**, **Borthakur A**, **Hecht GA**, **Dudeja PK**, **Alrefai WA**. Enteropathogenic Escherichia coli inhibits ileal sodium-dependent bile acid transporter ASBT. *Am J Physiol Gastrointest Liver Physiol* 302: G1216–22, 2012.

14. **Annaba F**, **Sarwar Z**, **Kumar P**, **Saksena S**, **Turner JR**, **Dudeja PK**, **Gill RK**, **Alrefai WA**. Modulation of ileal bile acid transporter (ASBT) activity by depletion of plasma membrane cholesterol: association with lipid rafts. *Am J Physiol Gastrointest Liver Physiol* 294: G489–97, 2008.

15. **Anwer MS**, **Stieger B**. Sodium-dependent bile salt transporters of the SLC10A transporter family: more than solute transporters. *Pflugers Arch - Eur J Physiol* 466: 77–89, 2014.

16. **Arab JP**, **Karpen SJ**, **Dawson PA**, **Arrese M**, **Trauner M**. Bile acids and nonalcoholic fatty liver disease: Molecular insights and therapeutic perspectives. *Hepatology* 65: 350–362, 2017.

17. **Bajor A**, **Gillberg P-G**, **Abrahamsson H**. Bile acids: short and long term effects in the intestine. *Scand J Gastroenterol* 45: 645–664, 2010.

18. **Balakrishnan A**, **Polli JE**. Apical sodium dependent bile acid transporter (ASBT, SLC10A2): a potential prodrug target. *Mol Pharm* 3: 223–230, 2006.

19. **Balakrishnan A**, **Wring SA**, **Coop A**, **Polli JE**. Influence of charge and steric bulk in the C-24 region on the interaction of bile acids with human apical sodium-dependent bile acid transporter. *Mol Pharm* 3: 282–292, 2006.

20. **Balistreri WF**, **Heubi JE**, **Suchy FJ**. Immaturity of the enterohepatic circulation in early life: factors predisposing to "physiologic" maldigestion and cholestasis. *J Pediatr Gastroenterol Nutr* 2: 346–354, 1983.

21. **Banerjee A**, **Hussainzada N**, **Khandelwal A**, **Swaan PW**. Electrostatic and potential cation-pi forces may guide the interaction of extracellular loop III with Na+ and bile acids for human apical Na+-dependent bile acid transporter. *Biochem J* 410: 391–400, 2008.

22. **Banerjee A**, **Ray A**, **Chang C**, **Swaan PW**. Site-directed mutagenesis and use of bile acid-MTS conjugates to probe the role of cysteines in the human apical sodium-dependent bile acid transporter (SLC10A2). *Biochemistry* 44: 8908–8917, 2005.

23. **Banerjee A**, **Swaan PW**. Membrane topology of human ASBT (SLC10A2) determined by dual label epitope insertion scanning mutagenesis. New evidence for seven transmembrane domains. *Biochemistry* 45: 943–953, 2006.

24. **Bannan BA**, **Van Etten J**, **Kohler JA**, **Tsoi Y**, **Hansen NM**, **Sigmon S**, **Fowler E**, **Buff H**, **Williams TS**, **Ault JG**, **Glaser RL**, **Korey CA**. The Drosophila protein palmitoylome: characterizing palmitoyl-thioesterases and DHHC palmitoyl-transferases. *Fly (Austin)* 2: 198–214, 2008.

25. **Baringhaus KH**, **Matter H**, **Stengelin S**, **Kramer W**. Substrate specificity of the ileal and the hepatic Na(+)/bile acid cotransporters of the rabbit. II. A reliable 3D QSAR pharmacophore model for the ileal Na(+)/bile acid cotransporter. *J Lipid Res* 40: 2158–2168, 1999.

26. **Benedict M**, **Zhang X**. Non-alcoholic fatty liver disease: An expanded review. *World J Hepatol* 9: 715–732, 2017.

27. **Bennion LJ**, **Grundy SM**. Effects of diabetes mellitus on cholesterol metabolism in man. *N Engl J Med* 296: 1365–1371, 1977.

28. **Beuling E**, **Kerkhof IM**, **Nicksa GA**, **Giuffrida MJ**, **Haywood J**, **aan de Kerk DJ**, **Piaseckyj CM**, **Pu WT**, **Buchmiller TL**, **Dawson PA**, **Krasinski SD**. Conditional Gata4 deletion in mice induces bile acid absorption in the proximal small intestine. *Gut* 59: 888–895, 2010.

29. **Bhat BG**, **Rapp SR**, **Beaudry JA**, **Napawan N**, **Butteiger DN**, **Hall KA**, **Null CL**, **Luo Y**, **Keller BT**. Inhibition of ileal bile acid transport and reduced atherosclerosis in apoE-/- mice by SC-435. *J Lipid Res* 44: 1614–1621, 2003.

30. **Bijsmans ITGW**, **Bouwmeester RAM**, **Geyer J**, **Faber KN**, **van de Graaf SFJ**. Homo- and hetero-dimeric architecture of the human liver Na^+-dependent taurocholate co-transporting protein. *Biochem J* 441: 1007–1015, 2012.

31. **Björkhem I**, **Araya Z**, **Rudling M**, **Angelin B**, **Einarsson C**, **Wikvall K**. Differences in the regulation of the classical and the alternative pathway for bile acid synthesis in human liver. No coordinate regulation of CYP7A1 and CYP27A1. *J Biol Chem* 277: 26804–26807, 2002.

32. **Bradford MM**. A rapid and sensitive method for the quantitation of microgram quantities of protein utilizing the principle of protein-dye binding. *Anal Biochem* 72: 248–254, 1976.

33. **Brufau G**, **Bahr MJ**, **Staels B**, **Claudel T**, **Ockenga J**, **Böker KH**, **Murphy EJ**, **Prado K**, **Stellaard F**, **Manns MP**, **Kuipers F**, **Tietge UJ**. Plasma bile acids are not associated with energy metabolism in humans. *Nutr Metab (Lond)* 7: 73, 2010.

34. **Brufau G**, **Stellaard F**, **Prado K**, **Bloks VW**, **Jonkers E**, **Boverhof R**, **Kuipers F**, **Murphy EJ**. Improved glycemic control with colesevelam treatment in patients with type 2 diabetes is not directly associated with changes in bile acid metabolism. *Hepatology* 52: 1455–1464, 2010.

35. **Camilleri M**. Bile Acid Diarrhea: Prevalence, Pathogenesis, and Therapy. *Gut Liver* 9, 2015.

36. **Carr RM**, **Reid AE**. FXR agonists as therapeutic agents for non-alcoholic fatty liver disease. *Curr Atheroscler Rep* 17: 500, 2015.

37. **Casey WM**, **Gibson KJ**, **Parks LW**. Covalent attachment of palmitoleic acid (C16:1 delta 9) to proteins in Saccharomyces cerevisiae. Evidence for a third class of acylated proteins. *J Biol Chem* 269: 2082–2085, 1994.

38. **Centers for Disease Control and Prevention - Atlanta**, **GA: Centers for …**, **2017**. *National diabetes statistics report, 2017*. [no date].

39. **Chamberlain LH**, **Shipston MJ**. The Physiology of Protein S-acylation. *Physiological Reviews* 95: 341–376, 2015.

40. **Chavda B**, **Arnott JA**, **Planey SL**. Targeting protein palmitoylation: selective inhibitors and implications in disease. *Expert Opin Drug Discov* 9: 1005–1019, 2014.

41. **Chen F**, **Ananthanarayanan M**, **Emre S**, **Neimark E**, **Bull LN**, **Knisely AS**, **Strautnieks SS**, **Thompson RJ**, **Magid MS**, **Gordon R**, **Balasubramanian N**, **Suchy FJ**, **Shneider BL**. Progressive familial intrahepatic cholestasis, type 1, is associated with decreased farnesoid X receptor activity. *YGAST* 126: 756–764, 2004.

42. **Chen F**, **Ma L**, **Al-Ansari N**, **Shneider B**. The role of AP-1 in the transcriptional regulation of the rat apical sodium-dependent bile acid transporter. *J Biol Chem* 276: 38703–38714, 2001.

43. **Chen F**, **MA L**, **Dawson PA**, **Sinal CJ**, **Sehayek E**, **Gonzalez FJ**, **Breslow J**, **Ananthanarayanan M**, **Shneider BL**. Liver receptor homologue-1 mediates species- and cell line-specific bile acid-dependent negative feedback regulation of the apical sodium-dependent bile acid transporter. *J Biol Chem* 278: 19909–19916, 2003.

44. **Chen F**, **MA L**, **Sartor RB**, **Li F**, **Xiong H**, **Sun A-Q**, **Shneider B**. Inflammatory-mediated repression of the rat ileal sodium-dependent bile acid transporter by c-fos nuclear translocation. *Gastroenterology* 123: 2005–2016, 2002.

45. **Chen F**, **Shyu A-B**, **Shneider BL**. Hu antigen R and tristetraprolin: counter-regulators of rat apical sodium-dependent bile acid transporter by way of effects on messenger RNA stability. *Hepatology* 54: 1371–1378, 2011.

46. **Chen L**, **Yao X**, **Young A**, **McNulty J**, **Anderson D**, **Liu Y**, **Nystrom C**, **Croom D**, **Ross S**, **Collins J**, **Rajpal D**, **Hamlet K**, **Smith C**, **Gedulin B**. Inhibition of apical sodium-dependent bile acid transporter as a novel treatment for diabetes. *Am J Physiol Endocrinol Metab* 302: E68–76, 2012.

47. **Chen X**, **Chen F**, **Liu S**, **Glaeser H**, **Dawson PA**, **Hofmann AF**, **Kim RB**, **Shneider BL**, **Pang KS**. Transactivation of rat apical sodium-dependent bile acid transporter and increased bile acid transport by 1alpha,25-dihydroxyvitamin D3 via the vitamin D receptor. *Mol Pharmacol* 69: 1913–1923, 2006.

48. **Cheng K**, **Metry M**, **Felton J**, **Shang AC**, **Drachenberg CB**, **Xu S**, **Zhan M**, **Schumacher J**, **Guo GL**, **Polli JE**, **Raufman J-P**. Diminished gallbladder filling, increased fecal bile acids, and promotion of colon epithelial cell proliferation and

neoplasia in fibroblast growth factor 15-deficient mice. *Oncotarget* 9: 25572–25585, 2018.

49. **Cheng S**, **Zou M**, **Liu Q**, **Kuang J**, **Shen J**, **Pu S**, **Chen L**, **Li H**, **Wu T**, **Li R**, **Li Y**, **Jiang W**, **Zhang Z**, **He J**. Activation of Constitutive Androstane Receptor Prevents Cholesterol Gallstone Formation. *Am J Pathol* 187: 808–818, 2017.

50. **Chey WD**, **Camilleri M**, **Chang L**, **Rikner L**, **Graffner H**. A randomized placebo-controlled phase IIb trial of a3309, a bile acid transporter inhibitor, for chronic idiopathic constipation. *Am J Gastroenterol* 106: 1803–1812, 2011.

51. **Chiang JYL**, **Pathak P**, **Liu H**, **Donepudi A**, **Ferrell J**, **Boehme S**. Intestinal Farnesoid X Receptor and Takeda G Protein Couple Receptor 5 Signaling in Metabolic Regulation. *Dig Dis* 35: 241–245, 2017.

52. **Chiang JYL**. Bile acids: regulation of synthesis. *J Lipid Res* 50: 1955–1966, 2009.

53. **Chignard N**, **Mergey M**, **Veissière D**, **Parc R**, **Capeau J**, **Poupon R**, **Paul A**, **Housset C**. Bile acid transport and regulating functions in the human biliary epithelium. *Hepatology* 33: 496–503, 2001.

54. **Chothe PP**, **Czuba LC**, **Moore RH**, **Swaan PW**. Human bile acid transporter ASBT (SLC10A2) forms functional non-covalent homodimers and higher order oligomers. *Biochim Biophys Acta* 1860: 645–653, 2018.

55. **Chothe PP**, **Swaan PW**. Resveratrol promotes degradation of the human bile acid transporter ASBT (SLC10A2). *Biochem J* 459: 301–312, 2014.

56. **Chow ECY**, **Maeng H-J**, **Liu S**, **Khan AA**, **Groothuis GMM**, **Pang KS**. 1alpha,25-Dihydroxyvitamin D(3) triggered vitamin D receptor and farnesoid X receptor-like effects in rat intestine and liver in vivo. *Biopharm Drug Dispos* 30: 457–475, 2009.

57. **Chow ECY**, **Sondervan M**, **Jin C**, **Groothuis GMM**, **Pang KS**. Comparative effects of doxercalciferol (1α-hydroxyvitamin D_2) versus calcitriol (1α,25-dihydroxyvitamin D_3) on the expression of transporters and enzymes in the rat in vivo. *J Pharm Sci* 100: 1594–1604, 2011.

58. **Christie DM**, **Dawson PA**, **Thevananther S**, **Shneider BL**. Comparative analysis of the ontogeny of a sodium-dependent bile acid transporter in rat kidney and ileum. *Am J Physiol* 271: G377–85, 1996.

59. **Coon S**, **Kekuda R**, **Saha P**, **Sundaram U**. Glucocorticoids differentially regulate Na-bile acid cotransport in normal and chronically inflamed rabbit ileal villus cells. *AJP: Gastrointestinal and Liver Physiology* 298: G675–82, 2010.

60. **Craddock AL**, **Love MW**, **Daniel RW**, **Kirby LC**, **Walters HC**, **Wong MH**, **Dawson PA**. Expression and transport properties of the human ileal and renal sodium-dependent bile acid transporter. *Am J Physiol* 274: G157–69, 1998.

61. **Cui JY**, **Aleksunes LM**, **Tanaka Y**, **Fu ZD**, **Guo Y**, **Guo GL**, **Lu H**, **Zhong X-B**, **Klaassen CD**. Bile acids via FXR initiate the expression of major transporters involved in the enterohepatic circulation of bile acids in newborn mice. *Am J Physiol Gastrointest Liver Physiol* 302: G979–96, 2012.

62. **da Silva TC**, **Hussainzada N**, **Khantwal CM**, **Polli JE**, **Swaan PW**. Transmembrane helix 1 contributes to substrate translocation and protein stability of bile acid transporter SLC10A2. *Journal of Biological Chemistry* 286: 27322–27332, 2011.

63. **Dawson PA**, **Haywood J**, **Craddock AL**, **Wilson M**, **Tietjen M**, **Kluckman K**, **Maeda N**, **Parks JS**. Targeted deletion of the ileal bile acid transporter eliminates enterohepatic cycling of bile acids in mice. *J Biol Chem* 278: 33920–33927, 2003.

64. **Dawson PA**, **Lan T**, **Rao A**. Bile acid transporters. *J Lipid Res* 50: 2340–2357, 2009.

65. **Dawson PA**. Impact of Inhibiting Ileal Apical versus Basolateral Bile Acid Transport on Cholesterol Metabolism and Atherosclerosis in Mice. *Dig Dis* 33: 382–387, 2015.

66. **De Bruyn T**, **Sempels W**, **Snoeys J**, **Holmstock N**, **Chatterjee S**, **Stieger B**, **Augustijns P**, **Hofkens J**, **Mizuno H**, **Annaert P**. Confocal imaging with a fluorescent bile acid analogue closely mimicking hepatic taurocholate disposition. *J Pharm Sci* 103: 1872–1881, 2014.

67. **Di Daniele N**, **Noce A**, **Vidiri MF**, **Moriconi E**, **Marrone G**, **Annicchiarico-Petruzzelli M**, **D'Urso G**, **Tesauro M**, **Rovella V**, **De Lorenzo A**. Impact of Mediterranean diet on metabolic syndrome, cancer and longevity. *Oncotarget* 8: 8947–8979, 2017.

68. **Dietschy JM**. Mechanisms for the intestinal absorption of bile acids. *J Lipid Res* 9: 297–309, 1968.

69. **Duane WC**, **Xiong W**, **Lofgren J**. Transactivation of the human apical sodium-dependent bile acid transporter gene by human serum. *J Steroid Biochem Mol Biol* 108: 137–148, 2008.

70. **Duane WC**, **Xiong W**, **Wolvers J**. Effects of bile acids on expression of the human apical sodium dependent bile acid transporter gene. *Biochim Biophys Acta* 1771: 1380–1388, 2007.

71. **Dudeja PK**, **Baldwin ML**, **Harig JM**, **Cragoe EJ**, **Ramaswamy K**, **Brasitus TA**. Mechanisms of Na+ transport in human distal colonic apical membrane vesicles. *Biochim Biophys Acta* 1193: 67–76, 1994.

72. **Eggert T**, **Bakonyi D**, **Hummel W**. Enzymatic routes for the synthesis of ursodeoxycholic acid. *J Biotechnol* 191: 11–21, 2014.

73. **Einarsson K**, **Ericsson S**, **Ewerth S**, **Reihnér E**, **Rudling M**, **Ståhlberg D**, **Angelin B**. Bile acid sequestrants: mechanisms of action on bile acid and cholesterol metabolism. *Eur J Clin Pharmacol* 40 Suppl 1: S53–8, 1991.

74. **Erickson SK**, **Lear SR**, **Deane S**, **Dubrac S**, **Huling SL**, **Nguyen L**, **Bollineni JS**, **Shefer S**, **Hyogo H**, **Cohen DE**, **Shneider B**, **Sehayek E**, **Ananthanarayanan M**, **Balasubramaniyan N**, **Suchy FJ**, **Batta AK**, **Salen G**. Hypercholesterolemia and changes in lipid and bile acid metabolism in male and female cyp7A1-deficient mice. *J Lipid Res* 44: 1001–1009, 2003.

75. **Falany CN**, **Johnson MR**, **Barnes S**, **Diasio RB**. Glycine and taurine conjugation of bile acids by a single enzyme. Molecular cloning and expression of human liver bile acid CoA:amino acid N-acyltransferase. *J Biol Chem* 269: 19375–19379, 1994.

76. **Fallingborg J**, **Pedersen P**, **Jacobsen BA**. Small intestinal transit time and intraluminal pH in ileocecal resected patients with Crohn's disease. *Dig Dis Sci* 43: 702–705, 1998.

77. **Felton J**, **Cheng K**, **Said A**, **Shang AC**, **Xu S**, **Vivian D**, **Metry M**, **Polli JE**, **Raufman J-P**. Using Multi-fluorinated Bile Acids and In Vivo Magnetic Resonance Imaging to Measure Bile Acid Transport. *J Vis Exp* : e54597, 2016.

78. **Forman HJ**, **Zhang H**, **Rinna A**. Glutathione: overview of its protective roles, measurement, and biosynthesis. *Mol Aspects Med* 30: 1–12, 2009.

79. **Forrester MT**, **Hess DT**, **Thompson JW**, **Hultman R**, **Moseley MA**, **Stamler JS**, **Casey PJ**. Site-specific analysis of protein S-acylation by resin-assisted capture. *J Lipid Res* 52: 393–398, 2011.

80. **Foster JD**, **Vaughan RA**. Palmitoylation controls dopamine transporter kinetics, degradation, and protein kinase C-dependent regulation. *Journal of Biological Chemistry* 286: 5175–5186, 2011.

81. **Fracchia M**, **Pellegrino S**, **Secreto P**, **Pera A**, **Galatola G**. Biliary lipid composition in idiopathic bile acid malabsorption. *Gut* 43: 812–816, 1998.

82. **Frankenberg T**, **Miloh T**, **Chen FY**, **Ananthanarayanan M**, **Sun A-Q**, **Balasubramaniyan N**, **Arias I**, **Setchell KDR**, **Suchy FJ**, **Shneider BL**. The membrane protein ATPase class I type 8B member 1 signals through protein kinase C zeta to activate the farnesoid X receptor. *Hepatology* 48: 1896–1905, 2008.

83. **Friedman SL**, **Neuschwander-Tetri BA**, **Rinella M**, **Sanyal AJ**. Mechanisms of NAFLD development and therapeutic strategies. *Nat Med* 24: 908–922, 2018.

84. **Fritz KS**, **Green MF**, **Petersen DR**, **Hirschey MD**. Ethanol metabolism modifies hepatic protein acylation in mice. *PLoS ONE* 8: e75868, 2013.

85. **Frommherz L**, **Bub A**, **Hummel E**, **Rist MJ**, **Roth A**, **Watzl B**, **Kulling SE**. Age-Related Changes of Plasma Bile Acid Concentrations in Healthy Adults--Results from the Cross-Sectional KarMeN Study. *PLoS ONE* 11: e0153959, 2016.

86. **Gaebler A**, **Milan R**, **Straub L**, **Hoelper D**, **Kuerschner L**, **Thiele C**. Alkyne lipids as substrates for click chemistry-based in vitro enzymatic assays. *J Lipid Res* 54: 2282–2290, 2013.

87. **Gao T**, **Feridooni HA**, **Howlett SE**, **Pelis RM**. Influence of age on intestinal bile acid transport in C57BL/6 mice. *Pharmacology Research & Perspectives* 5: e00287, 2017.

88. **Garbutt JT**, **Kenney TJ**. Effect of cholestyramine on bile acid metabolism in normal man. *J Clin Invest* 51: 2781–2789, 1972.

89. **Ghosh A**, **Chen F**, **Banerjee S**, **Xu M**, **Shneider BL**. c-Fos mediates repression of the apical sodium-dependent bile acid transporter by fibroblast growth factor-19 in mice. *Am J Physiol Gastrointest Liver Physiol* 306: G163–71, 2014.

90. **Gill RK**, **Saksena S**, **Alrefai WA**, **Sarwar Z**, **Goldstein JL**, **Carroll RE**, **Ramaswamy K**, **Dudeja PK**. Expression and membrane localization of MCT isoforms along the length of the human intestine. *AJP: Cell Physiology* 289: C846–52, 2005.

91. **Gonzalez FJ**, **Jiang C**, **Xie C**, **Patterson AD**. Intestinal Farnesoid X Receptor Signaling Modulates Metabolic Disease. *Dig Dis* 35: 178–184, 2017.

92. **González PM**, **Hussainzada N**, **Swaan PW**, **MacKerell AD**, **Polli JE**. Putative irreversible inhibitors of the human sodium-dependent bile acid transporter (hASBT; SLC10A2) support the role of transmembrane domain 7 in substrate binding/translocation. *Pharm Res* 29: 1821–1831, 2012.

93. **Gould SJ**, **Subramani S**. Firefly luciferase as a tool in molecular and cell biology. *Anal Biochem* 175: 5–13, 1988.

94. **Greaves J**, **Munro KR**, **Davidson SC**, **Riviere M**, **Wojno J**, **Smith TK**, **Tomkinson NCO**, **Chamberlain LH**. Molecular basis of fatty acid selectivity in the zDHHC family of S-acyltransferases revealed by click chemistry. *Proc Natl Acad Sci USA* 114: E1365–E1374, 2017.

95. **Hagey LR**, **Crombie DL**, **Espinosa E**, **Carey MC**, **Igimi H**, **Hofmann AF**. Ursodeoxycholic acid in the Ursidae: biliary bile acids of bears, pandas, and related carnivores. *J Lipid Res* 34: 1911–1917, 1993.

96. **Hallén S**, **Brändén M**, **Dawson PA**, **Sachs G**. Membrane insertion scanning of the human ileal sodium/bile acid co-transporter. *Biochemistry* 38: 11379–11388, 1999.

97. **Halpern MD**, **Holubec H**, **Dominguez JA**, **Meza YG**, **Williams CS**, **Ruth MC**, **McCuskey RS**, **Dvorak B**. Hepatic inflammatory mediators contribute to intestinal damage in necrotizing enterocolitis. *Am J Physiol Gastrointest Liver Physiol* 284: G695–702, 2003.

98. **Halpern MD**, **Holubec H**, **Saunders TA**, **Dvorak K**, **Clark JA**, **Doelle SM**, **Ballatori N**, **Dvorak B**. Bile acids induce ileal damage during experimental necrotizing enterocolitis. *YGAST* 130: 359–372, 2006.

99. **Halpern MD**, **Weitkamp J-H**, **Mount Patrick SK**, **Dobrenen HJ**, **Khailova L**, **Correa H**, **Dvorak B**. Apical sodium-dependent bile acid transporter upregulation is associated with necrotizing enterocolitis. *Am J Physiol Gastrointest Liver Physiol* 299: G623–31, 2010.

100. **Han X**, **Sun J**, **Wang Y**, **He Z**. PepT1, ASBT-Linked Prodrug Strategy to Improve Oral Bioavailability and Tissue Targeting Distribution. *Curr Drug Metab* 16: 71–83, 2015.

101. **Handelsman Y**. Role of bile acid sequestrants in the treatment of type 2 diabetes. *Diabetes Care* 34 Suppl 2: S244–50, 2011.

102. **Harig JM**, **Dudeja PK**, **Knaup SM**, **Shoshara J**, **Ramaswamy K**, **Brasitus TA**. Apical plasma membrane vesicles formed from organ donor colon demonstrate Na+ and H+ conductances and Na+/H+ exchange. *Biochem Biophys Res Commun* 167: 438–443, 1990.

103. **Henkin AH**, **Cohen AS**, **Dubikovskaya EA**, **Park HM**, **Nikitin GF**, **Auzias MG**, **Kazantzis M**, **Bertozzi CR**, **Stahl A**. Real-time noninvasive imaging of fatty acid uptake in vivo. *ACS Chem Biol* 7: 1884–1891, 2012.

104. **Heubi JE**, **Balistreri WF**, **Fondacaro JD**, **Partin JC**, **Schubert WK**. Primary bile acid malabsorption: defective in vitro ileal active bile acid transport. *YGAST* 83: 804–811, 1982.

105. **Heubi JE**, **Balistreri WF**, **Partin JC**, **Schubert WK**, **McGraw CA**. Refractory infantile diarrhea due to primary bile acid malabsorption. *J Pediatr* 94: 546–551, 1979.

106. **Heubi JE**, **Balistreri WF**, **Suchy FJ**. Bile salt metabolism in the first year of life. *J Lab Clin Med* 100: 127–136, 1982.

107. **Ho RH**, **Leake BF**, **Urquhart BL**, **Gregor JC**, **Dawson PA**, **Kim RB**. Functional characterization of genetic variants in the apical sodium-dependent bile acid transporter (ASBT; SLC10A2). *J Gastroenterol Hepatol* 26: 1740–1748, 2011.

108. **Hofmann AF**, **Hagey LR**, **Krasowski MD**. Bile salts of vertebrates: structural variation and possible evolutionary significance. *J Lipid Res* 51: 226–246, 2010.

109. **Hofmann AF**, **Mangelsdorf DJ**, **Kliewer SA**. Chronic diarrhea due to excessive bile acid synthesis and not defective ileal transport: a new syndrome of defective fibroblast growth factor 19 release. *Clin Gastroenterol Hepatol* 7: 1151–1154, 2009.

110. **Hofmann AF**, **Mysels KJ**. Bile salts as biological surfactants. *Colloids and Surfaces* 30: 145–173, 1987.

111. **Hofmann AF**. The continuing importance of bile acids in liver and intestinal disease. *Arch Intern Med* 159: 2647–2658, 1999.

112. **Hong V**, **Steinmetz NF**, **Manchester M**, **Finn MG**. Labeling live cells by copper-catalyzed alkyne--azide click chemistry. *Bioconjug Chem* 21: 1912–1916, 2010.

113. **Hruz P**, **Zimmermann C**, **Gutmann H**, **Degen L**, **Beuers U**, **Terracciano L**, **Drewe J**, **Beglinger C**. Adaptive regulation of the ileal apical sodium dependent bile acid transporter (ASBT) in patients with obstructive cholestasis. *Gut* 55: 395–402, 2006.

114. **Hu L-L**, **Wan S-B**, **Niu S**, **Shi X-H**, **Li H-P**, **Cai Y-D**, **Chou K-C**. Prediction and analysis of protein palmitoylation sites. *Biochimie* 93: 489–496, 2011.

115. **Hu N-J**, **Iwata S**, **Cameron AD**, **Drew D**. Crystal structure of a bacterial homologue of the bile acid sodium symporter ASBT. *Nature* 478: 408–411, 2011.

116. **Huff MW**, **Telford DE**, **Edwards JY**, **Burnett JR**, **Barrett PHR**, **Rapp SR**, **Napawan N**, **Keller BT**. Inhibition of the apical sodium-dependent bile acid transporter reduces LDL cholesterol and apoB by enhanced plasma clearance of LDL apoB. *Arterioscler Thromb Vasc Biol* 22: 1884–1891, 2002.

117. **Hussainzada N**, **Banerjee A**, **Swaan PW**. Transmembrane domain VII of the human apical sodium-dependent bile acid transporter ASBT (SLC10A2) lines the substrate translocation pathway. *Mol Pharmacol* 70: 1565–1574, 2006.

118. **Hussainzada N**, **Claro Da Silva T**, **Swaan PW**. The cytosolic half of helix III forms the substrate exit route during permeation events of the sodium/bile acid cotransporter ASBT. *Biochemistry* 48: 8528–8539, 2009.

119. **Hussainzada N**, **da Silva TC**, **Zhang EY**, **Swaan PW**. Conserved aspartic acid residues lining the extracellular loop 1 of sodium-coupled bile acid transporter ASBT Interact with Na+ and 7alpha-OH moieties on the ligand cholestane skeleton. *J Biol Chem* 283: 20653–20663, 2008.

120. **Hussainzada N**, **Khandewal A**, **Swaan PW**. Conformational flexibility of helix VI is essential for substrate permeation of the human apical sodium-dependent bile acid transporter. *Mol Pharmacol* 73: 305–313, 2008.

121. **Hwang ST**, **Henning SJ**. Ontogenic regulation of components of ileal bile acid absorption. *Exp Biol Med (Maywood)* 226: 674–680, 2001.

122. **Ishibashi S**, **Schwarz M**, **Frykman PK**, **Herz J**, **Russell DW**. Disruption of cholesterol 7alpha-hydroxylase gene in mice. I. Postnatal lethality reversed by bile acid and vitamin supplementation. *J Biol Chem* 271: 18017–18023, 1996.

123. **Jang D**, **Kwon H**, **Jeong K**, **Lee J**, **Pak Y**. Essential role of flotillin-1 palmitoylation in the intracellular localization and signaling function of IGF-1 receptor. *J Cell Sci* 128: 2179–2190, 2015.

124. **Jennings BC**, **Nadolski MJ**, **Ling Y**, **Baker MB**, **Harrison ML**, **Deschenes RJ**, **Linder ME**. 2-Bromopalmitate and 2-(2-hydroxy-5-nitro-benzylidene)-benzo[b]thiophen-3-one inhibit DHHC-mediated palmitoylation in vitro. *J Lipid Res* 50: 233–242, 2009.

125. **Jiang C**, **Xie C**, **Lv Y**, **Li J**, **Krausz KW**, **Shi J**, **Brocker CN**, **Desai D**, **Amin SG**, **Bisson WH**, **Liu Y**, **Gavrilova O**, **Patterson AD**, **Gonzalez FJ**. Intestine-selective farnesoid X receptor inhibition improves obesity-related metabolic dysfunction. *Nature Communications* 6: 10166, 2015.

126. **Jiang H**, **Zhang X**, **Chen X**, **Aramsangtienchai P**, **Tong Z**, **Lin H**. Protein Lipidation: Occurrence, Mechanisms, Biological Functions, and Enabling Technologies. *Chem Rev* 118: 919–988, 2018.

127. **Johnson MR**, **Barnes S**, **Kwakye JB**, **Diasio RB**. Purification and characterization of bile acid-CoA:amino acid N-acyltransferase from human liver. *J Biol Chem* 266: 10227–10233, 1991.

128. **Jones LR**, **Goun EA**, **Shinde R**, **Rothbard JB**, **Contag CH**, **Wender PA**. Releasable luciferin-transporter conjugates: tools for the real-time analysis of cellular uptake and release. *J Am Chem Soc* 128: 6526–6527, 2006.

129. **Josephson B**, **Rydin A**. The resorption of the bile acids from the intestines. *Biochem J* 30: 2224–2228, 1936.

130. **Jump DB**. The biochemistry of n-3 polyunsaturated fatty acids. *J Biol Chem* 277: 8755–8758, 2002.

131. **Jung D**, **Fantin AC**, **Scheurer U**, **Fried M**, **Kullak-Ublick GA**. Human ileal bile acid transporter gene ASBT (SLC10A2) is transactivated by the glucocorticoid receptor. *Gut* 53: 78–84, 2004.

132. **Jung D**, **Fried M**, **Kullak-Ublick GA**. Human apical sodium-dependent bile salt transporter gene (SLC10A2) is regulated by the peroxisome proliferator-activated receptor alpha. *J Biol Chem* 277: 30559–30566, 2002.

133. **Kazgan N**, **Metukuri MR**, **Purushotham A**, **Lu J**, **Rao A**, **Lee S**, **Pratt-Hyatt M**, **Lickteig A**, **Csanaky IL**, **Zhao Y**, **Dawson PA**, **Li X**. Intestine-specific deletion of SIRT1 in mice impairs DCoH2-HNF-1α-FXR signaling and alters systemic bile acid homeostasis. *Gastroenterology* 146: 1006–1016, 2014.

134. **Keller CA**, **Yuan X**, **Panzanelli P**, **Martin ML**, **Alldred M**, **Sassoè-Pognetto M**, **Lüscher B**. The gamma2 subunit of GABA(A) receptors is a substrate for palmitoylation by GODZ. *J Neurosci* 24: 5881–5891, 2004.

135. **Khantwal CM**, **Swaan PW**. Cytosolic half of transmembrane domain IV of the human bile acid transporter hASBT (SLC10A2) forms part of the substrate translocation pathway. *Biochemistry* 47: 3606–3614, 2008.

136. **Kitayama K**, **Nakai D**, **Kono K**, **van der Hoop AG**, **Kurata H**, **de Wit EC**, **Cohen LH**, **Inaba T**, **Kohama T**. Novel non-systemic inhibitor of ileal apical Na+-dependent bile acid transporter reduces serum cholesterol levels in hamsters and monkeys. *Eur J Pharmacol* 539: 89–98, 2006.

137. **Klomp LWJ**, **Vargas JC**, **van Mil SWC**, **Pawlikowska L**, **Strautnieks SS**, **van Eijk MJT**, **Juijn JA**, **Pabón-Peña C**, **Smith LB**, **DeYoung JA**, **Byrne JA**, **Gombert J**, **van der Brugge G**, **Berger R**, **Jankowska I**, **Pawlowska J**, **Villa E**, **Knisely AS**, **Thompson RJ**, **Freimer NB**, **Houwen RHJ**, **Bull LN**. Characterization of mutations in ATP8B1 associated with hereditary cholestasis. *Hepatology* 40: 27–38, 2004.

138. **Kolhatkar V**, **Polli JE**. Structural requirements of bile acid transporters: C-3 and C-7 modifications of steroidal hydroxyl groups. *Eur J Pharm Sci* 46: 86–99, 2012.

139. **Krag E**, **Phillips SF**. Active and passive bile acid absorption in man. Perfusion studies of the ileum and jejunum. *J Clin Invest* 53: 1686–1694, 1974.

140. **Kramer W**, **Burckhardt G**, **Wilson FA**, **Kurz G**. Bile salt-binding polypeptides in brush-border membrane vesicles from rat small intestine revealed by photoaffinity labeling. *J Biol Chem* 258: 3623–3627, 1983.

141. **Kramer W**, **Girbig F**, **Glombik H**, **Corsiero D**, **Stengelin S**, **Weyland C**. Identification of a ligand-binding site in the Na+/bile acid cotransporting protein from rabbit ileum. *J Biol Chem* 276: 36020–36027, 2001.

142. **Kramer W**, **Girbig F**, **Gutjahr U**, **Kowalewski S**, **Jouvenal K**, **Müller G**, **Tripier D**, **Wess G**. Intestinal bile acid absorption. Na(+)-dependent bile acid transport activity in rabbit small intestine correlates with the coexpression of an integral 93-kDa and a peripheral 14-kDa bile acid-binding membrane protein along the duodenum-ileum axis. *J Biol Chem* 268: 18035–18046, 1993.

143. **Kramer W**, **Girbig F**, **Gutjahr U**, **Kowalewski S**. Radiation-inactivation analysis of the Na+/bile acid co-transport system from rabbit ileum. *Biochem J* 306 (Pt 1): 241–246, 1995.

144. **Kramer W**, **Nicol SB**, **Girbig F**, **Gutjahr U**, **Kowalewski S**, **Fasold H**. Characterization and chemical modification of the Na(+)-dependent bile-acid transport system in brush-border membrane vesicles from rabbit ileum. *Biochim Biophys Acta* 1111: 93–102, 1992.

145. **Kramer W**, **Stengelin S**, **Baringhaus KH**, **Enhsen A**, **Heuer H**, **Becker W**, **Corsiero D**, **Girbig F**, **Noll R**, **Weyland C**. Substrate specificity of the ileal and the hepatic Na(+)/bile acid cotransporters of the rabbit. I. Transport studies with membrane vesicles and cell lines expressing the cloned transporters. *J Lipid Res* 40: 1604–1617, 1999.

146. **Kubitz R**, **Dröge C**, **Kluge S**, **Stindt J**, **Häussinger D**. Genetic variations of bile salt transporters. *Drug Discov Today Technol* 12: e55–67, 2014.

147. **Lammert F**, **Paigen B**, **Carey MC**. Localization of the ileal sodium-bile salt cotransporter gene (Slc10a2) to mouse chromosome 8. *Mamm Genome* 9: 173–174, 1998.

148. **Lan T**, **Haywood J**, **Dawson PA**. Inhibition of ileal apical but not basolateral bile acid transport reduces atherosclerosis in apoE$^{-/-}$ mice. *Atherosclerosis* 229: 374–380, 2013.

149. **Lazaridis KN**, **Pham L**, **Tietz P**, **Marinelli RA**, **deGroen PC**, **Levine S**, **Dawson PA**, **LaRusso NF**. Rat cholangiocytes absorb bile acids at their apical domain via the ileal sodium-dependent bile acid transporter. *J Clin Invest* 100: 2714–2721, 1997.

150. **Lazaridis KN**, **Tietz P**, **Wu T**, **Kip S**, **Dawson PA**, **LaRusso NF**. Alternative splicing of the rat sodium/bile acid transporter changes its cellular localization and transport properties. *Proc Natl Acad Sci USA* 97: 11092–11097, 2000.

151. **Le T-A**, **Chen J**, **Changchien C**, **Peterson MR**, **Kono Y**, **Patton H**, **Cohen BL**, **Brenner D**, **Sirlin C**, **Loomba R**, **San Diego Integrated NAFLD Research Consortium (SINC)**. Effect of colesevelam on liver fat quantified by magnetic resonance in nonalcoholic steatohepatitis: a randomized controlled trial. *Hepatology* 56: 922–932, 2012.

152. **Lee Y-K**, **Schmidt DR**, **Cummins CL**, **Choi M**, **Peng L**, **Zhang Y**, **Goodwin B**, **Hammer RE**, **Mangelsdorf DJ**, **Kliewer SA**. Liver receptor homolog-1 regulates bile acid homeostasis but is not essential for feedback regulation of bile acid synthesis. *Mol Endocrinol* 22: 1345–1356, 2008.

153. **Lemonidis K**, **Salaun C**, **Kouskou M**, **Diez-Ardanuy C**, **Chamberlain LH**, **Greaves J**. Substrate selectivity in the zDHHC family of S-acyltransferases. *Biochem Soc Trans* 45: 751–758, 2017.

154. **Lemonidis K**, **Werno MW**, **Greaves J**, **Diez-Ardanuy C**, **Sanchez-Perez MC**, **Salaun C**, **Thomson DM**, **Chamberlain LH**. The zDHHC family of S-acyltransferases. *Biochem Soc Trans* 43: 217–221, 2015.

155. **Levental I**, **Lingwood D**, **Grzybek M**, **Coskun U**, **Simons K**. Palmitoylation regulates raft affinity for the majority of integral raft proteins. *Proc Natl Acad Sci USA* 107: 22050–22054, 2010.

156. **Li H**, **Chen F**, **Shang Q**, **Pan L**, **Shneider BL**, **Chiang JYL**, **Forman BM**, **Ananthanarayanan M**, **Tint GS**, **Salen G**, **Xu G**. FXR-activating ligands inhibit rabbit ASBT expression via FXR-SHP-FTF cascade. *Am J Physiol Gastrointest Liver Physiol* 288: G60–6, 2005.

157. **Li H**, **Xu G**, **Shang Q**, **Pan L**, **Shefer S**, **Batta AK**, **Bollineni J**, **Tint GS**, **Keller BT**, **Salen G**. Inhibition of ileal bile acid transport lowers plasma cholesterol levels by inactivating hepatic farnesoid X receptor and stimulating cholesterol 7 alpha-hydroxylase. *Metab Clin Exp* 53: 927–932, 2004.

158. **Li T**, **Francl JM**, **Boehme S**, **Ochoa A**, **Zhang Y**, **Klaassen CD**, **Erickson SK**, **Chiang JYL**. Glucose and insulin induction of bile acid synthesis: mechanisms and implication in diabetes and obesity. *Journal of Biological Chemistry* 287: 1861–1873, 2012.

159. **Li-Hawkins J**, **Gåfvels M**, **Olin M**, **Lund EG**, **Andersson U**, **Schuster G**, **Björkhem I**, **Russell DW**, **Eggertsen G**. Cholic acid mediates negative feedback regulation of bile acid synthesis in mice. *J Clin Invest* 110: 1191–1200, 2002.

160. **Liang X**, **Nazarian A**, **Erdjument-Bromage H**, **Bornmann W**, **Tempst P**, **Resh MD**. Heterogeneous fatty acylation of Src family kinases with polyunsaturated fatty acids regulates raft localization and signal transduction. *J Biol Chem* 276: 30987–30994, 2001.

161. **Lin MC**, **Kramer W**, **Wilson FA**. Identification of cytosolic and microsomal bile acid-binding proteins in rat ileal enterocytes. *J Biol Chem* 265: 14986–14995, 1990.

162. **Lin MC**, **Mullady E**, **Wilson FA**. Timed photoaffinity labeling and characterization of bile acid binding and transport proteins in rat ileum. *Am J Physiol* 265: G56–62, 1993.

163. **Lionarons DA**, **Boyer JL**, **Cai S-Y**. Evolution of substrate specificity for the bile salt transporter ASBT (SLC10A2). *J Lipid Res* 53: 1535–1542, 2012.

164. **Lorent JH**, **Diaz-Rohrer B**, **Lin X**, **Spring K**, **Gorfe AA**, **Levental KR**, **Levental I**. Structural determinants and functional consequences of protein affinity for membrane rafts. *Nature Communications* 8: 1219, 2017.

165. **Lozano E**, **Monte MJ**, **Briz O**, **Hernández-Hernández A**, **Banales JM**, **Marin JJG**, **Macias RIR**. Enhanced antitumour drug delivery to cholangiocarcinoma through the apical sodium-dependent bile acid transporter (ASBT). *J Control Release* 216: 93–102, 2015.

166. **Ma L**, **Jüttner M**, **Kullak-Ublick GA**, **Eloranta JJ**. Regulation of the gene encoding the intestinal bile acid transporter ASBT by the caudal-type homeobox proteins CDX1 and CDX2. *Am J Physiol Gastrointest Liver Physiol* 302: G123–33, 2012.

167. **Magee AI**, **Gutierrez L**, **McKay IA**, **Marshall CJ**, **Hall A**. Dynamic fatty acylation of p21N-ras. *EMBO J* 6: 3353–3357, 1987.

168. **McClure M**, **DeLucas LJ**, **Wilson L**, **Ray M**, **Rowe SM**, **Wu X**, **Dai Q**, **Hong JS**, **Sorscher EJ**, **Kappes JC**, **Barnes S**. Purification of CFTR for mass spectrometry analysis: identification of palmitoylation and other post-translational modifications. *Protein Eng Des Sel* 25: 7–14, 2012.

169. **McClure ML**, **Wen H**, **Fortenberry J**, **Hong JS**, **Sorscher EJ**. S-palmitoylation regulates biogenesis of core glycosylated wild-type and F508del CFTR in a post-ER compartment. *Biochem J* 459: 417–425, 2014.

170. **McGettigan BM**, **McMahan RH**, **Luo Y**, **Wang XX**, **Orlicky DJ**, **Porsche C**, **Levi M**, **Rosen HR**. Sevelamer Improves Steatohepatitis, Inhibits Liver and Intestinal Farnesoid

X Receptor (FXR), and Reverses Innate Immune Dysregulation in a Mouse Model of Non-alcoholic Fatty Liver Disease. *Journal of Biological Chemistry* 291: 23058–23067, 2016.

171. **Metry M**, **Felton J**, **Cheng K**, **Xu S**, **Ai Y**, **Xue F**, **Raufman J-P**, **Polli JE**. Attenuated Accumulation of Novel Fluorine (19F)-Labeled Bile Acid Analogues in Gallbladders of Fibroblast Growth Factor-15 (FGF15)-Deficient Mice. *Mol Pharm* 15: 4827–4834, 2018.

172. **Miyata M**, **Matsuda Y**, **Nomoto M**, **Takamatsu Y**, **Sato N**, **Hamatsu M**, **Dawson PA**, **Gonzalez FJ**, **Yamazoe Y**. Cholesterol feeding prevents hepatic accumulation of bile acids in cholic acid-fed farnesoid X receptor (FXR)-null mice: FXR-independent suppression of intestinal bile acid absorption. *Drug Metab Dispos* 37: 338–344, 2009.

173. **Miyata M**, **Yamakawa H**, **Hamatsu M**, **Kuribayashi H**, **Takamatsu Y**, **Yamazoe Y**. Enterobacteria modulate intestinal bile acid transport and homeostasis through apical sodium-dependent bile acid transporter (SLC10A2) expression. *J Pharmacol Exp Ther* 336: 188–196, 2011.

174. **Miyata M**, **Yamakawa H**, **Hayashi K**, **Kuribayashi H**, **Yamazoe Y**, **Yoshinari K**. Ileal apical sodium-dependent bile acid transporter protein levels are down-regulated through ubiquitin-dependent protein degradation induced by bile acids. *Eur J Pharmacol* 714: 507–514, 2013.

175. **Molina H**, **Azocar L**, **Ananthanarayanan M**, **Arrese M**, **Miquel JF**. Localization of the Sodium-Taurocholate cotransporting polypeptide in membrane rafts and modulation of its activity by cholesterol in vitro. *Biochim Biophys Acta* 1778: 1283–1291, 2008.

176. **Monteiro I**, **David ES**, **Ferraris RP**. Ontogenetic development of rat intestinal bile acid transport requires thyroxine but not corticosterone. *Pediatr Res* 55: 611–621, 2004.

177. **Moore RH**, **Chothe P**, **Swaan PW**. Transmembrane domain V plays a stabilizing role in the function of human bile acid transporter SLC10A2. *Biochemistry* 52: 5117–5124, 2013.

178. **Moritz AE**, **Rastedt DE**, **Stanislowski DJ**, **Shetty M**, **Smith MA**, **Vaughan RA**, **Foster JD**. Reciprocal Phosphorylation and Palmitoylation Control Dopamine Transporter Kinetics. *Journal of Biological Chemistry* 290: 29095–29105, 2015.

179. **Mottino AD**, **Hoffman T**, **Dawson PA**, **Luquita MG**, **Monti JA**, **Sánchez Pozzi EJ**, **Catania VA**, **Cao J**, **Vore M**. Increased expression of ileal apical sodium-dependent bile acid transporter in postpartum rats. *Am J Physiol Gastrointest Liver Physiol* 282: G41–50, 2002.

180. **Mueller GM**, **Maarouf AB**, **Kinlough CL**, **Sheng N**, **Kashlan OB**, **Okumura S**, **Luthy S**, **Kleyman TR**, **Hughey RP**. Cys palmitoylation of the beta subunit modulates gating of the epithelial sodium channel. *Journal of Biological Chemistry* 285: 30453–30462, 2010.

181. **Mukherjee A**, **Mueller GM**, **Kinlough CL**, **Sheng N**, **Wang Z**, **Mustafa SA**, **Kashlan OB**, **Kleyman TR**, **Hughey RP**. Cysteine palmitoylation of the γ subunit has a dominant

role in modulating activity of the epithelial sodium channel. *Journal of Biological Chemistry* 289: 14351–14359, 2014.

182. **Mullins JG**, **Beechey RB**, **Gould GW**, **Campbell FC**, **Shirazi-Beechey SP**. Characterization of the ileal Na+/bile salt co-transporter in brush border membrane vesicles and functional expression in Xenopus laevis oocytes. *Biochem J* 285 (Pt 3): 785–790, 1992.

183. **Muszbek L**, **Haramura G**, **Cluette-Brown JE**, **Van Cott EM**, **Laposata M**. The pool of fatty acids covalently bound to platelet proteins by thioester linkages can be altered by exogenously supplied fatty acids. *Lipids* 34 Suppl: S331–7, 1999.

184. **Muthusamy S**, **Malhotra P**, **Hosameddin M**, **Dudeja AK**, **Borthakur S**, **Saksena S**, **Gill RK**, **Dudeja PK**, **Alrefai WA**. N-glycosylation is essential for ileal ASBT function and protection against proteases. *Am J Physiol, Cell Physiol* 308: C964–71, 2015.

185. **Nakao N**, **Kaneda H**, **Tsushima N**, **Ohta Y**, **Tanaka M**. Characterization of primary structure and tissue expression profile of the chicken apical sodium-dependent bile acid transporter mRNA. *Poult Sci* 94: 722–727, 2015.

186. **Neimark E**, **Chen F**, **Li X**, **Magid MS**, **Alasio TM**, **Frankenberg T**, **Sinha J**, **Dawson PA**, **Shneider BL**. c-Fos is a critical mediator of inflammatory-mediated repression of the apical sodium-dependent bile acid transporter. *YGAST* 131: 554–567, 2006.

187. **Neimark E**, **Chen F**, **Li X**, **Shneider BL**. Bile acid-induced negative feedback regulation of the human ileal bile acid transporter. *Hepatology* 40: 149–156, 2004.

188. **Nizamutdinov D**, **DeMorrow S**, **McMillin M**, **Kain J**, **Mukherjee S**, **Zeitouni S**, **Frampton G**, **Bricker PCS**, **Hurst J**, **Shapiro LA**. Hepatic alterations are accompanied by changes to bile acid transporter-expressing neurons in the hypothalamus after traumatic brain injury. *Sci Rep* 7: 40112, 2017.

189. **Nomoto M**, **Miyata M**, **Yin S**, **Kurata Y**, **Shimada M**, **Yoshinari K**, **Gonzalez FJ**, **Suzuki K**, **Shibasaki S**, **Kurosawa T**, **Yamazoe Y**. Bile acid-induced elevated oxidative stress in the absence of farnesoid X receptor. *Biol Pharm Bull* 32: 172–178, 2009.

190. **Nowicki MJ**, **Shneider BL**, **Paul JM**, **Heubi JE**. Glucocorticoids upregulate taurocholate transport by ileal brush-border membrane. *Am J Physiol* 273: G197–203, 1997.

191. **Oelkers P**, **Kirby LC**, **Heubi JE**, **Dawson PA**. Primary bile acid malabsorption caused by mutations in the ileal sodium-dependent bile acid transporter gene (SLC10A2). *J Clin Invest* 99: 1880–1887, 1997.

192. **Out C**, **Dikkers A**, **Laskewitz A**, **Boverhof R**, **van der Ley C**, **Kema IP**, **Wolters H**, **Havinga R**, **Verkade HJ**, **Kuipers F**, **Tietge UJF**, **Groen AK**. Prednisolone increases enterohepatic cycling of bile acids by induction of Asbt and promotes reverse cholesterol transport. *JOURNAL OF HEPATOLOGY* 61: 351–357, 2014.

193. **Out C**, **Patankar JV**, **Doktorova M**, **Boesjes M**, **Bos T**, **de Boer S**, **Havinga R**, **Wolters H**, **Boverhof R**, **van Dijk TH**, **Smoczek A**, **Bleich A**, **Sachdev V**, **Kratky D**, **Kuipers F**, **Verkade HJ**, **Groen AK**. Gut microbiota inhibit Asbt-dependent intestinal bile acid reabsorption via Gata4. *JOURNAL OF HEPATOLOGY* 63: 697–704, 2015.

194. **Paley MA**, **Prescher JA**. Bioluminescence: a versatile technique for imaging cellular and molecular features. *Medchemcomm* 5: 255–267, 2014.

195. **Pan DH**, **Chen F**, **Neimark E**, **Li X**, **Shneider BL**. FTF and LRH-1, two related but different transcription factors in human Caco-2 cells: their different roles in the regulation of bile acid transport. *Biochim Biophys Acta* 1732: 31–37, 2005.

196. **Pan W**, **Song I-S**, **Shin H-J**, **Kim M-H**, **Choi Y-L**, **Lim S-J**, **Kim W-Y**, **Lee S-S**, **Shin J-G**. Genetic polymorphisms in Na+-taurocholate co-transporting polypeptide (NTCP) and ileal apical sodium-dependent bile acid transporter (ASBT) and ethnic comparisons of functional variants of NTCP among Asian populations. *Xenobiotica* 41: 501–510, 2011.

197. **Pandak WM**, **Ren S**, **Marques D**, **Hall E**, **Redford K**, **Mallonee D**, **Bohdan P**, **Heuman D**, **Gil G**, **Hylemon P**. Transport of cholesterol into mitochondria is rate-limiting for bile acid synthesis via the alternative pathway in primary rat hepatocytes. *J Biol Chem* 277: 48158–48164, 2002.

198. **Park HM**, **Russo KA**, **Karateev G**, **Park M**, **Dubikovskaya E**, **Kriegsfeld LJ**, **Stahl A**. A System for In Vivo Imaging of Hepatic Free Fatty Acid Uptake. *Gastroenterology* 152: 78–81.e2, 2017.

199. **Pattni SS**, **Brydon WG**, **Dew T**, **Walters JRF**. Fibroblast Growth Factor 19 and 7α-Hydroxy-4-Cholesten-3-one in the Diagnosis of Patients With Possible Bile Acid Diarrhea. *Clin Transl Gastroenterol* 3: e18, 2012.

200. **Pawlikowska L**, **Groen A**, **Eppens EF**, **Kunne C**, **Ottenhoff R**, **Looije N**, **Knisely AS**, **Killeen NP**, **Bull LN**, **Elferink RPJO**, **Freimer NB**. A mouse genetic model for familial cholestasis caused by ATP8B1 mutations reveals perturbed bile salt homeostasis but no impairment in bile secretion. *Hum Mol Genet* 13: 881–892, 2004.

201. **Pellicoro A**, **van den Heuvel FAJ**, **Geuken M**, **Moshage H**, **Jansen PLM**, **Faber KN**. Human and rat bile acid-CoA:amino acid N-acyltransferase are liver-specific peroxisomal enzymes: implications for intracellular bile salt transport. *Hepatology* 45: 340–348, 2007.

202. **Perumpail BJ**, **Khan MA**, **Yoo ER**, **Cholankeril G**, **Kim D**, **Ahmed A**. Clinical epidemiology and disease burden of nonalcoholic fatty liver disease. *World J Gastroenterol* 23: 8263–8276, 2017.

203. **Quinn CM**, **Jessup W**, **Wong J**, **Kritharides L**, **Brown AJ**. Expression and regulation of sterol 27-hydroxylase (CYP27A1) in human macrophages: a role for RXR and PPARgamma ligands. *Biochem J* 385: 823–830, 2005.

204. **Rao A**, **Kosters A**, **Mells JE**, **Zhang W**, **Setchell KDR**, **Amanso AM**, **Wynn GM**, **Xu T**, **Keller BT**, **Yin H**, **Banton S**, **Jones DP**, **Wu H**, **Dawson PA**, **Karpen SJ**. Inhibition of ileal bile acid uptake protects against nonalcoholic fatty liver disease in high-fat diet-fed mice. *Sci Transl Med* 8: 357ra122–357ra122, 2016.

205. **Raufman J-P**, **Metry M**, **Felton J**, **Cheng K**, **Xu S**, **Polli J**. A 19F magnetic resonance imaging-based diagnostic test for bile acid diarrhea. *MAGMA* 92: 79–9, 2018.

206. **Reiss AB**, **Martin KO**, **Rojer DE**, **Iyer S**, **Grossi EA**, **Galloway AC**, **Javitt NB**. Sterol 27-hydroxylase: expression in human arterial endothelium. *J Lipid Res* 38: 1254–1260, 1997.

207. **Ren J**, **Wen L**, **Gao X**, **Jin C**, **Xue Y**, **Yao X**. CSS-Palm 2.0: an updated software for palmitoylation sites prediction. *Protein Eng Des Sel* 21: 639–644, 2008.

208. **Ren W**, **Jhala US**, **Du K**. Proteomic analysis of protein palmitoylation in adipocytes. *Adipocyte* 2: 17–28, 2013.

209. **Renner O**, **Harsch S**, **Schaeffeler E**, **Schwab M**, **Klass DM**, **Kratzer W**, **Stange EF**. Mutation screening of apical sodium-dependent bile acid transporter (SLC10A2): novel haplotype block including six newly identified variants linked to reduced expression. *Hum Genet* 125: 381–391, 2009.

210. **Repa JJ**, **Lund EG**, **Horton JD**, **Leitersdorf E**, **Russell DW**, **Dietschy JM**, **Turley SD**. Disruption of the sterol 27-hydroxylase gene in mice results in hepatomegaly and hypertriglyceridemia. Reversal by cholic acid feeding. *J Biol Chem* 275: 39685–39692, 2000.

211. **Rocks O**, **Gerauer M**, **Vartak N**, **Koch S**, **Huang Z-P**, **Pechlivanis M**, **Kuhlmann J**, **Brunsveld L**, **Chandra A**, **Ellinger B**, **Waldmann H**, **Bastiaens PIH**. The palmitoylation machinery is a spatially organizing system for peripheral membrane proteins. *Cell* 141: 458–471, 2010.

212. **Rocks O**, **Peyker A**, **Kahms M**, **Verveer PJ**, **Koerner C**, **Lumbierres M**, **Kuhlmann J**, **Waldmann H**, **Wittinghofer A**, **Bastiaens PIH**. An acylation cycle regulates localization and activity of palmitoylated Ras isoforms. *Science* 307: 1746–1752, 2005.

213. **Root C**, **Smith CD**, **Sundseth SS**, **Pink HM**, **Wilson JG**, **Lewis MC**. Ileal bile acid transporter inhibition, CYP7A1 induction, and antilipemic action of 264W94. *J Lipid Res* 43: 1320–1330, 2002.

214. **Russell DW**. The enzymes, regulation, and genetics of bile acid synthesis. *Annu Rev Biochem* 72: 137–174, 2003.

215. **Sabit H**, **Mallajosyula SS**, **MacKerell AD**, **Swaan PW**. Transmembrane domain II of the human bile acid transporter SLC10A2 coordinates sodium translocation. *Journal of Biological Chemistry* 288: 32394–32404, 2013.

216. **Saeki T**, **Kuroda T**, **Matsumoto M**, **Kanamoto R**, **Iwami K**. Effects of Cys mutation on taurocholic acid transport by mouse ileal and hepatic sodium-dependent bile acid transporters. *Biosci Biotechnol Biochem* 66: 467–470, 2002.

217. **Saeki T**, **Matoba K**, **Furukawa H**, **Kirifuji K**, **Kanamoto R**, **Iwami K**. Characterization, cDNA cloning, and functional expression of mouse ileal sodium-dependent bile acid transporter. *J Biochem* 125: 846–851, 1999.

218. **Saeki T**, **Mizushima S**, **Ueda K**, **Iwami K**, **Kanamoto R**. Mutational analysis of uncharged polar residues and proline in the distal one-third (Thr130-Pro142) of the highly conserved region of mouse Slc10a2. *Biosci Biotechnol Biochem* 73: 1535–1540, 2009.

219. **Saeki T**, **Munetaka Y**, **Ueda K**, **Iwami K**, **Kanamoto R**. Effects of Ala substitution for conserved Cys residues in mouse ileal and hepatic Na+-dependent bile acid transporters. *Biosci Biotechnol Biochem* 71: 1865–1872, 2007.

220. **Saeki T**, **Sato K**, **Ito S**, **Ikeda K**, **Kanamoto R**. Importance of uncharged polar residues and proline in the proximal two-thirds (Pro107-Ser128) of the highly conserved region of mouse ileal Na+-dependent bile acid transporter, Slc10a2, in transport activity and cellular expression. *BMC Physiol* 13: 4, 2013.

221. **Sanders SS**, **Martin DDO**, **Butland SL**, **Lavallée-Adam M**, **Calzolari D**, **Kay C**, **Yates JR**, **Hayden MR**. Curation of the Mammalian Palmitoylome Indicates a Pivotal Role for Palmitoylation in Diseases and Disorders of the Nervous System and Cancers. *PLoS Comput Biol* 11: e1004405, 2015.

222. **Sarwar Z**, **Annaba F**, **Dwivedi A**, **Saksena S**, **Gill RK**, **Alrefai WA**. Modulation of ileal apical Na+-dependent bile acid transporter ASBT by protein kinase C. *Am J Physiol Gastrointest Liver Physiol* 297: G532–8, 2009.

223. **Schwarz M**, **Lund EG**, **Setchell KD**, **Kayden HJ**, **Zerwekh JE**, **Bjorkhem I**, **Herz J**, **Russell DW**. Disruption of cholesterol 7alpha-hydroxylase gene in mice. II. Bile acid deficiency is overcome by induction of oxysterol 7alpha-hydroxylase. *J Biol Chem* 271: 18024–18031, 1996.

224. **Schwarz M**, **Russell DW**, **Dietschy JM**, **Turley SD**. Marked reduction in bile acid synthesis in cholesterol 7alpha-hydroxylase-deficient mice does not lead to diminished tissue cholesterol turnover or to hypercholesterolemia. *J Lipid Res* 39: 1833–1843, 1998.

225. **Shah S**, **Sanford UR**, **Vargas JC**, **Xu H**, **Groen A**, **Paulusma CC**, **Grenert JP**, **Pawlikowska L**, **Sen S**, **Elferink RPJO**, **Bull LN**. Strain background modifies phenotypes in the ATP8B1-deficient mouse. *PLoS ONE* 5: e8984, 2010.

226. **Shih DQ**, **Bussen M**, **Sehayek E**, **Ananthanarayanan M**, **Shneider BL**, **Suchy FJ**, **Shefer S**, **Bollileni JS**, **Gonzalez FJ**, **Breslow JL**, **Stoffel M**. Hepatocyte nuclear factor-1alpha is an essential regulator of bile acid and plasma cholesterol metabolism. *Nat Genet* 27: 375–382, 2001.

227. **Shipston MJ**. Ion channel regulation by protein S-acylation. *J Gen Physiol* 143: 659–678, 2014.

228. **Shneider BL**, **Dawson PA**, **Christie DM**, **Hardikar W**, **Wong MH**, **Suchy FJ**. Cloning and molecular characterization of the ontogeny of a rat ileal sodium-dependent bile acid transporter. *J Clin Invest* 95: 745–754, 1995.

229. **Shneider BL**, **Setchell KD**, **Crossman MW**. Fetal and neonatal expression of the apical sodium-dependent bile acid transporter in the rat ileum and kidney. *Pediatr Res* 42: 189–194, 1997.

230. **Sievänen E**. Exploitation of bile acid transport systems in prodrug design. *Molecules* 12: 1859–1889, 2007.

231. **Simon FR**, **Sutherland J**, **Sutherland E**. Identification of taurocholate binding sites in ileal plasma membrane. *Am J Physiol* 259: G394–401, 1990.

232. **Simrén M**, **Bajor A**, **Gillberg P-G**, **Rudling M**, **Abrahamsson H**. Randomised clinical trial: The ileal bile acid transporter inhibitor A3309 vs. placebo in patients with chronic idiopathic constipation--a double-blind study. *Aliment Pharmacol Ther* 34: 41–50, 2011.

233. **Sinha J**, **Chen F**, **Miloh T**, **Burns RC**, **Yu Z**, **Shneider BL**. beta-Klotho and FGF-15/19 inhibit the apical sodium-dependent bile acid transporter in enterocytes and cholangiocytes. *Am J Physiol Gastrointest Liver Physiol* 295: G996–G1003, 2008.

234. **Soler DM**, **Ghosh A**, **Chen F**, **Shneider BL**. A single element in the 3'UTR of the apical sodium-dependent bile acid transporter controls both stabilization and destabilization of mRNA. *Biochem J* 462: 547–553, 2014.

235. **Spinelli M**, **Fusco S**, **Grassi C**. Nutrient-Dependent Changes of Protein Palmitoylation: Impact on Nuclear Enzymes and Regulation of Gene Expression. *International Journal of Molecular Sciences* 19: 3820, 2018.

236. **Spinelli M**, **Fusco S**, **Mainardi M**, **Scala F**, **Natale F**, **Lapenta R**, **Mattera A**, **Rinaudo M**, **Li Puma DD**, **Ripoli C**, **Grassi A**, **D'Ascenzo M**, **Grassi C**. Brain insulin resistance impairs hippocampal synaptic plasticity and memory by increasing GluA1 palmitoylation through FoxO3a. *Nature Communications* 8: 2009, 2017.

237. **Srivastava A**. Progressive familial intrahepatic cholestasis. *J Clin Exp Hepatol* 4: 25–36, 2014.

238. **Staels B**. A review of bile acid sequestrants: potential mechanism(s) for glucose-lowering effects in type 2 diabetes mellitus. *Postgrad Med* 121: 25–30, 2009.

239. **Stelzner M**, **Hoagland V**, **Somasundaram S**. Distribution of bile acid absorption and bile acid transporter gene message in the hamster ileum. *Pflugers Arch - Eur J Physiol* 440: 157–162, 2000.

240. **Stross C**, **Helmer A**, **Weissenberger K**, **Görg B**, **Keitel V**, **Häussinger D**, **Kubitz R**. Protein kinase C induces endocytosis of the sodium taurocholate cotransporting polypeptide. *Am J Physiol Gastrointest Liver Physiol* 299: G320–8, 2010.

241. **Suchy FJ**, **Balistreri WF**, **Heubi JE**, **Searcy JE**, **Levin RS**. Physiologic cholestasis: elevation of the primary serum bile acid concentrations in normal infants. *YGAST* 80: 1037–1041, 1981.

242. **Suchy FJ**, **Balistreri WF**. Uptake of taurocholate by hepatocytes isolated from developing rats. *Pediatr Res* 16: 282–285, 1982.

243. **Suchy FJ**, **Courchene SM**, **Balistreri WF**. Ontogeny of hepatic bile acid conjugation in the rat. *Pediatr Res* 19: 97–101, 1985.

244. **Sun A-Q**, **Balasubramaniyan N**, **Chen H**, **Shahid M**, **Suchy FJ**. Identification of functionally relevant residues of the rat ileal apical sodium-dependent bile acid cotransporter. *J Biol Chem* 281: 16410–16418, 2006.

245. **Sun A-Q**, **Salkar R**, **Sachchidanand**, **Xu S**, **Zeng L**, **Zhou M-M**, **Suchy FJ**. A 14-amino acid sequence with a beta-turn structure is required for apical membrane sorting of the rat ileal bile acid transporter. *J Biol Chem* 278: 4000–4009, 2003.

246. **Sun AQ**, **Ananthanarayanan M**, **Soroka CJ**, **Thevananther S**, **Shneider BL**, **Suchy FJ**. Sorting of rat liver and ileal sodium-dependent bile acid transporters in polarized epithelial cells. *Am J Physiol* 275: G1045–55, 1998.

247. **Suzuki T**, **Oba K**, **Igari Y**, **Matsumura N**, **Watanabe K**, **Futami-Suda S**, **Yasuoka H**, **Ouchi M**, **Suzuki K**, **Kigawa Y**, **Nakano H**. Colestimide lowers plasma glucose levels and increases plasma glucagon-like PEPTIDE-1 (7-36) levels in patients with type 2 diabetes mellitus complicated by hypercholesterolemia. *J Nippon Med Sch* 74: 338–343, 2007.

248. **Swaan PW**, **Hillgren KM**, **Szoka FC**, **Oie S**. Enhanced transepithelial transport of peptides by conjugation to cholic acid. *Bioconjug Chem* 8: 520–525, 1997.

249. **Takahashi S**, **Fukami T**, **Masuo Y**, **Brocker CN**, **Xie C**, **Krausz KW**, **Wolf CR**, **Henderson CJ**, **Gonzalez FJ**. Cyp2c70 is responsible for the species difference in bile acid metabolism between mice and humans. *J Lipid Res* 57: 2130–2137, 2016.

250. **Thomas C**, **Landrier JF**, **Gaillard D**, **Grober J**, **Monnot M-C**, **Athias A**, **Besnard P**. Cholesterol dependent downregulation of mouse and human apical sodium dependent bile acid transporter (ASBT) gene expression: molecular mechanism and physiological consequences. *Gut* 55: 1321–1331, 2006.

251. **Thorne RF**, **Ralston KJ**, **de Bock CE**, **Mhaidat NM**, **Zhang XD**, **Boyd AW**, **Burns GF**. Palmitoylation of CD36/FAT regulates the rate of its post-transcriptional processing in the endoplasmic reticulum. *Biochim Biophys Acta* 1803: 1298–1307, 2010.

252. **Tiessen RG**, **Kennedy CA**, **Keller BT**, **Levin N**, **Acevedo L**, **Gedulin B**, **van Vliet AA**, **Dorenbaum A**, **Palmer M**. Safety, tolerability and pharmacodynamics of apical sodium-dependent bile acid transporter inhibition with volixibat in healthy adults and patients with type 2 diabetes mellitus: a randomised placebo-controlled trial. *BMC Gastroenterol* 18: 3, 2018.

253. **Van de Wiel S**, **Merkx M**, **Van de Graaf S**. Real Time Monitoring of Intracellular Bile Acid Dynamics Using a Genetically Encoded FRET-based Bile Acid Sensor. *J Vis Exp* : e53659–e53659, 2016.

254. **van der Mark VA**, **de Waart DR**, **Ho-Mok KS**, **Tabbers MM**, **Voogt HW**, **Oude Elferink RPJ**, **Knisely AS**, **Paulusma CC**. The lipid flippase heterodimer ATP8B1-CDC50A is essential for surface expression of the apical sodium-dependent bile acid transporter (SLC10A2/ASBT) in intestinal Caco-2 cells. *Biochim Biophys Acta* 1842: 2378–2386, 2014.

255. **van der Velden LM**, **Golynskiy MV**, **Bijsmans ITGW**, **van Mil SWC**, **Klomp LWJ**, **Merkx M**, **van de Graaf SFJ**. Monitoring bile acid transport in single living cells using a genetically encoded Förster resonance energy transfer sensor. *Hepatology* 57: 740–752, 2013.

256. **van der Velden LM**, **Golynskiy MV**, **Bijsmans ITGW**, **van Mil SWC**, **Klomp LWJ**, **Merkx M**, **van de Graaf SFJ**. Monitoring bile acid transport in single living cells using a genetically encoded Förster resonance energy transfer sensor. *Hepatology* 57: 740–752, 2013.

257. **Van Itallie CM**, **Gambling TM**, **Carson JL**, **Anderson JM**. Palmitoylation of claudins is required for efficient tight-junction localization. *J Cell Sci* 118: 1427–1436, 2005.

258. **Vivian D**, **Cheng K**, **Khurana S**, **Xu S**, **Dawson PA**, **Raufman J-P**, **Polli JE**. Design and evaluation of a novel trifluorinated imaging agent for assessment of bile acid transport using fluorine magnetic resonance imaging. *J Pharm Sci* 103: 3782–3792, 2014.

259. **Vivian D**, **Cheng K**, **Khurana S**, **Xu S**, **Kriel EH**, **Dawson PA**, **Raufman J-P**, **Polli JE**. In vivo performance of a novel fluorinated magnetic resonance imaging agent for functional analysis of bile acid transport. *Mol Pharm* 11: 1575–1582, 2014.

260. **Vivian D**, **Cheng K**, **Khurana S**, **Xu S**, **Whiterock V**, **Witter D**, **Lentz KA**, **Santone KS**, **Raufman J-P**, **Polli JE**. Design and characterization of a novel fluorinated magnetic resonance imaging agent for functional analysis of bile Acid transporter activity. *Pharm Res* 30: 1240–1251, 2013.

261. **Wagner M**, **Halilbasic E**, **Marschall H-U**, **Zollner G**, **Fickert P**, **Langner C**, **Zatloukal K**, **Denk H**, **Trauner M**. CAR and PXR agonists stimulate hepatic bile acid and bilirubin detoxification and elimination pathways in mice. *Hepatology* 42: 420–430, 2005.

262. **Wahlström A**, **Sayin SI**, **Marschall H-U**, **Bäckhed F**. Intestinal Crosstalk between Bile Acids and Microbiota and Its Impact on Host Metabolism. *Cell Metab* 24: 41–50, 2016.

263. **Wang DQ-H**, **Tazuma S**, **Cohen DE**, **Carey MC**. Feeding natural hydrophilic bile acids inhibits intestinal cholesterol absorption: studies in the gallstone-susceptible mouse. *Am J Physiol Gastrointest Liver Physiol* 285: G494–502, 2003.

264. **Weerachayaphorn J**, **Mennone A**, **Soroka CJ**, **Harry K**, **Hagey LR**, **Kensler TW**, **Boyer JL**. Nuclear factor-E2-related factor 2 is a major determinant of bile acid homeostasis in the liver and intestine. *Am J Physiol Gastrointest Liver Physiol* 302: G925–36, 2012.

265. **Weihrauch D**, **Kanchanapoo J**, **Ao M**, **Prasad R**, **Piyachaturawat P**, **Rao MC**. Weanling, but not adult, rabbit colon absorbs bile acids: flux is linked to expression of putative bile acid transporters. *Am J Physiol Gastrointest Liver Physiol* 290: G439–50, 2006.

266. **Weinman SA**, **Carruth MW**, **Dawson PA**. Bile acid uptake via the human apical sodium-bile acid cotransporter is electrogenic. *J Biol Chem* 273: 34691–34695, 1998.

267. **Weinman SA**. Electrogenicity of Na(+)-coupled bile acid transporters. *Yale J Biol Med* 70: 331–340, 1997.

268. **Werno MW**, **Chamberlain LH**. S-acylation of the Insulin-Responsive Aminopeptidase (IRAP): Quantitative analysis and Identification of Modified Cysteines. *Sci Rep* 5: 12413, 2015.

269. **West KL**, **Zern TL**, **Butteiger DN**, **Keller BT**, **Fernandez ML**. SC-435, an ileal apical sodium co-dependent bile acid transporter (ASBT) inhibitor lowers plasma cholesterol and reduces atherosclerosis in guinea pigs. *Atherosclerosis* 171: 201–210, 2003.

270. **Wong MH**, **Oelkers P**, **Craddock AL**, **Dawson PA**. Expression cloning and characterization of the hamster ileal sodium-dependent bile acid transporter. *J Biol Chem* 269: 1340–1347, 1994.

271. **Wong MH**, **Oelkers P**, **Dawson PA**. Identification of a mutation in the ileal sodium-dependent bile acid transporter gene that abolishes transport activity. *J Biol Chem* 270: 27228–27234, 1995.

272. **Wong MH**, **Rao PN**, **Pettenati MJ**, **Dawson PA**. Localization of the ileal sodium-bile acid cotransporter gene (SLC10A2) to human chromosome 13q33. *Genomics* 33: 538–540, 1996.

273. **Wu Y**, **Aquino CJ**, **Cowan DJ**, **Anderson DL**, **Ambroso JL**, **Bishop MJ**, **Boros EE**, **Chen L**, **Cunningham A**, **Dobbins RL**, **Feldman PL**, **Harston LT**, **Kaldor IW**, **Klein R**, **Liang X**, **McIntyre MS**, **Merrill CL**, **Patterson KM**, **Prescott JS**, **Ray JS**, **Roller SG**, **Yao X**, **Young A**, **Yuen J**, **Collins JL**. Discovery of a highly potent, nonabsorbable apical sodium-dependent bile acid transporter inhibitor (GSK2330672) for treatment of type 2 diabetes. *J Med Chem* 56: 5094–5114, 2013.

274. **Xia X**, **Roundtree M**, **Merikhi A**, **Lu X**, **Shentu S**, **LeSage G**. Degradation of the Apical Sodium-dependent Bile Acid Transporter by the Ubiquitin-Proteasome Pathway in Cholangiocytes. *J Biol Chem* 279: 44931–44937, 2004.

275. **Xiao Y**, **Yan W**, **Zhou K**, **Cao Y**, **Cai W**. Glucocorticoid treatment alters systemic bile acid homeostasis by regulating the biosynthesis and transport of bile salts. *Dig Liver Dis* 48: 771–779, 2016.

276. **Xie Y**, **Zheng Y**, **Li H**, **Luo X**, **He Z**, **Cao S**, **Shi Y**, **Zhao Q**, **Xue Y**, **Zuo Z**, **Ren J**. GPS-Lipid: a robust tool for the prediction of multiple lipid modification sites. *Sci Rep* 6: 28249, 2016.

277. **Xu Z**, **Zhong L**. New insights into the posttranslational regulation of human cytosolic thioredoxin by S-palmitoylation. *Biochem Biophys Res Commun* 460: 949–956, 2015.

278. **Yap MC**, **Kostiuk MA**, **Martin DDO**, **Perinpanayagam MA**, **Hak PG**, **Siddam A**, **Majjigapu JR**, **Rajaiah G**, **Keller BO**, **Prescher JA**, **Wu P**, **Bertozzi CR**, **Falck JR**, **Berthiaume LG**. Rapid and selective detection of fatty acylated proteins using omega-alkynyl-fatty acids and click chemistry. *J Lipid Res* 51: 1566–1580, 2010.

279. **Younossi Z**, **Anstee QM**, **Marietti M**, **Hardy T**, **Henry L**, **Eslam M**, **George J**, **Bugianesi E**. Global burden of NAFLD and NASH: trends, predictions, risk factors and prevention. *Nat Rev Gastroenterol Hepatol* 15: 11–20, 2018.

280. **Yount JS**, **Moltedo B**, **Yang Y-Y**, **Charron G**, **Moran TM**, **López CB**, **Hang HC**. Palmitoylome profiling reveals S-palmitoylation-dependent antiviral activity of IFITM3. *Nat Chem Biol* 6: 610–614, 2010.

281. **Zeidman R**, **Jackson CS**, **Magee AI**. Protein acyl thioesterases (Review). *Mol Membr Biol* 26: 32–41, 2009.

282. **Zhang EY**, **Phelps MA**, **Banerjee A**, **Khantwal CM**, **Chang C**, **Helsper F**, **Swaan PW**. Topology scanning and putative three-dimensional structure of the extracellular binding domains of the apical sodium-dependent bile acid transporter (SLC10A2). *Biochemistry* 43: 11380–11392, 2004.

283. **Zhao L**, **Zhang C**, **Luo X**, **Wang P**, **Zhou W**, **Zhong S**, **Xie Y**, **Jiang Y**, **Yang P**, **Tang R**, **Pan Q**, **Hall AR**, **Luong TV**, **Fan J**, **Varghese Z**, **Moorhead JF**, **Pinzani M**, **Chen Y**, **Ruan XZ**. CD36 palmitoylation disrupts free fatty acid metabolism and promotes tissue inflammation in non-alcoholic steatohepatitis. *JOURNAL OF HEPATOLOGY* 69: 705–717, 2018.

284. **Zheng X**, **Pan Y**, **Acharya C**, **Swaan PW**, **Polli JE**. Structural requirements of the ASBT by 3D-QSAR analysis using aminopyridine conjugates of chenodeoxycholic acid. *Bioconjug Chem* 21: 2038–2048, 2010.

285. **Zhou B**, **An M**, **Freeman MR**, **Yang W**. Technologies and Challenges in Proteomic Analysis of Protein S-acylation. *J Proteomics Bioinform* 7: 256–263, 2014.

286. **Zhou F**, **Xue Y**, **Yao X**, **Xu Y**. CSS-Palm: palmitoylation site prediction with a clustering and scoring strategy (CSS). *Bioinformatics* 22: 894–896, 2006.

287. **Zhou X**, **Levin EJ**, **Pan Y**, **McCoy JG**, **Sharma R**, **Kloss B**, **Bruni R**, **Quick M**, **Zhou M**. Structural basis of the alternating-access mechanism in a bile acid transporter. *Nature* 505: 569–573, 2014.

Chapter VI: Appendices

A. Appendix A

UIC UNIVERSITY OF ILLINOIS AT CHICAGO

Office of Animal Care and Institutional
Biosafety Committee (M/C 672)
Office of the Vice Chancellor for Research
206 Administrative Office Building
1737 West Polk Street
Chicago, Illinois 60612

April 16, 2018

Waddah A. Alrefai
Medicine/Gastroenterology and Hepatology
Jesse Brown VA Medical Center
R&D Room 7227, MP115-2030 W. Taylor St.
Chicago IL 60612-

Dear Dr. Alrefai:

The modifications requested in modification indicated below pertaining to your approved protocol indicated below have been reviewed and approved in accordance with the Animal Care Policies of the University of Illinois at Chicago on ***4/16/2018***.

Title of Application: Gut-Liver Crosstalk in Bile acid-induced Diarrhea

ACC Number: 16-063

Modification Number: ***1***

Nature of Modification:
1) Addition of FVB-Luciferase Tg (Total 124) Mice will be bred at VA and transferred to UIC, one week prior to IVIS study under the supervision of the veterinary staff. Mice will be used for the following: 1) pilot study to determine proper dose of the luciferase probe. To confirm that the bioluminescence is emanating from CA-SS-Luc that is absorbed in the distal ileum, excised intestine will be imaged. 2) Study to compare prenatal and preweaning exposure of offspring born from breeders fed a methyl donor-supplemented diet (MS diet) or control (CT diet) in order to determine the effect of prenatal exposure to hypermethylating conditions on bile acid absorption. On the day of IVIS imaging, they will be gavaged with CA-SS-Luc and imaged as above once every other week until 30 weeks of age. This will allow quantification of bile acid absorption during development. In addition, intestinal enteroids from isolated intestinal crypts for in vitro IVIS experiments
2) Addition of Fgf15 Tg mice (Total 188) overexpression Fgf15 specifically in the intestine (BL6 background) in order to examine the effect of MS diet and Fgf15 overexpression on experimental DSS-induced colitis. Breeders will be fed diets as outlined above through weaning and the offspring switched to normal chow at weaning. At 8 weeks, colitis will be induced as outlined in original protocol. These studies will be at VA.
3) Addition of C57 WT mice in order to examine the effect of MS diet on gene expression and DNA methylation in the intestine and liver, as well as plasma bile acid levels. Breeders will be fed diets as above through weaning and offspring switched to normal chow at weaning. Offspring will be euthanized at 4, 8 and 16 weeks of age. Breeders will also be analyzed. These studies will be at VA.
4) Addition of C57 WT (280) for administration of Ad-viral vector expressing hepatic Cyp7a1 or control vector to investigate the effect of disrupting ileal FGF15-hepatic CYP7A1 axis on the development of intestinal inflammation of diarrhea. This work will be at BSL2. These studies will be at VA.

5) Addition of F30 grant under institutional # 00401353.

Protocol Approved: ***4/25/2016***

Current Approval Period: ***4/19/2017*** to ***4/19/2018.***
Approval Period for Year 3*: 4/19/2018* to ***4/19/2019. Continuation has been submitted and approved***

Current Funding: ***Portions of this protocol are supported by the funding sources indicated in the table below.***
Number of funding sources: 2

Funding Agency	**Funding Title**			**Portion of Funding Matched**
NIH	*Gut Liver Crosstalk in Bile-Acid Included Diarrhea*			*All matched*
Funding Number	**Current Status**	**UIC PAF NO.**	**Performance Site**	**Funding PI**
RO1 DJ109709 (years 1-5)	*Funded*	*201600739*	*JBVAMC*	*Waddah Alrefai*
Funding Agency	**Funding Title**			**Portion of Funding Matched**
NIH	*Epigenetic regulation of bile acids in health and disease (Institutional # 00401353)*			*All matched*
Funding Number	**Current Status**	**UIC PAF NO.**	**Performance Site**	**Funding PI**
F30DK117535 (A1 version years 1-4)	*Pending*		*UIC and JBVAMC* *IVIS study at UIC*	*Alexander Ticho*

This institution has Animal Welfare Assurance Number A3460.01 on file with the Office of Laboratory Animal Welfare, NIH. **This letter may only be provided as proof of IACUC approval for those specific funding sources listed above in which all portions of the grant are matched to this ACC protocol.**

Thank you for complying with the Animal Care Policies and Procedures of UIC.

Sincerely yours,

Timothy J. Koh, PhD
Chair, Animal Care Committee
TJK /*mbb*
cc: BRL, ACC File, Pooja Malhotra, Ravinder Gill

B. Appendix B

Permission for articles published in the American Journal of Physiology – GI & Liver and Comprehensive Physiology

Copyright and Permissions

Reuse by Authors of Their Work Published by APS

Reuse by Non-authors of APS Published Content

Reuse in APS Publications of non-APS Published Content

Reuse by Authors of Their Work Published by APS

The APS Journals are copyrighted for the protection of authors and the Society. The Mandatory Submission Form serves as the Society's official copyright transfer form. Author's rights to reuse their APS-published work are described below:

Republication in New Works	Authors may republish parts of their final-published work (e.g., figures, tables), without charge and without requesting permission, provided that full citation of the source is given in the new work.
Meeting Presentations and Conferences	Authors may use their work (in whole or in part) for presentations (e.g., at meetings and conferences). These presentations may be reproduced on any type of media in materials arising from the meeting or conference such as the proceedings of a meeting or conference. A copyright fee will apply if there is a charge to the user or if the materials arising are directly or indirectly commercially supported[1]. Full citation is required.
Theses and Dissertations	Authors may reproduce whole published articles in dissertations and post to thesis repositories without charge and without requesting permission. Full citation is required.

https://journals.physiology.org/author-info.permissions

Permission for article published in the Journal of Biological Chemistry

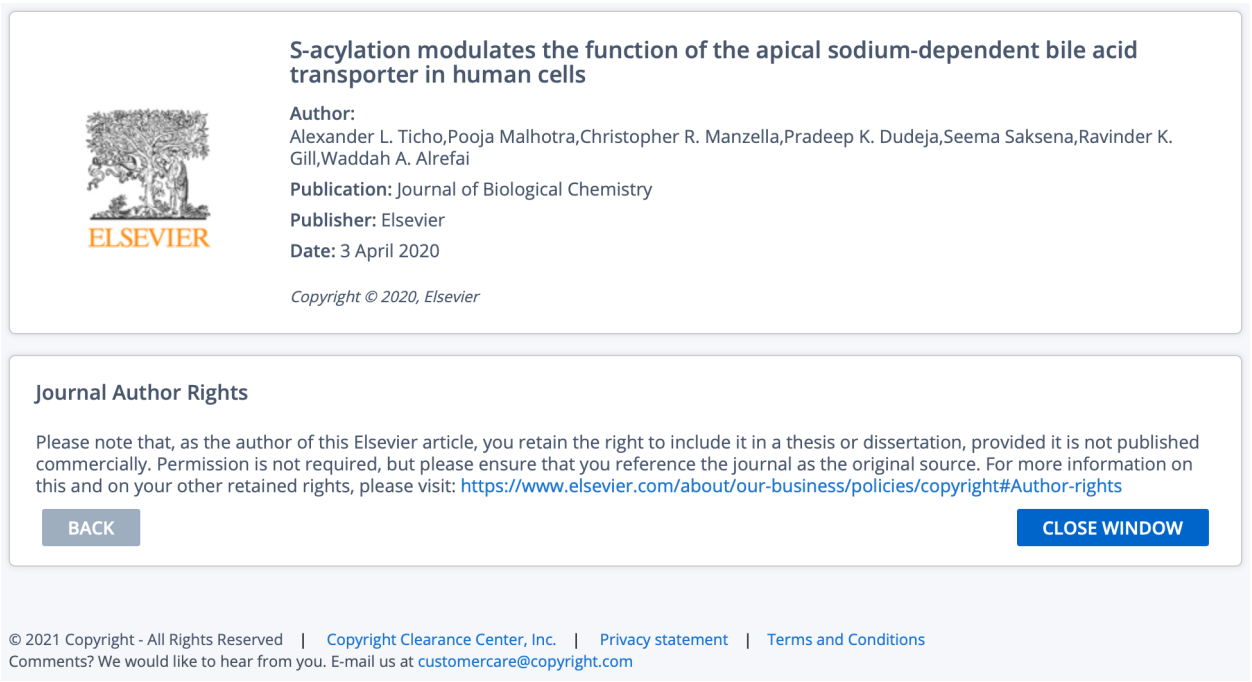

S-acylation modulates the function of the apical sodium-dependent bile acid transporter in human cells

Author:
Alexander L. Ticho,Pooja Malhotra,Christopher R. Manzella,Pradeep K. Dudeja,Seema Saksena,Ravinder K. Gill,Waddah A. Alrefai

Publication: Journal of Biological Chemistry

Publisher: Elsevier

Date: 3 April 2020

Copyright © 2020, Elsevier

Journal Author Rights

Please note that, as the author of this Elsevier article, you retain the right to include it in a thesis or dissertation, provided it is not published commercially. Permission is not required, but please ensure that you reference the journal as the original source. For more information on this and on your other retained rights, please visit: https://www.elsevier.com/about/our-business/policies/copyright#Author-rights

BACK CLOSE WINDOW

Chapter VII: Vita

Education

2013 – MD, PhD
University of Illinois at Chicago College of Medicine, Medical Scientist Training Program, Department of Physiology and Biophysics, Chicago, IL

2009 – 2012 BA *summa cum laude*, Chemistry
St Olaf College, Northfield, MN

Publications

1. **Ticho AL**, Calzadilla N, Malhotra P, Lee H, Anbazhagan AN, Saksena S, Dudeja PK, Lee D, Gill RK, Alrefai WA. NPC1L1-dependent transport of 27-alkyne cholesterol in intestinal epithelial cells. *Am J Physiol Cell Physiol. Under revision.*
2. Holton NW, Singhal M, Kumar A, **Ticho AL**, Manzella CR, Malhotra P, Jarava D, Saksena S, Dudeja PK, Alrefai WA, Gill RK. Hepatocyte Nuclear Factor 4α regulates transcription of the serotonin transporter in intestinal epithelial cells. *Am J Physiol Cell Physiol* 318: C1294-C1304, 2020.
3. **Ticho AL**, Malhotra P, Manzella CR, Dudeja PK, Saksena S, Gill RK, Alrefai WA. S-acylation modulates the function of the apical sodium-dependent bile acid transporter in human cells. *Journal of Biological Chemistry* 295: 4488-4497, 2020.
4. Manzella C, Ackerman M, Singhal M, **Ticho AL**, Ceh J, Alrefai WA, Saksena S, Dudeja PK, Gill RK. Serotonin modulates AhR activation by interfering with CYP1A1-mediated clearance of AhR ligands. *Cellular Physiology and Biochemistry* 54: 126-141, 2020.
5. **Ticho AL**, Malhotra P, Gill RK, Dudeja PK, Alrefai WA. Intestinal bile acid absorption in health and disease. *Comprehensive Physiology* 10: 21-56, 2020.
6. **Ticho AL**, Malhotra P, Dudeja PK, Gill RK, Alrefai WA. Bile acid receptors and gastrointestinal functions. *Liver Research* 3: 31-39, 2019.
7. **Ticho AL**, Lee H, Gill RK, Dudeja PK, Saksena S, Lee D, Alrefai WA. A novel bioluminescence-based method to investigate uptake of bile acids in living cells. *Am J Physiol Gastrointest Liver Physiol* 315: G529–G537, 2018.
8. Sharma M, **Ticho AL**, Samankumara L, Zeller M, Brückner C. Conformational Landscapes of Metal(II) Porphyrinato, Chlorinato, and Morpholinochlorinato Complexes. *Inorg Chem* 56: 11490–11502, 2017.
9. **Ticho AL**, Alrefai WA. Chronic ethanol exposure closes the door to vitamin C in pancreatic acinar cells. Focus on "Uptake of ascorbic acid by pancreatic acinar cells is negatively impacted by chronic alcohol exposure". *Am J Physiol Cell Physiol* 311: C127–8, 2016.

Research support

Source: National Institutes of Health (NIDDK) F30 Predoctoral Fellowship – F30DK117535
Dates: 5/2018 – 5/2021
Title: Epigenetic regulation of bile acids in health and disease
Role: PI
Goals: Elucidate the mechanisms by which DNA methylation causes bile acid dysregulation

Source: UIC Center for Clinical and Translational Science PECTS Fellowship
Dates: 8/2017 – 7/2018
Title: Regulation of the ileal bile acid transporter ASBT
Role: PI

Goals: Develop a bioluminescence-based probe to evaluate ASBT-dependent, real-time bile acid uptake

Source: National Science Foundation Research Experience for Undergraduates Fellowship – CHE-1062946
Dates: 6/2011 – 8/2011
Role: Trainee
Goals: Synthesize and characterize a series of metal(II) porphyrinato, chlorinato, and morpholinochlorinato complexes

Honors and awards

2019 Early Career Investigator Award, American Gastroenterological Association
2018 Honorable Mention for Poster Presentations by PhD and MD/PhD Students, UIC COM Research Forum
2018 Editor's Pick (October 2018), American Journal of Physiology – GI & Liver
2018 APS Select Nominee (October 2018), American Physiological Society
2018 International Bile Acid Congress Travel Award, Falk Foundation
2017 Poster of Distinction, American Physiological Society GI & Liver Section, Experimental Biology
2017 Predoctoral Travel Award, American Physiological Society GI & Liver Section, Experimental Biology
2017 Cover Article (October 2017), Inorganic Chemistry
2012 Bachelor of Arts *summa cum laude*, St Olaf College
2012 Phi Beta Kappa Honor Society, St Olaf College
2012 Phi Lambda Upsilon Honor Society, St Olaf College
2012 Merck Award, St Olaf College and Merck & Co.

Research experience

2013 – MD, PhD Candidate. University of Illinois at Chicago College of Medicine, Medical Scientist Training Program, Chicago, IL
Advisor: Waddah A Alrefai, MD
Thesis: S-Acylation is Crucial for ASBT-Mediated Bile Acid Uptake: Monitoring the Transport Activity in Real Time

2012 – 2013 Research Assistant. Loyola University Chicago Stritch School of Medicine, Department of Cell and Molecular Physiology, Maywood, IL
Advisor: Seth Robia, PhD
Project: **Structure transitions of the sodium, potassium-ATPase investigated by intramolecular FRET**

2011 Undergraduate Researcher – National Science Foundation REU Fellowship. University of Connecticut, Department of Chemistry, Storrs, CT
Advisor: Christain Brückner, PhD
Project: Conformational Landscapes of Metal(II) Porphyrinato, Chlorinato, and Morpholinochlorinato Complexes

2010 – 2011 Undergraduate Researcher – CURI Program. St Olaf College, Department of Chemistry, Northfield, MN
Advisor: Peter Gittins, PhD

Project: A greener approach to the synthesis of meso-monosubstituted porphyrins

Teaching experience

2017 – 2018 Lecturer, Gastrointestinal Physiology. Summer Pre-matriculation Program, University of Illinois at Chicago College of Medicine, Chicago, IL
2010 – 2011 Chemistry Tutor, St Olaf College, Northfield, MN

Volunteer experience

2015 – Alumni Mentor, Davidson Institute for Talent Development
2009 – 2010 Mentor, TRiO Educational Talent Search, St Olaf College

Abstracts and presentations

1. Malhotra P, **Ticho AL**, Calzadilla N, Saksena S, Gill RK, Dudeja PK, Alrefai WA. Omega-3 fatty acids reduce association with lipid rafts and inhibit the function of ileal apical sodium-dependent bile acid transporter (ASBT). May 2021. Digestive Disease Week, National Meeting of the American Gastroenterological Association. Poster Presentation
2. **Ticho AL**, Malhotra P, Lee H, Anbazhagan AN, Dudeja PK, Saksena S, Gill RK, Lee D, Alrefai WA. NPC1L1-dependent transport of 27-alkyne cholesterol to measure intestinal cholesterol absorption. May 2020. Digestive Disease Week, National Meeting of the American Gastroenterological Association; Chicago, IL. Oral Presentation
3. **Ticho AL**, Malhotra P, Manzella CR, Dudeja PK, Saksena S, Gill RK, Alrefai WA. A Novel Role of S-Acylation in the Modulation of Ileal Apical Sodium-Dependent Bile Acid Transporter (ASBT) Function. May 2019. Digestive Disease Week, National Meeting of the American Gastroenterological Association; San Diego, CA. Oral Presentation
4. Manzella C, **Ticho AL**, Ackerman M, Singhal M, Saksena S, Alrefai WA, Dudeja PK, Gill RK. Serotonin modulates Aryl hydrocarbon receptor (AhR) activation in the intestine by interfering with CYP1A1-mediated clearance of AhR ligands. May 2019. Digestive Disease Week, National Meeting of the American Gastroenterological Association; San Diego, CA. Oral Presentation
5. Manzella C, **Ticho AL**, Ackerman M, Singhal M, Saksena S, Alrefai WA, Dudeja PK, Gill RK. Serotonin modulates Aryl hydrocarbon receptor (AhR) activation in the intestine by interfering with CYP1A1-mediated clearance of AhR ligands. February 2019. Crohn's & Colitis Congress; Las Vegas, NV. Poster Presentation
6. Manzella C, **Ticho AL**, Ackerman M, Singhal M, Saksena S, Alrefai WA, Dudeja PK, Gill RK. Serotonin modulates AhR activation by interfering with CYP1A1-mediated ligand clearance. August 2018. AhR International Meeting; Paris, France. Poster Presentation
7. **Ticho AL**, Lee H, Gill RK, Dudeja PK, Saksena S, Lee D, Alrefai WA. A novel bioluminescence-based method to investigate uptake of bile acids in living cells. October 2018. American Physiological Society Video Abstract; https://www.youtube.com/watch?v=rnx3mp6GoRs. Video Abstract
8. **Ticho AL**, Lee H, Gill RK, Dudeja PK, Saksena S, Lee D, Alrefai WA. A real-time bioluminescent method for assessing bile acid transporter activity. July 2018. International Bile Acid Congress, Falk Foundation; Dublin, Ireland. Poster Presentation
9. **Ticho AL**, Lee H, Gill RK, Dudeja PK, Saksena S, Lee D, Alrefai WA. A novel method for measuring bile acid transporter activity in real time. June 2018. Digestive Disease Week,

National Meeting of the American Gastroenterological Association; Washington, DC. Poster Presentation

10. **Ticho AL**, Malhotra P, Manzella CR, Saksena S, Gill RK, Dudeja PK, Alrefai WA. The 5'-UTR of Niemann-Pick C1-Like 1 enhances translation efficiency. April 2017. Experimental Biology, National Meeting of the American Physiological Society; Chicago, IL. Poster Presentation
11. Malhotra P, Muthusamy S, Kumar A, **Ticho AL**, Saksena S, Gill RK, Dudeja PK, Alrefai WA. TNF decreases intestinal FGF15/19 expression via activation of NF-kB. April 2016. Digestive Disease Week, National Meeting of the American Gastroenterological Association; San Diego, CA. Poster Presentation
12. Manzella CR, Singhal M, Kumar A, Coffing H, **Ticho AL**, Priyamvada S, Anbazhagan AN, Saksena S, Alrefai WA, Dudeja PK, Gill RK. Gene expression and miRNA profiling in ileal mucosa of SERT knock-out mouse using microarray approaches. April 2016. Digestive Disease Week, National Meeting of the American Gastroenterological Association; San Diego, CA. Poster Presentation
13. **Ticho AL, Abrol N, Bossuyt J, Bers DM, Robia SL. Structure transitions of the sodium, potassium-ATPase investigated by intramolecular FRET. February 2013. Biophysical Society Annual Meeting; Philadelphia, PA.** Poster Presentation
14. **Ticho AL**, Samankumara L, Zeller M, Brückner C. Metallomorpholinochlorins: Mapping the conformational space of morpholinochlorins. April 2012. National Meeting of the American Chemical Society; San **Diego**, CA. Poster Presentation